Mobility Modelling and Simulation In Tactical Networks and Smart Cities

Younes Regragui

جامعة شعيب الدكالي
Université Chouaib Doukkali

THÈSE

En vue de l'obtention du

DOCTORAT DE L'UNIVERSITÉ CHOUAÏB DOUKKALI

Délivré par :

Faculté des Sciences

Spécialité doctorale : **INFORMATIQUE**

présentée et soutenue publiquement par :

Younes REGRAGUI

le 26 décembre 2019

Titre :

Mobility Modelling and Simulation In Tactical Networks and Smart Cities

---

Directeur de thèse : **Prof. NAJEM MOUSSA**

Membres du jury :

Mr. Abdessadek AAROUD,	PES-Faculté des Sciences, El Jadida	Président
Mr. Najib EL KAMOUN,	PES-Faculté des Sciences, El Jadida	Rapporteur
Mr. Abdellah MADANI,	PH-Faculté des Sciences, El Jadida	Rapporteur
Mr. Khalid ZINE-DINE,	PH-Faculté des Sciences, Rabat	Rapporteur
Mr. Abderrahim BENI-HSSANE,	PES-Faculté des Sciences, El Jadida	Examinateur
Mr. A. EL MOUTAOUAKKIL,	PES-Faculté des Sciences, El Jadida	Examinateur
Mr. Mohamed KISSI,	PES-Faculté des Sciences et Techniques, Mohammedia	Examinateur
Mr. Najem MOUSSA,	PES-Faculté des Sciences, El Jadida	Dir. de thèse

---

Laboratoire de Recherche en Optimisation, Systèmes Émergents, Réseaux et Imagerie (LAROSERI)

Abstract

Recently, we have observed a continuous interest in mobility modeling and simulation either for tactical mobility or for intelligent mobility in traffic systems. The rapid advent of ad hoc networks and their ability to provide efficient wireless applications have encouraged researchers to think about new solutions and application fields for tactical networks and Intelligent Transportation Systems (ITS). As an essential feature of ad hoc networks, the mobility of devices and their ability to communicate with each other without the need of a pre-established infrastructure, based on a self-organization mechanism, is considered to be an attractive feature in order to build realistic applications and protocols. Therefore, the need for mobility models is one of the most important components to enable extensive evaluation, analysis, and comparison of such applications and protocols, before they are officially adopted for use. Since most of the scenarios in the real world are based on nodes mobility including, intelligent vehicles, persons and drones, we are interested in studying mobility modeling, in order to search, as realistically as possible, for the efficient mobility behaviors for such real-world scenarios.

We focus principally on mobility modeling as a basic component to provide efficient analyzing of the dynamicity of nodes in tactical networks, and also to understand traffic systems behaviors in order to design intelligent mobility schemes for transportation systems and smart cities. We began our research by investigating the mobility behaviors to extract their intrinsic properties and to be able to propose more accurate approaches. After that, our attention is oriented to adopt specifications and tools needed to design mobility behaviors of tactical networks, as well as to realize intelligent mobility strategies for providing efficient services in smart cities.

In this thesis, we are interested on studying some mobility models of tactical scenarios in Mobile Ad Hoc Networks (MANETs) and Wireless Sensor Networks (WSNs) in order to provide strong simulation tools for studying and analyzing some frequently encountered challenges in wireless networks, including topology change, communication reliability, and energy efficiency. We have been interested in the dynamicity of the tactical network and in particular in dismounted soldiers dynamic which is very interesting for modern wars. Moreover, we provided extensive simulations of sensor networks based on a tactical scenario, to highlight the relationship between tactical mobility and energy efficiency. Another subject of interest we are concerned with is smart city. Before we gain insight into the specificities of intelligent mobility in traffic systems and smart cities, our interest was oriented first to mobility modeling based on cellular automata, which are known as a microscopic model. The purpose behind this choice is to take a first step towards understanding traffic systems before going through intelligent mobility in smart cities. Then, our attention is directed towards both mobility and communication in vehicular environment called VANETs, which enables us to study the real-time interaction either between Vehicles (V2V) or either between vehicles and infrastructure (V2I). This study allowed us to consider new solutions of the problems related to ITS, including traffic conges-

tion, traffic jams, and accidents. We address precisely both the problem of traffic congestion and collision situations at traffic intersections. The purpose of such a study is to improve traffic flow in transportation systems by profiting from new wireless technologies to immigrate towards smart traffic mobility, which is currently one of the most fundamental service that must be available in smart cities. We adopted cooperative strategies between vehicles (V2V) and between vehicles and infrastructure (V2I). Accordingly, we introduced a path planning strategy to avoid traffic problems by reducing travel times on-road segments. This developed path planning strategy allows the driver to get timely short paths based on received information about the traffic state in each road segment. In the context of intersection collisions, we developed an approach based on a periodic exchange of beacons between approaching vehicles to the intersection to estimate and to avoid collisions at the intersection.

Key words : Self-Organized Behavior, Mobility Models, Ad hoc Networks, Group mobility, Dismounted soldiers, Battlefield, Vehicular traffic flow, Mobility, Smart Mobility, Smart Cities, Tactical network, ITS, Collision detection, Flocking, Sensor networks, Energy efficiency.

Acknowledgment

This thesis work has given me an excellent opportunity to have a deeper level understanding of the computer networks and several tools of simulation. I am grateful to my PhD advisor Prof. Najem Moussa for all the necessary support and guidance during these years. His great support in scientific and academic life, sharing his ideas and thoughts with us, and that he managed well the way of raising right questions and solving problems.

I would like to thank my jury members for reading my manuscript and showing interest in my work.

I would also like to thank all colleagues and friends for their support and camaraderie during these years. The experience and the education before beginning my PhD have definitely contributed to make this journey easier to start. Therefore, I am thankful to my school teachers, university professors during my professional career.

Finally, a special thanks to my parents. Without their understanding, support and patience during my PhD study period it would be much more difficult for me to finish my PhD degree. I am very grateful to their efforts to grant me well education, love, and a continue support since childhood.

Contents

List of Figures

List of Tables

List of Acronyms

AODV	Ad Hoc On-Demand Distance Vector
CA	Cellular Automata
CGM	Coordinated Group Member
CAMs	Cellular Automata Models
CCH	Control Channel
CMM	Community Based Mobility
DSRC	Dedicated Short-Range Communication
GAMs	Gap Acceptance Models
GM	Gipps Model
GFMM	Group Force Mobility Model
GPS	Global Position System
IDM	Intelligent-Driver Model
ITS	Intelligent Transportation Systems
IDM	Intelligent-Driver Model
IGM	Individual Group Member
IEEE	Institute of Electrical and Electronics Engineers
ICWSs	Intersection Collision Warning Systems
LCMs	Lane Changing Models
LLC	Logical Link Control
MANETs	Mobile Ad Hoc Networks
MTN	Mobile Tactical Network
MLME	MAC Layer Management Entity
MGCM	Multi-Group Coordination Mobility
NaSch	Nagel and Schreckenberg Model
NCMM	Nomadic Community Mobility Model
NS	Network Simulator
PLME	PHY Layer Management Entity
PBGM	Point-Based Group Mobility
RBGM	Region-Based group mobility

RPGM	Reference Point Group Mobility
RWM	Random Waypoint Model
RVGM	Reference Velocity Group Mobility
RSUs	Roadside Units
RRGM	Reference Region Group Mobility
RF	Radio Frequency
STEPS	Spatio-Temporal Parametric Stepping
SLAW	Self-similar Least Action Walk
SCH	Service Channel
V2I	Vehicle-to-Infrastructure
V2V	Vehicle-to-Vehicle
VANETs	Vehicular Ad Hoc Networks
VTGM	Virtual Track Group Mobility
WSMP	Short Message Protocol
WAVE	Wireless Access in Vehicular Environments
WSNs	Wireless Sensor Networks

Chapter 1

Introduction

« *Everybody is a genius. But if you judge a fish by its ability to climb a tree, it will live its whole life believing that it is stupid.* »

Albert Einstein

Contents

1.1 Context and motivations

The rapid advent of MANETs, in the last decades, has encouraged the research community to think about adopting new solutions for different categories of applications. The success of MANETs is related to the fact that they allow a flexible exchange of information between mobile devices without the existence of a predefined infrastructure. This rapid evolution in communication technologies has completely changed the way people communicate. These networks have the ability to provide a wide range of promising applications, including data transmission in disaster areas, battlefields, inter-vehicular communications, vehicle tracking, real-time path planning, and intelligent traffic lights control. It is widely believed that the node's mobility is among the most important reasons behind the revolution in MANETs. Indeed, mobility is considered as an essential feature that allows us to develop and simulate applications constrained to high dynamism such as tactical networks and Vehicular Ad Hoc Networks (VANETs), where cooperation and coordination mechanisms can lead to improved efficiency and reliability in such networks. However, MANETs are sensitive to nodes' mobility due to frequent topology changes, which may cause considerable link failures. This can lead to a catastrophic situation whereby source nodes cannot successfully send data packets to their destination. In addition, in certain critical situations, like that related to dismounted soldiers in battlefield, it is very important to maintain path length and end-to-end delays in order to carry out the desired mission.

In recent years, there has been an increasing interest in mobility modeling for both tactical networks and transportation systems. Therefore, several studies and researches have been proposed in the literature. For example, in order to provide a performance analysis of wireless networks, some researchers have tried to introduce mobility models based on different techniques including, enhanced random mobility by using movement tracing [1], mathematical formulation for systematic tracking of the random movement of a mobile station [2], microscopic modelling for individual human mobility [3] and realistic mobility modeling based on the movement of vehicles on real street maps [4]. Other researchers have proposed mobility models to simulate tactical scenarios in the real-world scenarios. For example, in [5], the authors proposed a mobility modeling tool called SWarMM (Synthetic Warfare Mobility Modeller) to produce mobility that more closely represents tactical military deployments. In [6], a Mobile Tactical Network (MTN) operating in the VHF/UHF military radio is introduced to investigate both characteristics of tactical mobility and the network properties including, connectivity, distribution of hop counts, etc. Accordingly, to provide simulation and emulation for performance evaluation of wireless multi-hop networks, open-source Java software called BonnMotion has been introduced to create and analyze mobility scenarios [7]. These scenarios can also be exported for the network simulators ns-2, GloMoSim/QualNet, COOJA, and MiXiM. To discover interesting strategies for Intelligent Transportation Systems, researchers create a microscopic traffic simulator based on cellular automata models [8]. This simulator tends to define drivers as intelligent agents in a cellular automata environment. In [9], an open-source simulation platform is used to improve road traffic safety and efficiency, characterized by a modular architecture that allows integrating traffic and wireless simulation models to develop cooperative ITS applications. In [10], a reservation-based approach to intersection control was proposed to provide intelligent coordination between vehicles and intersections in terms of the time and space that a vehicle will occupy when approaching the intersection. Each vehicle is attempting to claim its right to a reservation of crossing the intersection to an intersection coordinator (an electronic device installed at the intersection) via a wireless network.

The continuous development of communication technologies may encourage researchers to further discover new collective motions, inspired from nature such as humans and animals.

Motivated by the importance of mobility modeling and its ability to build more realistic simulations of mobile wireless networks, our contributions tackled tactical networks as well as intelligent transportation systems which are considered to serve fundamental services for smart cities. Our main purpose is to design such mobility models capable of reflecting as closely as possible those existing in the real world, in order to improve the efficiency and the reliability in tactical networks and to avoid traffic problems by performing traffic control and planning in road networks.

In the context of tactical mobility, our interests are oriented specifically to realizing mobility modeling of tactical scenarios in MANETs and WSNs, so as to provide a strong simulation tool for studying some encountered challenges, including topology change, communications reliability and energy efficiency. To gain insights into tactical mobility modeling, we paid attention to the dynamic of dismounted soldiers as a suitable subject that is very interesting for modern wars. As dismounted soldiers are constrained by high dynamics within the battlefield, we show how this can have an impact on both topology conditions and wireless communications reliability. In addition, we also are interested in tactical mobility modeling in order to highlight the problem of energy efficiency in WSNs. We try to make efforts to find a relationship that links energy consumption to the dynamic of nodes of WSNs for different kinds of tactical scenarios.

In the context of mobility modeling in traffic systems, our interest was oriented first to model mobility based on cellular automata Cellular Automata (CA). The reason behind this choice is that CA is very useful for rapid simulations, since it is discrete in both space and time. After that, our attention will focus on how combining both mobility modeling and wireless communications to migrate towards more intelligent mobility needed for designing smart cities. Our aim here is to provide efficient and intelligent strategies to overcome some problems related to transportation systems including, for example, traffic congestion or traffic jams, reducing travel time, and avoiding accidents at intersections. We address mainly two main issues : the first one is devoted to improving the traffic state and reducing vehicles travel time, while the second focus is avoiding collisions at intersections between approaching vehicles. We adopted a cooperative strategy to the mobility of nodes, based on Vehicle-to-Vehicle (V2V) and Vehicle-to-Infrastructure (V2I) communications. Accordingly, we introduced a path planning strategy to avoid congestion problems and we demonstrated that this strategy is capable of improving traffic flow and reducing vehicles' travel time. Indeed, our proposed strategy allows drivers to get timely short paths based on a real-time exchange of information between vehicles and infrastructure. Furthermore, we developed a new strategy related to collision estimation and avoidance at intersection, based on a periodic exchange of beacons between vehicles approaching the intersection, so as to estimate and avoid collisions via the calculation of collision probability.

1.2 Overview and Contributions

In the following, an overview of the content of this thesis is provided :

1. First, we review mobility models in Chapter 2, because we believe that they are very important in the context of this thesis. These mobility models include both microscopic traffic models and group mobility models. Secondly, we propose a two-dimensional CA model based on discrete-time and space. This model is capable of simulating the traffic in an urban environment with multiple roundabouts. Based on our microscopic mobility model, we perform an analysis of traffic state and accident probability in roundabouts in terms of car density. Thirdly, we propose a group mobility model based on a multi-agents technique for studying the impact of heterogeneity within the agents' group. The group

may contain a proportion of informed agents who already have knowledge about the target, and the question is how the group will be attracted to this target based on a predefined level (ω). We assume that the value of ω may represent the quality of information about the location of the target. Indeed, the objective of this chapter is to provide support for related knowledge of mobility modeling, in order to be able to design more accurate scenarios for both tactical networks and smart cities.

2. In Chapter 3, we propose three tactical mobility scenarios for studying and analyzing some frequently encountered challenges in tactical networks including, topology change, communications reliability and energy efficiency. Firstly, we are interested in particular in the dismounted soldiers dynamic as a suitable subject for simulation of battlefield in modern war. So, we provide an appropriate environment to study and analyze the dynamicity of dismounted soldiers under different factors such as soldiers' speed, noise which affects the soldiers' movement direction, enemy attacks, etc. Our proposed scenarios include simulation of a dismounted soldiers' group, simulation of dismounted soldiers' group with the presence of enemy and simulation of a dismounted soldiers' squad. Then, we extended our previous mobility model proposed in chapter 2 to analyze the relationship between tactical mobility and energy efficiency. For this purpose, we developed a new wireless sensor model composed of a network model which defines how sensor nodes will communicate between them, a buffering mechanism to manage related and unrelated data packets, a probabilistic flooding algorithm, and an energy model to determine energy consumption during sending, receiving and sensing states.

3. In Chapter 4, we provide two main parts. In the first part, we propose a Real-Time Path Planning strategy developed to reduce vehicle traveling time. As an important component in a smart city, smart mobility should be characterized by a high flexibility of traffic flow management, less travel time and low risk of car accidents. Thus, our strategy can request a real-time short path from a central server, which performs a central analysis of vehicle travel times in every road segment received via V2V and V2I communications. We evaluated our proposed path planning strategy in terms of average speed, travel time and the density of vehicles and by considering two realistic scenarios. Secondly, we propose a prediction strategy of collision at intersections between approaching vehicles an intersection by using Dedicated Short-Range Communication (DSRC) based V2V Communications. Our method is based on the estimation of risk for each pair of approaching vehicles an intersection based on the calculation of collision probability. Our strategy is evaluated and compared in terms of maximum collision probability and by considering two classifications of situations awareness (Crash and No Crash).

4. Finally, Chapter 5 summarizes our contributions and shows possible future research directions based on the findings of this thesis.

Chapter 2

On the mobility Modeling

« *In the middle of difficulty lies opportunity.* »

Albert Einstein

Contents

2.1 Introduction

Mobility modeling is aimed at accurately representing mobility descriptions based on different conceptual models to give an understanding of some existing behaviors in the real-world such as traffic in an urban environment, animal groups, and human mobility. Interaction and relationships defined by each mobility model depend on mathematical/logical concepts in most cases. Some mobility models are based on a combination of mathematical formulations and real experiments' traces to recreate the same behaviors. However, a lot of experiments of real-world scenarios are not feasible mathematically since the analytical cost can be too high and sometimes it is even impossible. Therefore, a simulation environment can very attractive for evaluating and studying varying types of problems associated with complex mobility processes that cannot readily be described in analytical terms. Typically, the utilization of a simulation environment is intended to respond to the needs and reflect important results with a high level of satisfaction.

2.2 Mobility models

Traffic simulation modeling is considered to be a very popular and effective tool of great importance for analyzing and studying a wide variety of behaviors and challenging problems in Transportation Systems, including traffic jams problems, accident probability and other types of traffic problems. Usually, these scenarios are characterized by the interaction between many components, including vehicles of different types, driver's behaviors, traffic lights, traffic signals, traffic rules and infrastructure settings which are considered to have a significant effect on traffic dynamics. All these components or entities whose interactions are complex make simulation not easy to do. However, most simulations tools try to simplify the problems by adopting some techniques capable of redefinition of the problems with simple logic representation such as using models based on discrete-time and space.

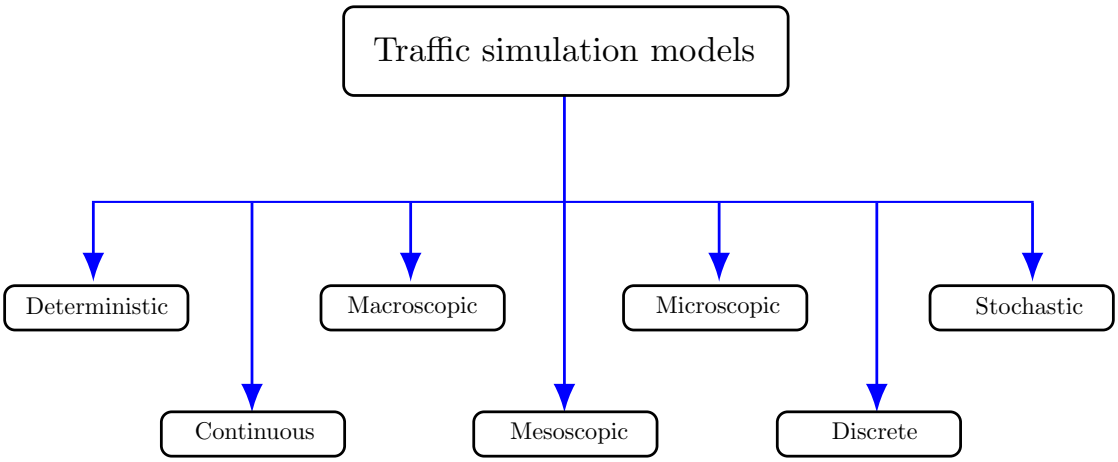

Figure 2.1 – Classification of Traffic simulation models.

2.2.1 Microscopic Traffic Models

Microscopic mobility modeling tries to describes various real-world objects explicitly (pedestrians, vehicles, animals, etc.). This type of modeling can describe both objects' activities and interactions at a much lower level of detail. In traffic systems, microscopic modeling in-

cludes more details like speed, traffic flow, length, density, car's acceleration/deceleration, driver's behavior and vehicle neighborhood. In the literature, several microscopic models were introduced, including car-following models such as the Krauss model and the Intelligent-Driver Model (IDM), Lane Changing Models (LCMs), Gap Acceptance Models (GAMs) and Cellular Automata Models (CAMs).

2.2.1.1 Car–following–models

The car-following models' theories are in most cases based on the assumption that the motion of vehicle i depends directly on the motion of the preceding vehicle (i + 1). This can be the basic foundation of steady-state in traffic systems which requires that the velocity of all vehicles should be equal (otherwise they would collide). This means that the desired velocity of a car is equal to the velocity of the car it is following as given with the following equation :

$$\frac{d\,v_i(t)}{\delta t} = \frac{v_{i+1}(t) - v_i(t)}{\tau} \tag{2.1}$$

Intelligent Driver's Model (IDM) : IDM describes the instantaneous dynamics of single vehicles based on the positions, velocities, and accelerations under the constraint that a driver is following a lead vehicle and respecting a limited speed. This can be described as that a car driver belongs to a platoon of vehicles without being able to change its lane. For vehicle i of length l_i located at position x_i, moves with a speed v_i and respecting a maximum acceleration a, the dynamics of vehicle i is then described by the following equations as follows :

$$\mathbf{a}_i = \left(1 - \left(\frac{v_i}{v_\alpha}\right)^\delta - \left(\frac{\mathrm{S}^*(v_i, \Delta v_i)}{\mathrm{S}_i}\right)^2\right) \tag{2.2}$$

$$\mathbf{a}_i^{free} = \left(1 - \left(\frac{v_i}{v_\alpha}\right)^\delta\right) \tag{2.3}$$

where v_i is the current vehicle speed, $\mathrm{S}_i = x_{i-1} - x_i - l_i$ is the net distance and v_α is the desired velocity.

Krauss Model : Unlike IDM, Krauss model describes vehicle dynamics as discrete in time domain based on stimulus response approach. The Krauss model allows a vehicle to change acceleration/deceleration based on an adjusting parameter called μ. It simply changes the current speed for a unit step time by allowing a regular increase/decrease in speed.

Wiedemann Mobility Model (WMM) : This is considered as a psycho-physical model i.e. the driver's behavior is related to its mentality and the current situation on the road. Accordingly, driver behavior is taken into consideration to predict multiple responses for the same input stimulus. Thus, several driver' profiles may exit corresponding to each situation on the road as follows :

1. In the case of no leading vehicle : the driver accelerates without restrictions.
2. In the case of a leading vehicle : the driver decelerates till reaching a suitable safe distance in between.
3. Following mode : the driver tries to adjust its speed with the lead vehicle by adding smooth acceleration and deceleration.
4. Breaking mode : a Crash avoidance approach is triggered to get away from the leading vehicle using deep sudden deceleration.

2.2.1.2 Lane Changing Models

Lane changing models are introduced in a variety of traffic and transportation studies including transportation planning and development [11] of traffic management policies [12] and performing a partly empirical and partly theoretical analysis of lane changing on two-lane–freeways [13]. Several studies were introduced in the literature to examine how lane changing strategies can have an effect on increasing freeway traffic state and traffic safety on the road.

Gipps Model : it is a lane-changing model based on an estimation of driver's behavior in making a lane change for a specific situation and at a specific time. The execution of lane changes can be done on freeways and urban streets. The lane-changing decisions described by Gipps Model (GM) can be executed as the result of three factors, including the lane-changing possibility, the necessity for changing lanes and lane-changing desirability. GM includes several factors that can be considered as constraints when executing each lane-changing decision, such as the existence of safety gap, locations of permanent obstructions, the intent of turning movement, the presence of heavy vehicles, and speed advantage. It also considers several lane-changing reasons : avoiding a heavy vehicle's influence, gaining speed advantage, avoiding special purpose lanes such as transit lanes, turning at downstream intersections and avoiding permanent obstructions.

Wiedemann Lane changing model : this model distinguishes between two types of driver' behaviors, including the wish to change lanes and the decision to change lanes as follows :

1. **Wish :** To change lanes if on any of the two lanes there is another vehicle ahead and obstructing.
2. **Decision :** To make a lane change if there is enough space in the other lane.

The Wiedemann-approach is based on obstructing phenomenon which is defined in terms of so-called psycho-physiological thresholds. The obstructing phenomenon or psycho-physiological thresholds depends on speed difference and distance, where a vehicle reaction depends on the crossed threshold.

2.2.1.3 Cellular Automata Models (CAM)

By using cellular automata, it is possible to update the velocity in discrete time steps directly instead of solving a differential equation. Thus, as cellular automata are based on discrete-time, it gives us extra details and simplification to reduce computational complexity. They are based on both discrete-time and space, respectively. These models describe lanes as a lattice of cells of equal size and incorporate a binary state for each cell and some rules such as acceleration, deceleration, and breaking. In each time step, a vehicle movement can move at least to the next cell depending on its previous speed state and the available headway in front of it. This means that the velocity of a vehicle i at time step t is calculated in terms of the previous state of vehicle [14, 15] as follows :

$$\mathbf{v}_i^t = f\big(v_i(t-\Delta t), v_{i+1}(t-\Delta t), x_{i+1}(t-\Delta t), x_{i-1}(t-\Delta t)\big) \tag{2.4}$$

CA Model proposed by Cremer and Ludwig : Among the first proposed models based on CAMs. This model is capable of simulating traffic flow through urban networks. On each street, it simulates the progression of cars by moving 1-bit variables through binary positions of bytes in the storage which are arranged to copy the topology of a specified network. Based on an application of boolean operations, this model can perform different types of vehicle behaviors such as driving at a constant speed, lane changing, passing, decelerating and accelerating, queueing and turning at intersections. Also, this model has supplementary advantages, it needs low computational requirements to perform both storage and computation and can

simulate large traffic networks on personal computers.
Nagel and Schreckenberg Model (NaSch) : This is a CA model based on discrete-time and space, respectively, where the road segments are discretized into cells of about 7.5 meters length. Each cell can either be empty or be occupied by a vehicle at each time step. The velocity of a vehicle is an integer number that represents the number of cells the vehicle jumps per time step from its current position. The calculation of a vehicle' velocity is done by considering some constraints such as current velocity, possible acceleration/deceleration, maximum velocity and the gap in front of a vehicle. NaSch is a stochastic model that incorporates imperfections of driving using a noise term in the update rules. The discrete rules governance provided by NaSch reproduces the empirical speed-density relation with more details and precision in handling different drivers' behaviors on the road.

2.2.2 Group Mobility Models

In group mobility models, mobile nodes are divided into groups, each mobile node belonging to a specific group based on some criteria and parameters. Usually, mobile nodes can make interactions with other mobile nodes in the same group or with neighbors of the nearest groups based on different zones or radius, where each zone is corresponding to a specific behavior. As each node belongs to a specific group, its mobility within the group is constrained by the group's coverage area. In contrast, each group can move to any location within the simulation environment depending on an already predefined destination or a shared trajectory between groups. As a result, an effective leadership emerges between groups and the trajectory selected is usually due to consensus decision making between groups. The Classification of Group Mobility Models is based on different perspectives related to how mobile nodes can move as a group. For example, in some group mobility models, the mobile nodes follow a lead point, whose movement dictates that of an entire group, where the lead point can represent either a real physical node or a logical point that represents the center of the group. These types of group mobility models are referred to in the literature as Point-Based Group Mobility (PBGM) models. Another class of group mobility models in [16–18] uses a different principle, where mobile nodes can follow a path through a sequence of regions or areas instead of following a lead point. These models are referred to in the literature as Region-Based group mobility (RBGM) models. The third class of group mobility models is considered different from class one and two, but it inherits some characteristics from them. Mobile nodes for this class move independently of each other ; however, their movements are influenced only by their lead point or targeted regions. These models are referred to as Individual Group Member (IGM) models. The last class of group mobility models defines relationships between mobile nodes completely different from the previous classes. The movement of nodes is influenced by or correlated with other group members due only to some interaction or relationships that exist between them. These models are referred to as Coordinated Group Member (CGM) movements.

2.2.2.1 Point Based Group Mobility Models

In PBGM models, each mobile node can follow the movements of a physical or logical lead point that exists within the group, which represents the group' center or mobile node leader.

1. **Reference Point Group Mobility (RPGM)[19] :** This model is the most widely known of the group mobility models. The entire group has a logical "center" or a lead point that defines the entire group's motion behavior, including location, speed, direction, and acceleration. The trajectory of the logical center can be predefined or obtained based on a particular entity mobility model. The entire group is composed of multiple independent

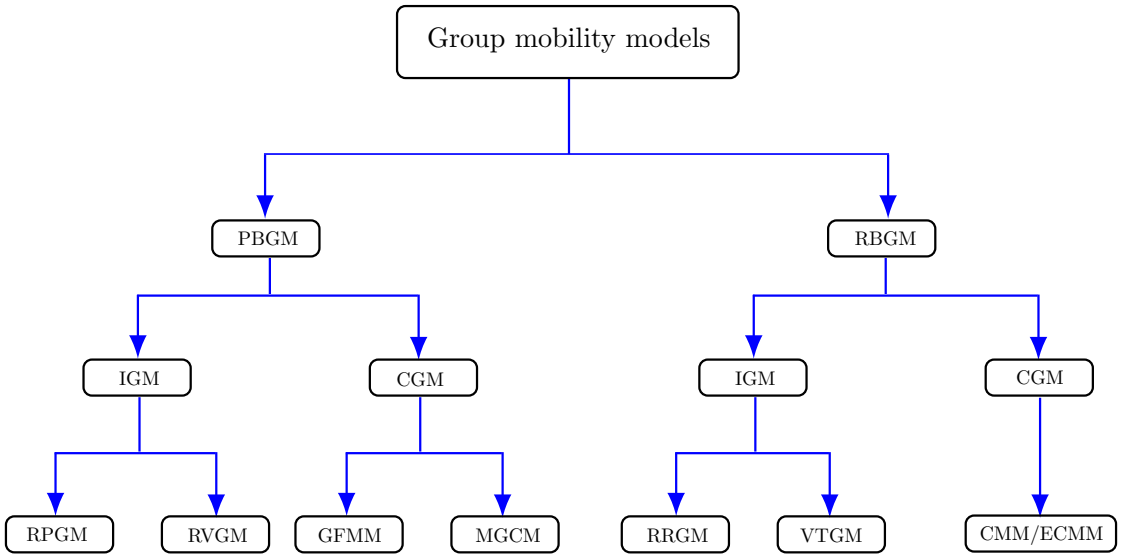

Figure 2.2 – Classification of group mobility models.

groups, where each one is characterized by a reference point. In each group, members follow its group' reference point that in its turn follows the lead point and maintains a constant distance and direction from it. Every member moves to a randomly chosen location within a circular neighborhood of radius R around its reference point location. The movement around the reference point is based on the Random Waypoint Model (RWM). The analysis and the simulation experiments demonstrated that the greater the radius, the higher the fluctuation and the uncertainty in the mobility.

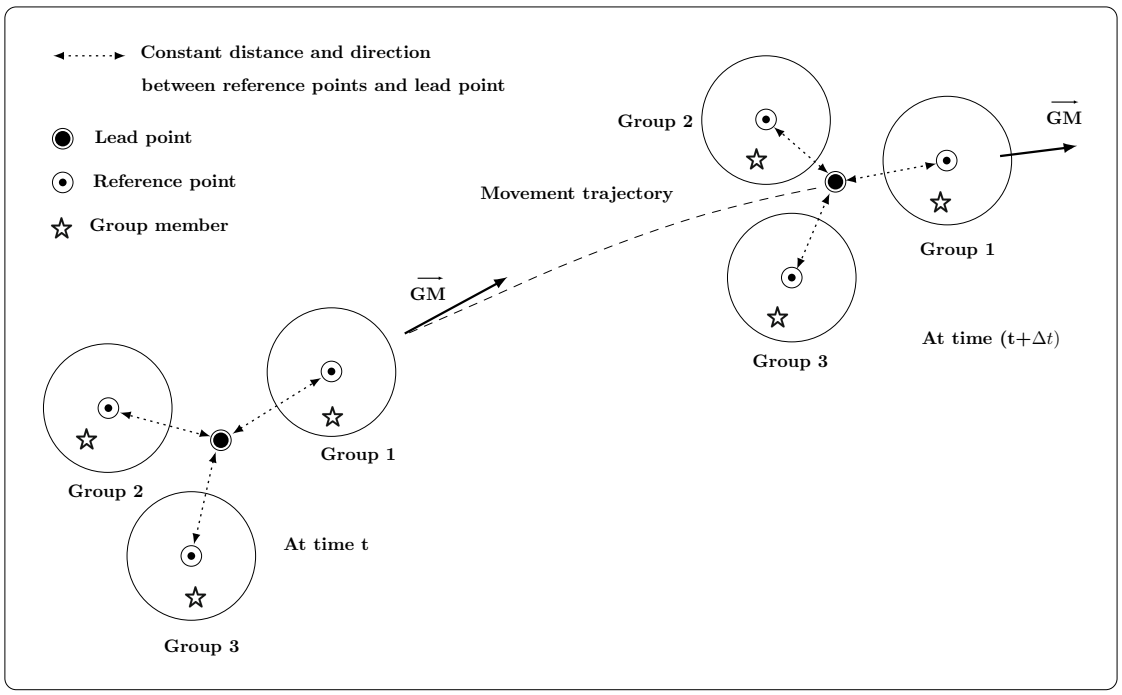

Figure 2.3 – Representation of mobile nodes movement in RPGM model.

2. **Reference Velocity Group Mobility (RVGM) :** The RVGM[20] model extends the RPGM model by proposing two velocity vectors : group velocity of the logical center or the lead point, and the local deviation velocity of each group member. In RVGM, the movement of a lead point is defined in terms of speed and direction, whereas the deviation level of a

group member from that of the lead point is defined only in terms of velocity. Thus, each group member movement is given by the sum of these two velocity vectors, whereas the movement of the lead point determines the entire group mobility in terms of both velocity and direction, respectively. Also, the group can either follows a predefined trajectory or either follows a common direction in the case the lead point direction is given based on the average velocity of all members within the group.

3. **PBGM models used with CGM Movement :** In this model, the movement of a group member is not only influenced by its lead point, but also by other group members
4. **Group Force Mobility Model (GFMM) :** The GFMM[21] takes into consideration the environmental changes such as collision avoidance and congestion in the group mobility based on exerting forces (repulsion and attraction) between nodes. As for humans, in the simulation, mobile nodes try to move together sharing the same goal, such as having the same destination location. To realize this point, mobile nodes try adapting their mobility to get similar speed and direction. In general, GFMM is similar to RVGM in that the velocity of a group member follows the velocity of its lead point with a small random deviation. GFMM not only focuses on group interaction and movement but also provides the capability to incorporate obstacles into a simulation area and gives the groups the ability to maneuver around them.
5. **Multi-Group Coordination Mobility (MGCM) [22] :** This model supports multiple groups, where all groups move in a coordinated manner towards a predefined target or a common object. In MGCM, a two-level group architecture is introduced, where each group has its lead point. One of the lead points is selected as the lead point of the entire group. The lead points of other groups are considered as members of the entire group's lead point. During simulation execution, the groups try to keep the same distance between each other by exerting a peer force, when the distance between groups is smaller than a predefined threshold. The velocity of each group's lead point is determined in terms of different velocity vectors, including the velocity vector of the entire group's lead point, the velocity vector of other groups' lead points and a small random deviation velocity vector. Also, MGCM supports repulsion behavior to avoid collision between groups and group members. This can make MGCM adaptable with scenarios that need collision avoidance, such as in tactical networks.

2.2.2.2 Region Based Group Mobility Models

In RBGM models, each group member may follow a path through a predefined or real-time dynamically determined sequence of regions or areas.

2.2.2.2.1 RBGM models used with IGM Movement

1. **Reference Region Group Mobility (RRGM) :** In this model [16], the movement of group members is provided based on a predefined path consisting of a sequence of referenced regions. The sequence of reference regions defines the group members to move from a source to a target destination. Each group first tries to identify a reference region in real-time that nodes will move towards it. Once a reference region is identified, group members start moving towards it and once they arrive, they select a location within the region. Within this region, group members continue moving according to the random waypoint model while waiting for the arrival of other nodes members. When all group members

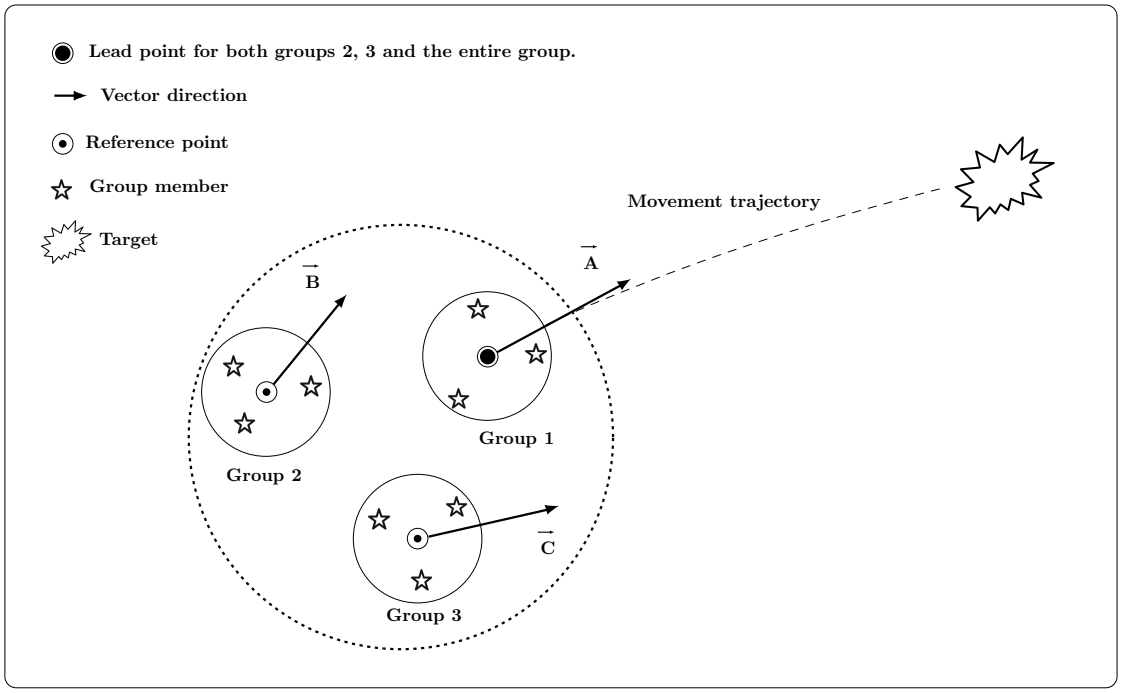

Figure 2.4 – Representation of mobile nodes movement in MGCM model.

have arrived at the reference region, they wait for a certain time interval considered as a pause time. After this step, group members will try to identify the next reference region. This process repeats until the target reference region is reached. Also, RRGM supports multiple targets for the same group, which makes group members split into small groups as each set of members will try to move towards a specific target. Moreover, small groups can merge into a larger group when they share the same target. These real mission-oriented behaviors make RRGM model more efficient to support more realistic scenarios.

2. **Virtual Track Group Mobility (VTGM) :** The VTGM model focuses on predefined paths called virtual tracks for each group member. Each track terminates at junction points known as switch stations. Each switch station is placed at a junction point that links between multiple virtual tracks, where each switch station has a certain track width. Members of the same group are distributed on the same track and move according to this track. Each member tries to move towards the next switch station in a way similar to the RWM. The movement of group members is confined within the same track ; however, the group can merge with other groups or split into smaller groups at switch stations. Also, VTGM supports free node mobility without constraints of the group or virtual tracks. VTGM is to be considered very useful for many practical scenarios depending on the applied constraints of node movements. In some cases, switch stations and virtual tracks can be treated as traffic intersections and road segments, respectively. Moreover, Groups' movements can be treated as buses with onboard passengers traveling along, whereas non-group nodes can represent pedestrians.

2.2.2.2.2 RBGM models used with CGM Movement

1. **Community Based Mobility (CMM)) :** The CMM model is based on social network theory, where group members have strong relationships related to their social environment and they share social links with each other. Each member has a value ranging from 0 to 1

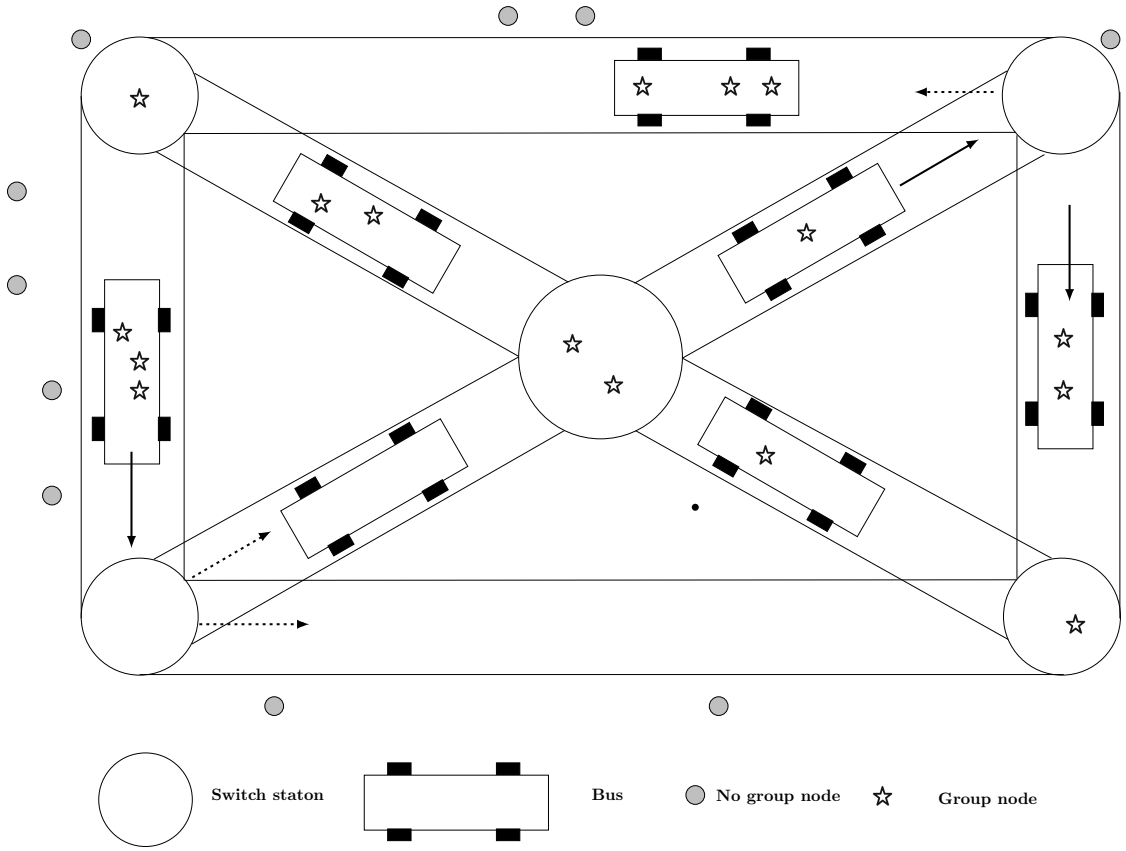

Figure 2.5 – Representation of mobile nodes movement in VTGM model.

(low to high) used to represent the degree of social link with another member. An interaction matrix (IM) is used to store all social link degree of social interaction between any two members. The IM matrix will allow us to identify a highly connected set of members which will be grouped to form a group membership. This means that each group member will select a location within a community region based on its level of social attraction. The social level attractively excreted by a community region allows a group member to choose the next location based on the average strength of the social links between it and members of that community. Once a location is chosen, the member will move towards that location using any mobility model. This process repeats until the group members reach the target location.

2.3 Contribution 1 : Modeling and studying vehicular traffic using Cellular Automata

Improving the traffic flow in a given network of streets is among the main objectives of transportation systems. However, transportation systems suffer from traffic congestion which is becoming one of the biggest problems found in urban environments [15]. To understand the traffic congestion phenomenon, scientists have carried out many studies based on different models and methods. The CA model developed by NaSch [23] is one of the efficient models for traffic flow problems.

Traffic flow is governed by several factors, among them drivers' behavior (e.g., imperfect driving styles, slower cars and car accidents) which play an important role in the formation of traffic jams within the transportation system, especially when it is combined with the increase

in car density (for a review, see [24, 25]). Indeed, when the density of cars increases, a phase transition from free flow phase to congestion phase occurs. In the free-flow phase, cars move close to the speed limit, and an increase in density leads to an increase in traffic flow. However, the congested phase is characterized by a negative linear relationship between traffic flow and density. It has been shown that, in the congested phase, the drivers' behavior has a major effect on the spatial distribution of vehicles relative to each other over the road [26, 27].

The modern roundabout is a type of intersection with no traffic lights. It is a circular intersection with design features that offer benefits in terms of circulation safety, delays and capacity. It was first developed in the United Kingdom and now is widely used in most countries. Drivers approaching a roundabout must reduce their speeds and look for potential conflicts with vehicles already in the circle. Many technical reports stated that the average accident risk at roundabouts has found important reductions in crashes compared to other conventional crossroads or T-junction, with or without traffic signals [28–30]. However, car accidents inside roundabouts are one of the most frequent contributing factors to jam formation. Among the reasons for car accidents are the high velocity and the violation of some safety conditions related to priority rules. Despite the demonstrated safety benefits of roundabouts, some crashes still occur. An Institute study of crashes at 38 roundabouts in Maryland found that collisions occurred more frequently at entrances to roundabouts than within the circulatory roadway or at exits [31]. The researchers concluded that unsafe speeds were an important crash factor, since drivers may not have seen the roundabout in time to slow down sufficiently.

Several models have been proposed to study the characteristics of vehicular traffic flow at a roundabout based on Cellular Automata models. For example, investigation the characteristics of traffic at an isolated roundabout by using car-following models [32], or studying unsigned multi-lane urban roundabouts [33]. Cellular Automata can be a suitable tool to analyze traffic flow around a traffic roundabout by analyzing different transitions, including the transition between free-flowing and gridlock and bottleneck [34]. An exciting issue of using cellular automata is studying the probability of car accidents for various traffic scenarios [35–37].

Cellular automata models have been also used to study the probability of car accidents for various traffic scenarios [35–37]. The first CA model including dangerous situations have been proposed by Boccara *et al* [35]. In this context, the conditions for the occurrence of car accidents, based on the delayed reaction time of the successor car has been investigated in [36]. Moreover, the probability of entering/circulating car accidents occurring at a single-lane roundabout when the incoming vehicles ignore the priority rules was studied in [37].

The urban traffic, where traffic lights are installed to regulate traffic flow at intersections, has been well studied. In contrast, only a small number of studies have provided models for urban traffic with multiple roundabouts to significantly highlight the interactions between them. In this chapter, we introduce a two-dimensional CA model based on discrete events capable of simulating traffic in urban contexts with roundabouts. Figure 2.6 gives an illustration of our proposed structure of the urban environment. Our objective is to provide a study of the impact of turning movement based on using different turning probabilities and also are interested in the impact of geometric factors on the traffic flow such as the distance between roundabouts.

We consider a CA model described in the two-dimensional system with periodic boundary conditions. The underlying structure is a $L \times L$ cell grid, where L is the system size. All streets are two-way, with one lane in each direction [15]. The distance between each pair of roundabouts is configured with a parameter K (see Figure 2.7).

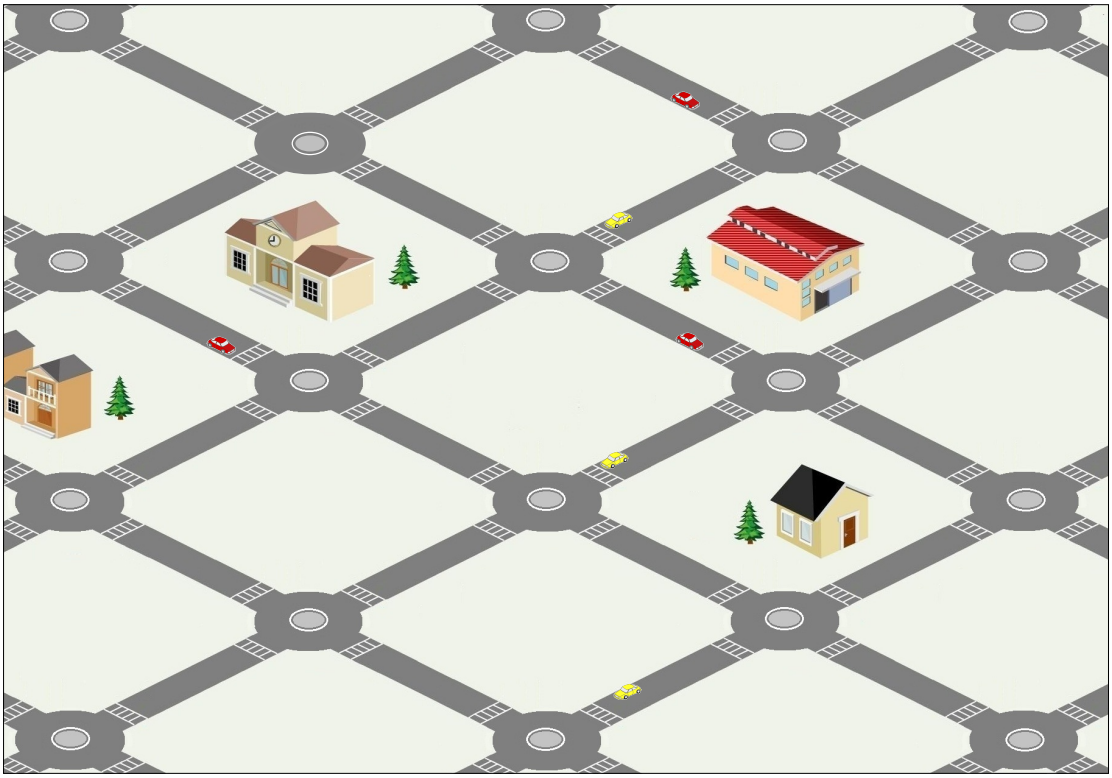

Figure 2.6 – The illustration of proposed structure of urban environment.

2.3.1 Mobility modelling in urban streets

Following the NaSch model, we modeled our urban streets as a set of cells where each cell can either be empty or occupied by exactly one vehicle (see Figure 2.7). The length of a single cell is set to $7.5m$. The vehicles move within each route with periodic boundary conditions without changing lane. In each simulation setup, vehicles are either eastbound or westbound or southbound or northbound. The global density is defined by $\rho = N/L^2$. Here the city size L is defined as $L = 2\sqrt{K * N_r}$, where N_r is the number of roundabouts in the city.

Algorithm 1 : Turning rules for roundabouts

```
1:  if the vehicle is on the entry leg then
2:      if ( thenγ > rand(0,1))
3:          p=0.5 // to make a right turn or left turn with equal probability.
4:          if (p > rand(0,1)) then
5:              the vehicle turn right, d2.
6:          else
7:              the vehicle turn left, d3.
8:          end if
9:      else
10:         the vehicle move strait, d1.
11:     end if
12: end if
```

At each discrete time step $t \longrightarrow t+1$, the system update is performed in parallel according to the following rules :

1. Acceleration outside roundabouts : $v_n(t+1) = min(v_n(t)+1, v_{max})$

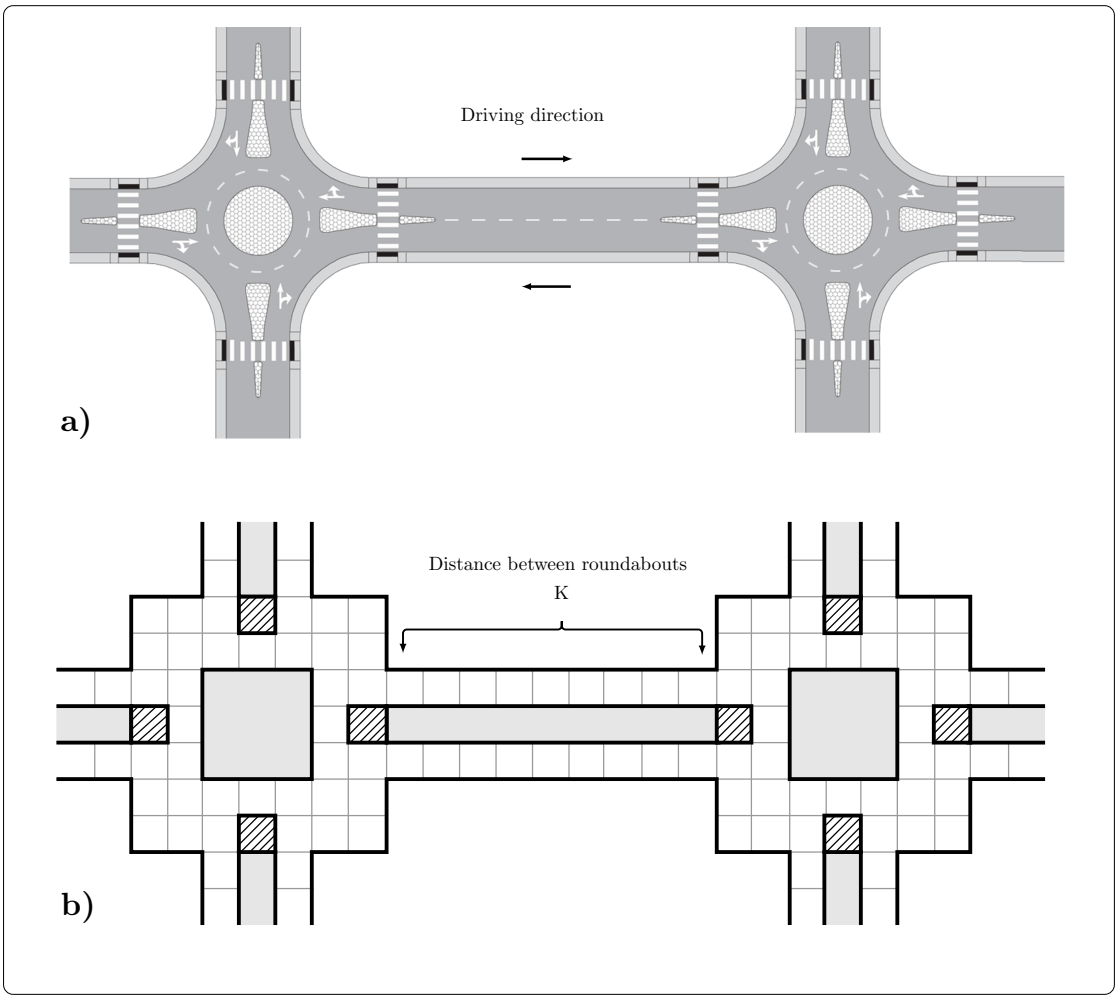

Figure 2.7 – Urban streets : (a) Realistic environment (b) CA model.

2. Deceleration : $v_n(t+1) = min(v_n(t), d_n(t))$
3. Randomization, braking : $v_n(t+1) = min(v_n(t) - 1, 0)$ with probability p.
4. Car motion : each vehicle will move according to its new velocity.

where $v_n(t)$ denotes the velocity of the vehicle. v_{max} denotes the maximum velocity in urban streets. $d_n(t)$ denotes the gap (*number of empty cells*) between the vehicle n and its immediate predecessor or between the vehicle n and the last cell in the lane (*cell that is right next to the roundabout*).

2.3.2 Mobility model and car accidents detection in roundabout

At each intersection between streets, we introduce a roundabout designed to allow drivers to change direction during their travel. Figure 2.8 illustrates the type of roundabout considered in this chapter. In addition, before entering the roundabout, each vehicle n is assigned a turning probability ($p_{turn}(n)$), which allows driver to choose his preferred driving direction (see Figure 2.9). Note that in the real world, the turning probability of different drivers may be distinct. For the sake of simplicity, we assume that all drivers have the same turning probability ($p_{turn}(n) = \gamma$). The turning behavior of vehicles at roundabouts is implemented by using the Algorithm 1 .

The majority of roundabouts were operated based on the offside priority rule, which implies that a vehicle V_A approaching a roundabout (on the entry leg) is usually required to give

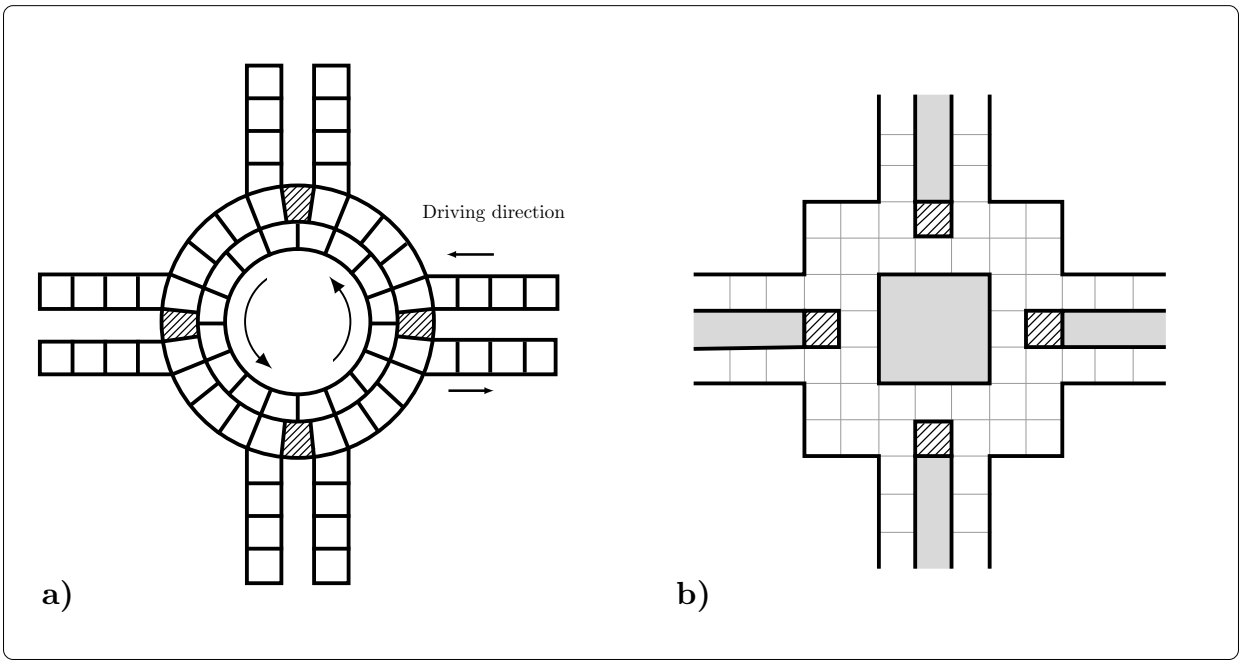

Figure 2.8 – Illustration of our proposed models of roundabout based on CA concept.

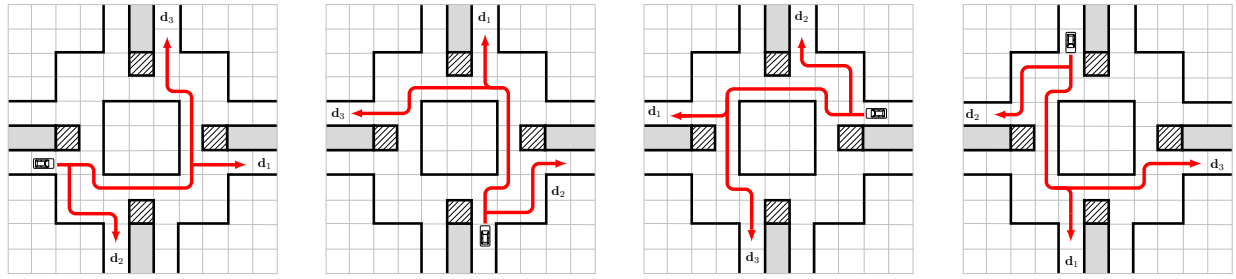

Figure 2.9 – Illustration of allowed driving directions for drivers entering the roundabout.

way to the traffic already in the roundabout. Another priority rule contemplated here concerns another vehicle V_A entering a roundabout and wishing to exit via the exit leg without using the circle of the roundabout. Let V_B be a circulating vehicle in the roundabout that V_A may encounter (see Figure 2.11). Now, we define the set of gaps used to control the entering vehicle V_A to roundabout based on offside priority rule. The gap $gap^1_A(t)$ (resp. $gap^1_B(t)$) represents the number of empty cells in front of the vehicle V_A (resp. V_B) in its travel path at time t.

For example in Figure 2.11 a, if the vehicle V_A turn right then $gap^1_A = gap'_a$ else $gap^1_A = gap_a$. Similarly, in Figure 2.11 b, if the vehicle V_B turn left then $gap^1_B = gap_d$ else $gap^1_B = gap'_d$. The gap $gap^2_A(t)$ (resp. $gap^2_B(t)$) represents the number of empty cells in front of the vehicle V_A (resp. V_B) and the collision cell at time t. Remember that there are two different cells where a conflict may occur; the first is at the entry leg while the second is on the exit leg of the roundabout. In the situation where a conflict occurred at the entry leg (see Figure 2.11 c), we have $gap^2_A = gap_a$ and $gap^2_B = gap_b$. However, at the exit leg (see Figure 2.11 d), we have $gap^2_A = gap_e$ and $gap^2_B = gap_f$. The offside priority rule is implemented by using the Algorithm 2 . So, if the speed of V_A is large enough then the algorithm must be executed (line 1). The condition in line 2 means that when V_B is far away from the cell of the collision, V_A enters safely to the roundabout. If not, V_A will move to just behind the cell of collision (line 6). On the other hand, it is believed that roundabouts are very important for the limitation of traffic jams,

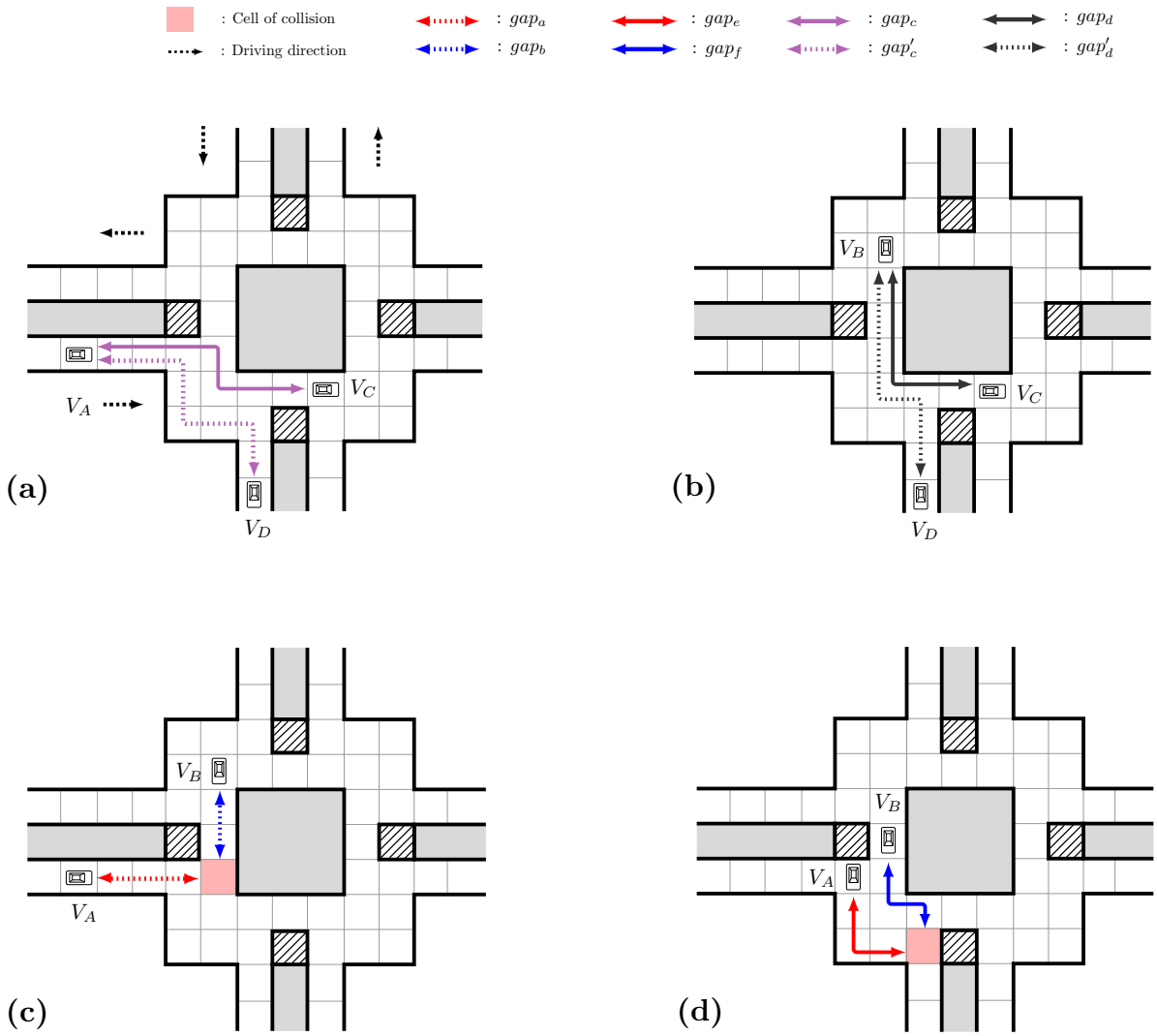

Figure 2.10 – Illustration of different gaps used to manage priority between entering vehicles and circulating vehicles and to determine car accidents at entry and exit legs of roundabout.

the reduction of accidents and contribute to slow down speeding cars [38]. Nevertheless, roundabouts suffer from the occurrence of car accidents when entering vehicles violate the priority rules. The violation of safety conditions is mainly related to the inability to accurately estimate the available gap, a lack of attention concerning the offside priority rule or the long reaction time τ of the driver. The conditions of the occurrence of these accidents are defined as shown in Algorithm 3 .

2.3.2.1 Performance Metrics

Here, several performance metrics are developed to assess our urban traffic system behavior. We monitor the impact of cars' density ρ and turning probability γ on traffic flow, accident probability and the average waiting time. Similarly, we will investigate the impact of the urban geometric characteristics by varying the distance between roundabouts K, while keeping fixed the number of roundabouts N_r in the urban city.

1. **Average velocity :** We define the average velocity of vehicles as the sum velocities of all vehicles during the simulation time divided by time interval. The average velocity is then given as follows :

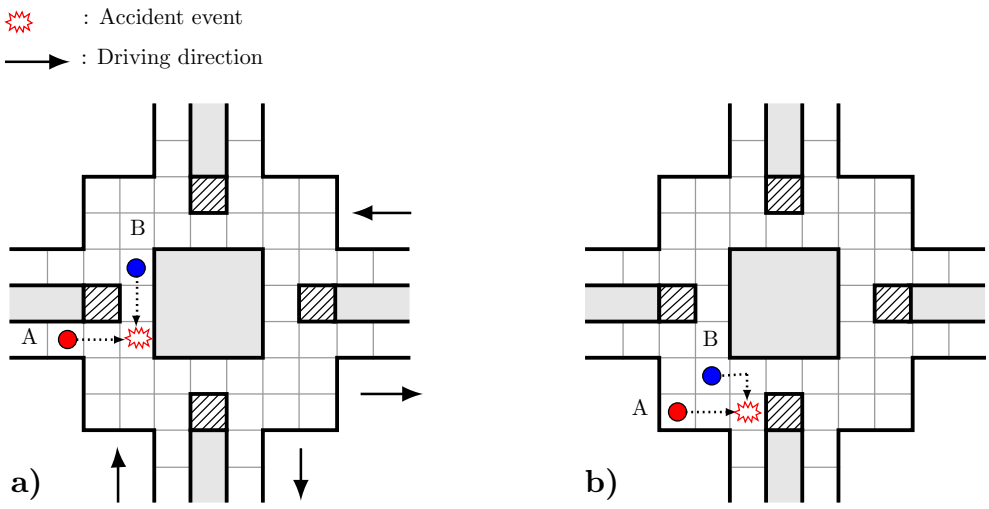

Figure 2.11 – Illustration of different gaps used to manage priority between entering vehicles and circulating vehicles and to determine car accidents at entry and exit legs of roundabout.

Algorithm 2 : Offside priority rule

if $(v_A(t) >= gap_A^2(t))$ **then**
  if $(gap_B^2(t) >= v_{max_{rp}})$ **then**
    $v_A(t+1) = min(v_A(t)+1, gap_A^1(t), v_{max_{rp}})$
    $v_B(t+1) = min(v_B(t)+1, v_{max_{rp}})$
  else
    $v_A(t+1) = gap_A^2(t)$
    $v_B(t+1) = min(v_A(t)+1, gap_B^1(t), v_{max_{rp}})$
  end if
end if

$$\textbf{Average velocity} = \sum_{i=1}^{N} \frac{v_i(t)}{N \times T} \tag{2.5}$$

where T is the time interval and N is the number of vehicles.

2. **Traffic flow :** We define the traffic flow as the car density ρ multiplied to the average velocity. The traffic flow in the city is then given as follows :

$$\textbf{Traffic flow} = \rho \times \sum_{i=1}^{N} \frac{v_i(t)}{N \times T} \tag{2.6}$$

3. **Accident probability :** We define the accident probability as the total number of accidents ($\mathbf{n}_{ac}$) committed by vehicles within the roundabout during the simulation time

Algorithm 3 : Detecting car accidents

if (conflict between V_A and V_B occurs in the roundabout) **then**
  $\widetilde{v}_B(t+1) = min(v_B(t)+1, gap_B^1(t), v_{max_{rp}})$
  if $(\tau v_A(t) > gap_A^2(t)$ **And** $\widetilde{v}_B(t+1) > gap_B^2(t)$ **And** $\beta > rand(0,1))$ **then**
    $n_{ac}++$
  end if
end if

divided by the number of vehicles and the simulation time. The accident probability is then given as follows :

$$\textbf{Accident probability} = \frac{n_{ac}}{\mathrm{N} \times \mathrm{T}_s} \tag{2.7}$$

4. **Average waiting time :** We define the waiting time as the time between the arrival time ($\mathbf{t}^i_{arr}$) of a vehicle i in the entry cell of a roundabout, and the moment of its departure ($\mathbf{t}^i_{dep}$) from this cell. Let $\mathbf{N}_c$ be the number of vehicles that have left the entry cells. The waiting time is then given as follows :

$$\textbf{Average waiting time} = \frac{\sum_{i=1}^{\mathrm{N}_c} (t^i_{dep} - t^i_{arr})}{\mathrm{N}_c} \tag{2.8}$$

2.3.3 Results and discussion

In this section, we present the simulation results for our indicators of system performance to investigate the relationship between the states of our transportation system and the model parameters. The model parameters which have been considered in this work are given in Table 3.2 . In this chapter, we are interested in the effect of the turning rate and the city structure on the capacity of urban traffic. The impact of the city size is provided by varying the distance K between roundabouts (Large cities correspond to high values of K).

Table 2.1 – Mobility pattern parameters used in the simulation.

Parameter	Symbol	Value
Roadmap size	$\mathrm{L} \times \mathrm{L}$	-
Simulation time	T_s	-
NaSch randomization probability	p	0
Turning rate	γ	-
Reaction time of driver	τ	1s
Car accident probability	β	0.3
Maximum velocity for vehicles outside the roundabout	v_{max}	3
Maximum velocity for vehicles inside the roundabout	$v_{max_{rp}}$	2
Number of roundabouts in the city	N_r	16
Roundabout size	R_s	36
Distance between roundabouts	K	-
Time step increment	dt	1s

First, we will analyze the different traffic states present in the transportation system. With increasing the density, we find that the traffic flow increases almost linearly and then begins to decrease beyond certain value of the density. This critical density ρ_c represents a transition between free flow and congested state.

As illustrated in Figure 2.12 , this congested state is unstable and it depends greatly on the simulation time. A detailed study of this behavior leads to the discovery that congested states change over time to gridlock state when $\gamma \neq 0$. In this case, the model presents a state transition from free low to gridlock at a critical car density ρ_c. Figure 2.13 shows a snapshot illustration of the two states present in the model when $\gamma = 0.30$. In free-flow state (see Figure 2.13 a) vehicles move freely while in gridlock state (see Figure 2.13 b), vehicles pile up around some roundabouts, forming a single immobile cluster with zero mean velocity. However, on the other hand,

for $\gamma = 0$, we observe from Figure 2.15 a,c that the average velocity is stable with time and decreases when the density is diminished, thus showing the existence of the congested state. However, if $\gamma \neq 0$, the average velocity is stable with time for low values of the density ; but as soon as this density exceeds ρ_c the average velocity decreases with time and vanishes at $t = t_{grid}$; showing that the system has reached the gridlocked state (see Figure 2.15 b,d).

Based on our simulations, we can see that the main cause of the gridlock is the conflict of circulation between vehicles who circulate in a roundabout and those who want to leave. In such situations, no one can move because everyone is in someone else's way (see Figure 2.14). More precisely, when several exits of a roundabout present simultaneously conflict of circulation, a local deadlock emerges. This situation allows other circulating vehicles to slow down and stop because there is not a free space in front of exiting vehicles. This leads to the propagation of a traffic jam wave towards other roads linked to this roundabout and thus causing a global gridlock.

To determine the critical density ρ_c, several simulations were carried out by examining the time evolution of the average velocity for different car densities. Figure 2.16 shows the obtained results for different values of γ and K. It is shown that the gridlocked state can take longer time (t_{grid}) to occur as the car density decreases, and t_{grid} will become infinity when approaching to the critical density. Our experimental simulations show that the model parameters have no obvious impact on the values of ρ_c. Moreover, since critical densities are found to be in the range of about 0.160 to 0.190, Based on a detailed analysis of the gridlocked state, it appears that the gridlock occurs due to right-turning vehicles which may be trapped in loops when the car density exceeds a critical car ρ_c. This means that a loop formation can occur when the car density becomes sufficient to form a loop of vehicles. This loop is governed by the rate of right-turning vehicles especially when they are located in the head of road segments and waiting to access the roundabout, but the destination lanes are not empty which leads to a local gridlock. This local gridlock can propagate toward other sides of the city causing a global gridlock. As the appearance of gridlock is mainly related to an increase in the rate of right-turning vehicles in the road segments (e.g., $\gamma > 0$) which leads to the formation of the square loop.

However, when $\gamma = 0$, the gridlock can occur, but with a much lower probability as compared with the occurrence of the square loop formed by the right-turning vehicles, and therefore the transition between free flow and gridlock can take much longer time. As the right-turning vehicles are absent, the gridlock can occur only due to an intersection between fully saturated road segments that lead to making obstacles in front of exiting vehicles from the circulating

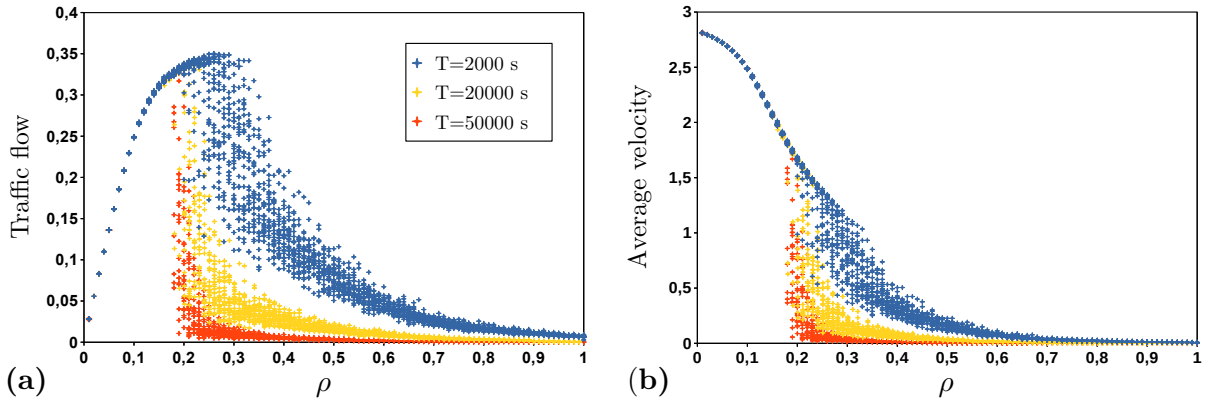

Figure 2.12 – Fundamental diagrams for different values of simulation time with parameters K = 40 and $\gamma = 0.3$. Each point represents one simulation run result and for each density we plot 30 points. (a) Traffic flow diagram (b) Mean velocity diagram.

ring of the roundabout. We limited our results to ($\gamma = 0.3$) because the detection of gridlock can take much long time (e.g., several days and months). But, when the density increases enough, it's possible to have a gridlock quickly as illustrated in (see Figure 2.13 c) for ($\rho = 0.3$). Indeed,

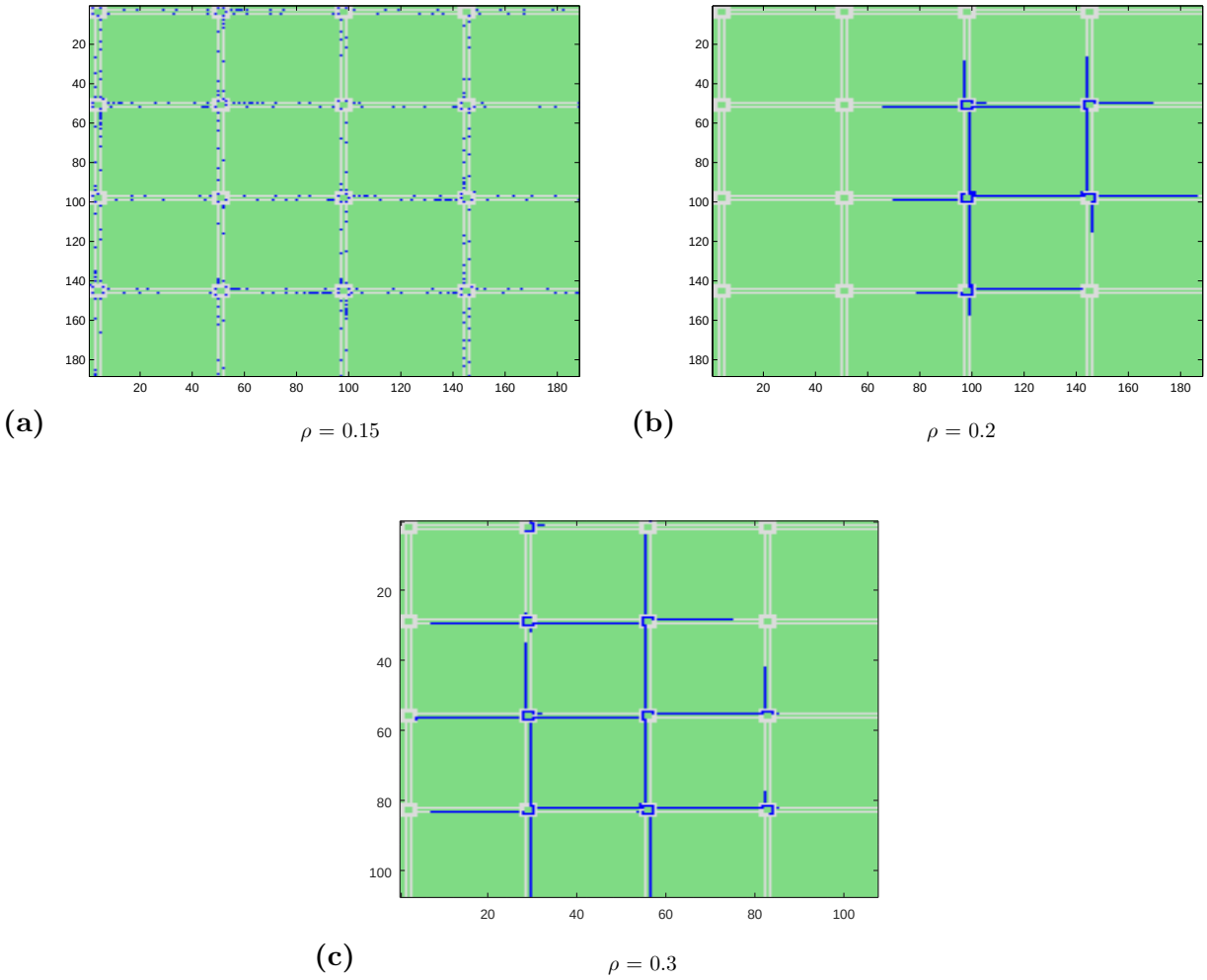

Figure 2.13 – Snapshot illustration of traffic states with parameters K = 40 and $v_{max} = 3$. (a) $\rho = 0.15$ and $\gamma = 0.3$, (b) $\rho = 0.2$ and $\gamma = 0.3$, and (c) $\rho = 0.3$ and $\gamma = 0$.

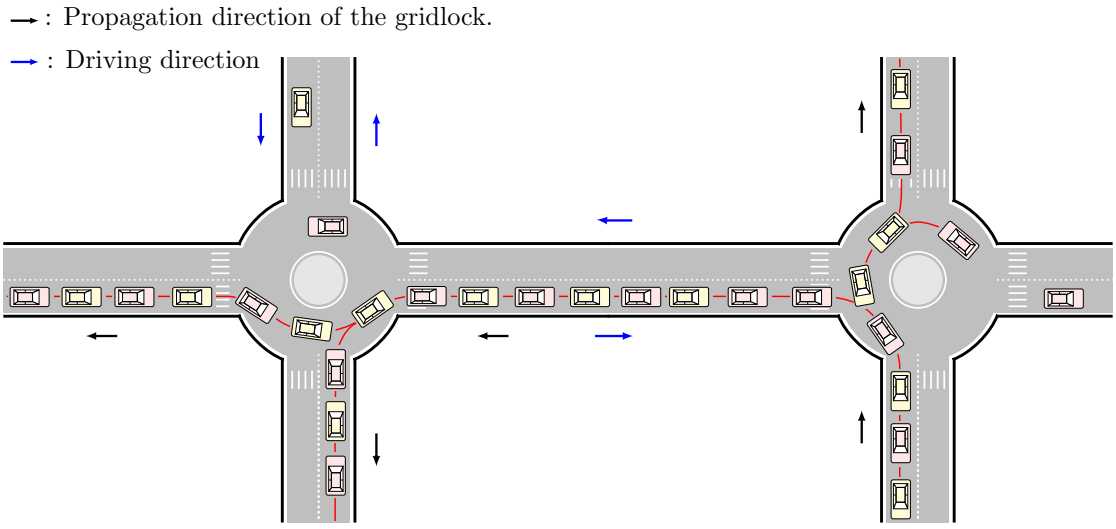

Figure 2.14 – Snapshot illustration of gridlock at roundabout.

we found that critical car density can be given as follows :

$$\rho_c = \frac{4 \times (K + R_s)}{32 \times K} \tag{2.9}$$

Moreover, since critical densities are found to be in the range of about 0.160 to 0.190, we limit our simulations and analysis up to the density of 0.160.

We begin our investigation by examining the impact of the turning rate on our traffic system. Figure 2.17 shows the characteristics of traffic flow, average velocity, car accident and waiting time as a function of the density for different values of the turning probability γ. As plotted on Figure 2.17 a, the traffic flow versus the density reproduces the free flow state observed in real traffic flow, regardless of the value of γ. In this state, the traffic flow increases almost linearly with ρ because almost all the vehicles move with their maximum speed $v = v_{free}$, due to the availability of large headways occurring in the traffic stream.

Furthermore, it is shown that γ has no visible effect on the traffic flow and the average velocity for low car densities. As the car density increases ($\rho > 0.1$), the turning movement starts to affect the transportation system. It is shown that both traffic flow and average velocity increase with increasing γ, in accordance with the results of the model considered in [39]. This can be explained by the fact that under high values of γ, the number of right-turning movements is higher and so several exit possibilities will be available for rotating vehicles. These exciting vehicles create opportunities for other entering vehicles, and therefore new gaps will be created inside roundabouts. Figure 2.17 c shows the car accident probability for different values of γ, as a function of car density. In this part, we study the causes of car accidents at roundabouts, without taking into account their impacts on the traffic flow. This means that the car accident does not happen, but only that we monitor the car accident probability without

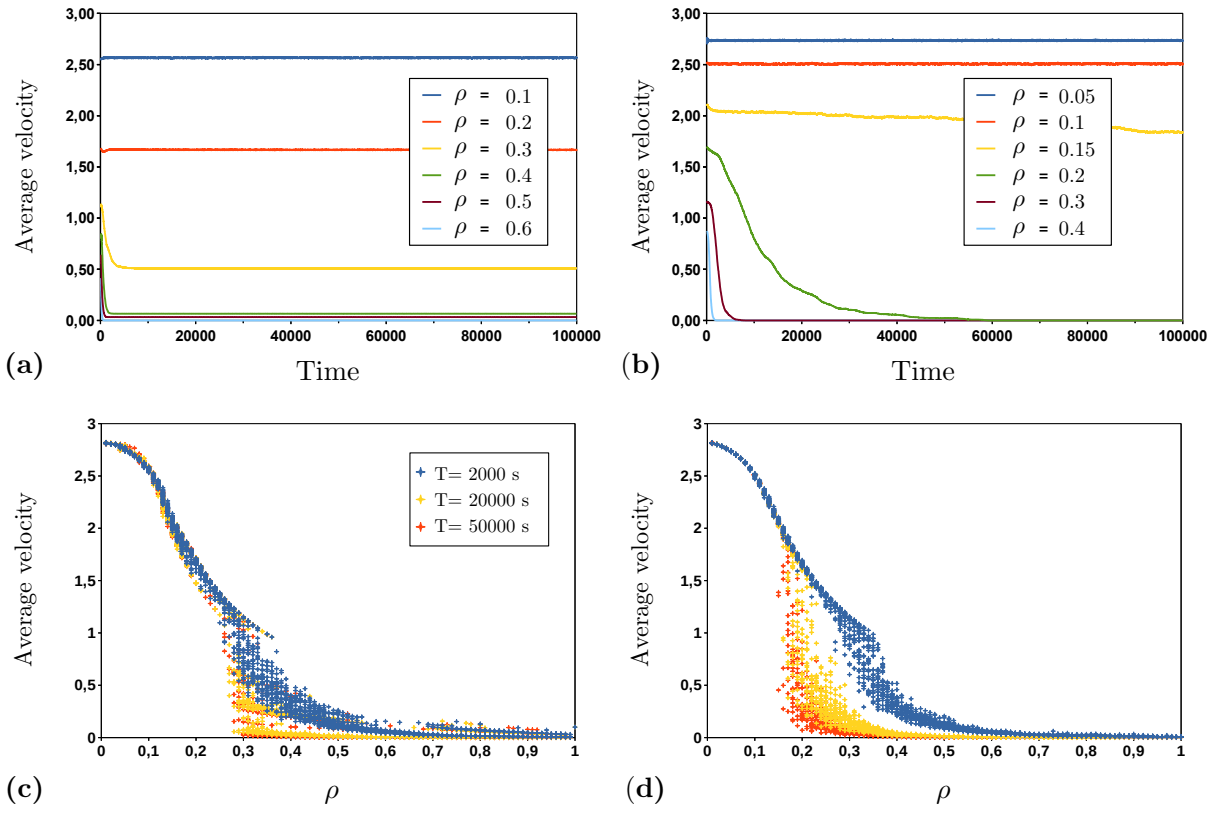

Figure 2.15 – Evolution of the average velocity for different car densities and simulation times with parameters K = 40 and γ = 0.3. (a) and (c) : γ = 0 ; (b) and (d) : γ = 0.05.

affecting the traffic flow. We observe that unlike accidents in highways, which usually do not occur until the car density exceeds some critical value [36], accidents at roundabouts can exist even if the density is very low. Indeed, at low densities, vehicles access roundabouts at maximal speed and the probability to collide with other circulating vehicles will be considerable. Moreover, with increasing density, the car accident rate increases until it reaches a maximum and then decreases with further density. It can be observed that the higher the turning rate, the more frequent the accidents at roundabouts. Indeed, with higher values of γ, the traffic system creates more opportunities for entering vehicles and, as a result, these vehicles access the roundabouts with relatively high speeds, which increases the risk of collisions with rotating vehicles. On the other hand, for a given value of γ, the waiting time increases as the density increases due to the excessive number of vehicles at roundabouts (see Figure 2.17 d). Moreover, at fixed density, the waiting time decreases with increasing γ. Once again, this is the result of the fluidity of traffic caused by an increase of γ.

To get a better understanding of the effect of urban network structure on the traffic dynamics, the plots of traffic flow, car accident probability, average velocity and waiting time against

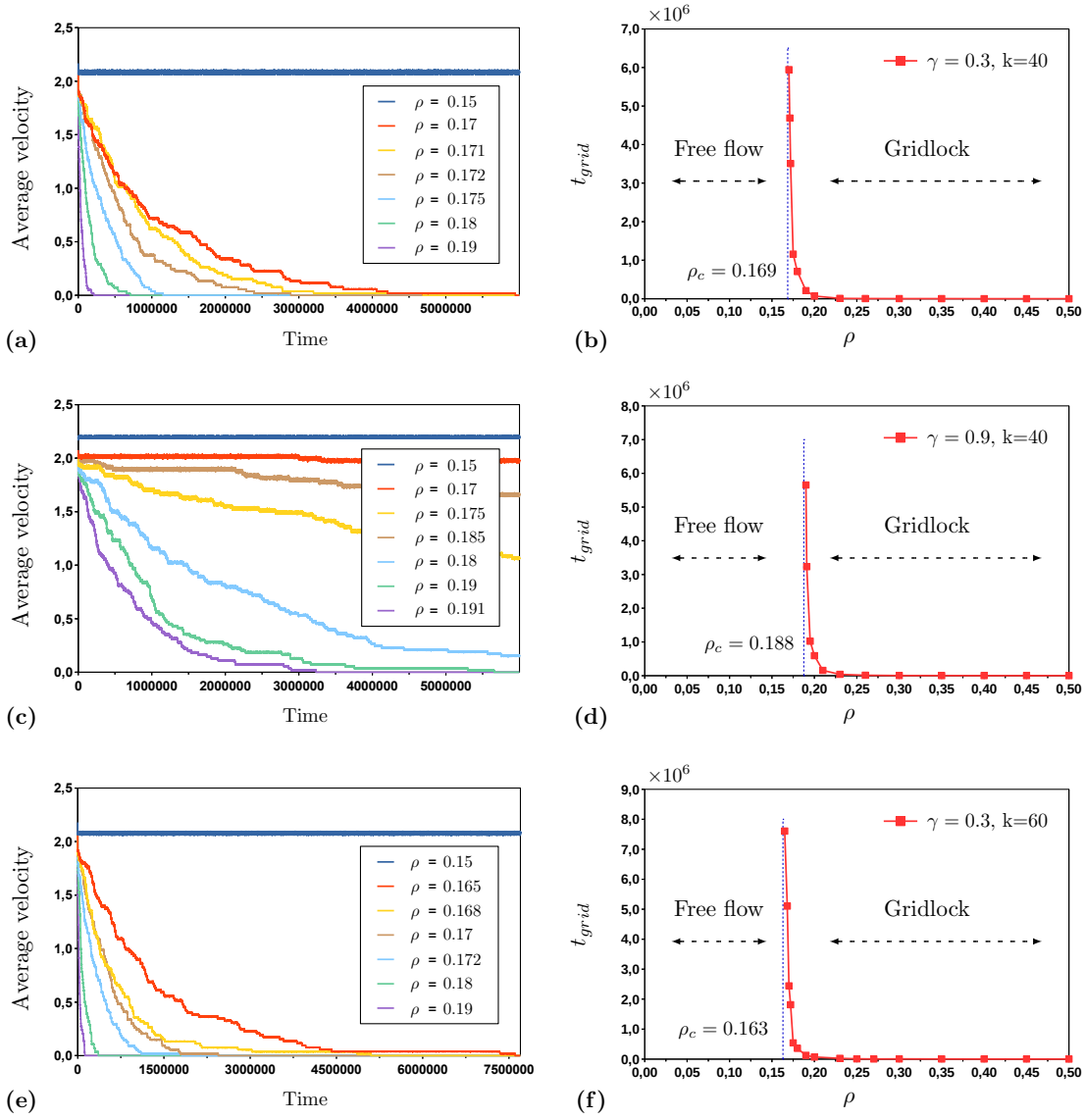

Figure 2.16 – Illustration of the transition between free flow and gridlock for different values of γ and K. (a) and (b) : γ = 0.3 and K = 40 ; (c) and (d) : γ = 0.9 and K = 40 ; (e) and (f) : γ = 0.3 and K = 60.

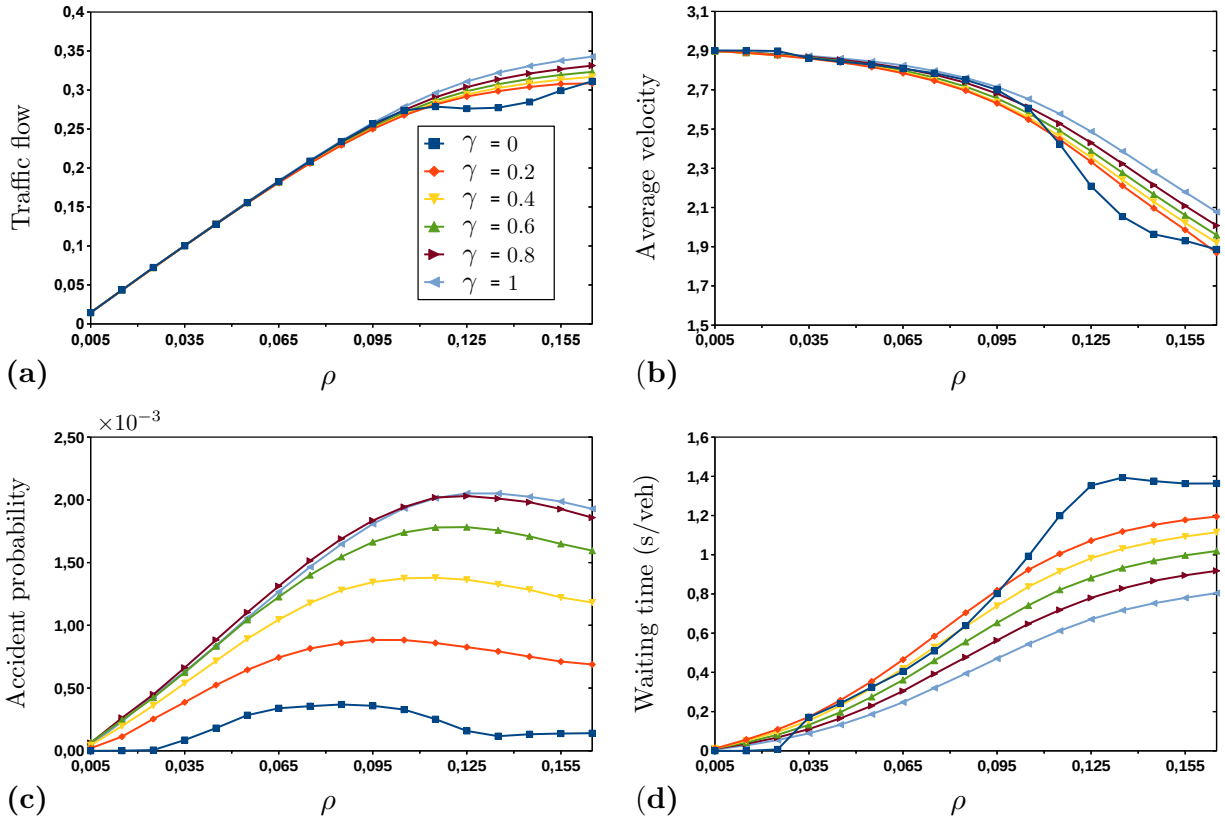

Figure 2.17 – Effect of increasing the turning probability γ with K = 80.

the density for varying values of K are shown in Figure 2.18 . Note that, when we vary K, the number of roundabouts present in the urban structure remains fixed. Figure 2.18 a,b show that, as the distance between roundabouts K decreases, the traffic flow and the average velocity decrease significantly. This can be explained by the fact that in the case of low values of K (small cities), vehicles can reach the roundabouts quickly and therefore they are forced to either slow down or stop to avoid collisions with other circulating vehicles. This affects significantly the traffic flow and imposes a speed reduction of the vehicles every time they want to access the roundabouts (see Figure 2.18 b). From the obtained curves of Figure 2.18 c, it is clear that, at fixed car density, the high rate of car accidents corresponds to low values of K. As mentioned before, the smaller the distance between two successive roundabouts, the more quickly vehicles reach the roundabouts. Therefore, during one simulation period, the frequency of violation of the safety conditions will become higher. Furthermore, for a given density, the waiting time increases with increasing K. To understand this phenomenon, it is necessary to remember that the number of roundabouts remains fixed when K is increased. Moreover, for a fixed density, the increase in K automatically leads to an increase in the number of vehicles ($\rho = N/(4 * N_r * K)$). As a result, the traffic capacity of roundabouts is particularly limited if the number of vehicles exceeds some limit. This will result in many stops in the entry legs and thus the average waiting time becomes more important.

Finally, our results can be summarized as follows : **1.** Urban traffic without turning behavior exhibits a transition from free flow to the congested state as the density exceeds a critical density of ρ_c. **2.** The principal cause of the appearance of gridlock is the turning movement of vehicles. **3.** Flow, accidents and waiting time are influenced by the turning rate as well as by the geometry of the urban city : - A high turning rate can lead to an increase in the urban traffic capacity, but also it can be a factor that increases the risk of an accident. - Urban traffic is

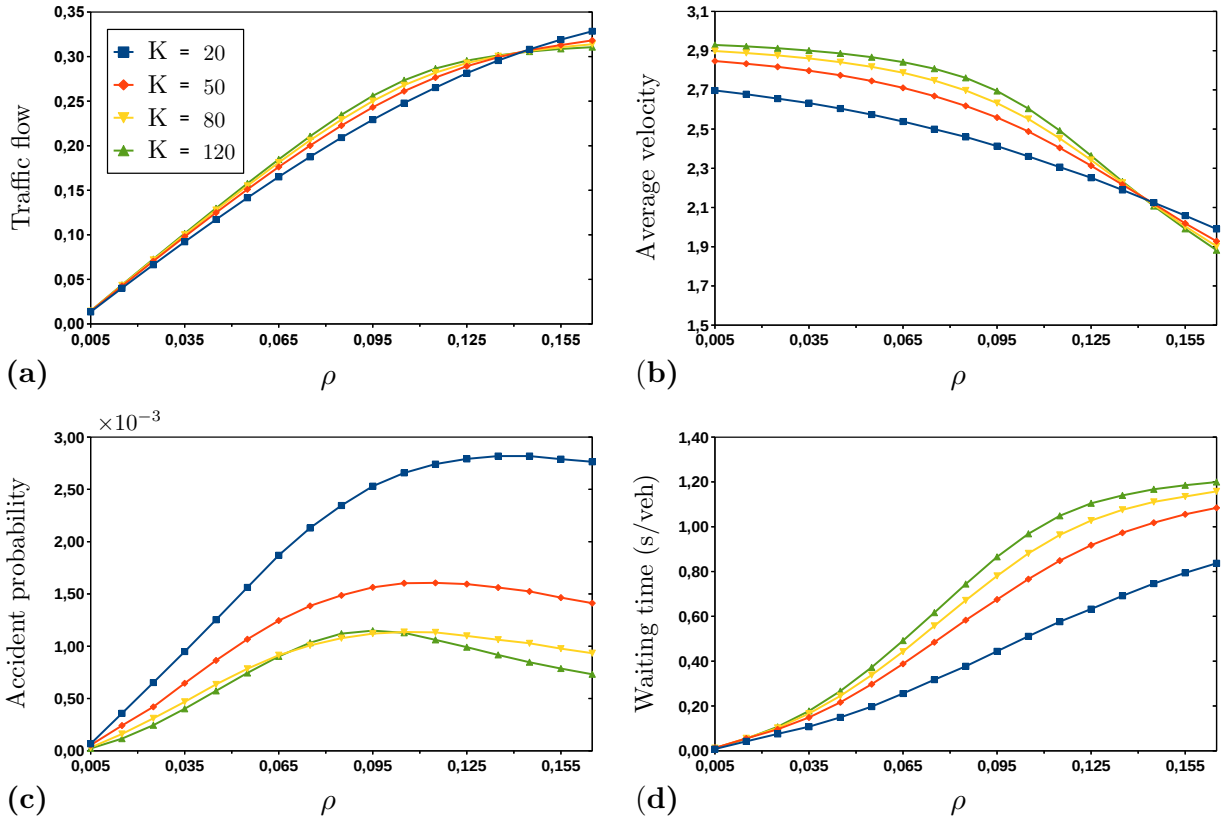

Figure 2.18 – Effect of increasing the distance between roundabouts K with $\gamma = 0.3$. The city size L^2 depends on the value of K : $L^2 = 7200$ for K = 50, $L^2 = 5760$ for K = 40, $L^2 = 4320$ for K = 30 and $L^2 = 2880$ for K = 20.

significantly better in large cities than in small ones. On the other hand, we have shown that ρ_c varies very little when we vary the model parameters ($0.160 < \rho_c < 0.190$). Then, it would be very interesting to implement intelligent strategies to increase ρ_c. This idea is under study and will be considered in future work.

2.4 Contribution 2 : Studying Agents' Heterogeneity with Group Mobility

In this contribution, we study the collective motion exhibited by some groups in nature (e.g., human and animal groups) and its impact on decisions making and leadership emergence within the groups. The existence of heterogeneity inside the group (e.g., differences in physiology, energetic state, social status) plays an important role in determining the dynamical equilibrium of such systems [40, 41]. Also, other factors can be responsible on the heterogeneity such as binary mixtures [42, 43], presence of leaders [44] and agents with different velocities [45]. This means that an expected hierarchical organization will arise for such a group when the interaction is not the same for all individuals [46]. In some cases, heterogeneity can allow the appearance of different phase transitions with a different rate within the group depending on the degree of heterogeneity [47]. In other cases, introducing heterogeneity may alter the nature of the suffered phase transition or even its universality class [48, 49].

In this chapter, we analyze and investigate the leadership aspect within a group of heterogeneous agents in terms of spatial knowledge, where a proportion of the individuals are given

information about a preferred direction (e.g., food location or a known destination), whereas other members are naive and have no information about any particular direction. For this purpose, we consider several performance metrics of interest, such as polarization, group elongation, group movement accuracy and crossed distance by the agents' group.

2.4.1 Modeling of agents mobility within the group

This section describes the considered flock mobility model specifically designed for governing the dynamics of agents in the simulation area. It illustrates how autonomous agents can make different interactions based on a superposition of some simple rules that define different interaction behaviors between each other, and where agents carry out their tasks collectively to contribute to a common goal (e.g., destination or location of the enemy). Accordingly, each agent can make interaction with other agents in its neighborhood-based on three basic rules [50–52].

1. Cohesion : An attempt to stay close to each other.
2. Separation : Behavior that avoids collisions by causing an agent to steer away from all of its neighbors.
3. Alignment : Behavior that causes a particular agent to line up with soldiers close by.

In our model, we consider N agents that move at a constant speed of v_0 units per second with periodic boundary conditions. Each agent is characterized by his location $\mathbf{c}_i(t)$ and velocity $\mathbf{v}_i(t) = v_0 \times \mathbf{d}_i(t)$ of direction $\mathbf{d}_i(t)$ at time t.

2.4.1.1 Repulsion behavior

Each agent i attempts to maintain a minimum distance from neighbors within the repulsion zone, modeled as a circle, centered on the agent i with radius ρ. If n neighbors are present in this zone at time t, the direction of repulsion from neighbors is given as follows :

$$\mathbf{d}_i(t+\Delta t) = -\sum_{j\neq i}^{n} \frac{(\mathbf{X}_j - \mathbf{X}_i)}{|(\mathbf{X}_j - \mathbf{X}_i)|} \tag{2.10}$$

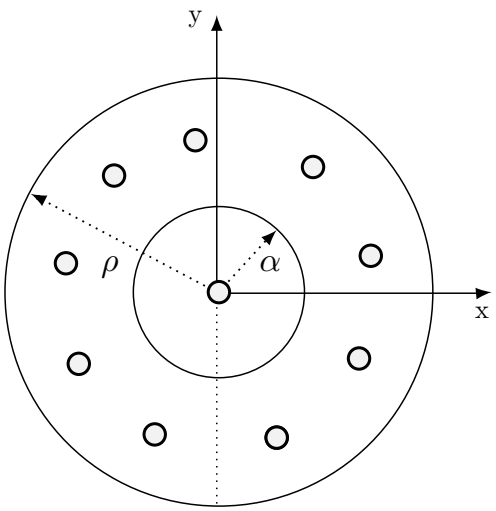

Figure 2.19 – Representation of an agent in the model with different behavioral zones : α is the zone of repulsion and ρ represent both the zone of orientation and the zone of attraction, respectively.

2.4.1.2 Orientation and attraction behavior

Both orientation and attraction behaviors are trigged when neighbors are not detected within the region of radius α. Then, the agent i will tend to become attracted towards, and aligned with, m neighbors within a local interaction range of radius between α and ρ (see Figure 2.19) :

$$\mathbf{d}_i(t+\Delta t) = \sum_{j=1}^{m} \frac{\mathbf{v}_j}{|\mathbf{v}_j|} + \sum_{j\neq i} \frac{(\mathbf{X}_j - \mathbf{X}_i)}{|(\mathbf{X}_j - \mathbf{X}_i)|} \tag{2.11}$$

Here $\mathbf{d}_i(t+\Delta t)$ is converted to the corresponding unit vector $\hat{\mathbf{d}}_i(t+\Delta t) = \mathbf{d}_i(t+\Delta t)/|\mathbf{d}_i(t+\Delta t)|$.

To incorporate the influence of informed group agents [53], a proportion P of the agents are given information about a preferred direction (simulated as a unit vector $\mathbf{g}$) representing the destination to a known resource or enemy location. All other individuals are naïve and are not aware that there is a preferred direction, nor do they know which agents of the group have this information. Then, the informed individuals balance the influence of their preferred direction towards a target $\mathbf{T}$ and their social interactions with weighting term ω, as follows :

$$\mathbf{d}'_i(t+\Delta t) = \frac{\hat{\mathbf{d}}_i(t+\Delta t) + \omega \mathbf{g}_i}{|\hat{\mathbf{d}}_i(t+\Delta t) + \omega \mathbf{g}_i|} \tag{2.12}$$

where $\mathbf{g}_i$ is the unit vector from the location point of agent i in the direction of a target $\mathbf{T}$ as follows :

$$\mathbf{g}_i = \frac{\mathbf{X}_i - \mathbf{T}}{|\mathbf{X}_i - \mathbf{T}|} \tag{2.13}$$

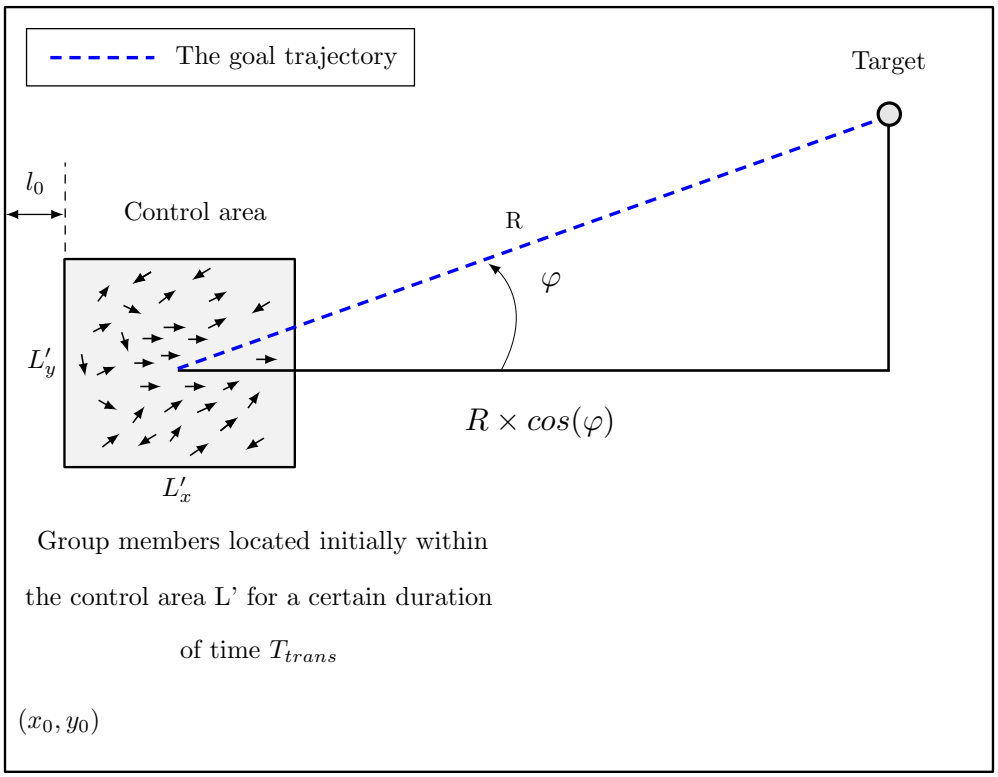

Figure 2.20 – Illustration of the considered scenarios, where agents group in the simulation area L of size ($L_x \times L_y$) and are located initially in the control area L' of size ($L'_x \times L'_y$). The gray ball represent the target.

Table 2.2 – Mobility pattern parameters used in the simulation.

Parameter	Symbol	Value
Simulation area	-	4200m×4200m
Simulation time	-	10000 (s)
Number of agents	N	100
Zone of repulsion	Z*o*R	10 m
Zone of orientation	Z*o*O	50 m
Zone of attraction	Z*o*A	250 m
Weighting term	ω	0.5
circle radius	R	2000
Initial velocity of nodes	v_0	1 (m/s)
Time step	dt	0.1 (s)

The target location $(T_{x,y})$ (see Figure 2.20) is given as follows :

$$T_{x,y} = (x_0 + l_0 + \frac{L'_x}{2} + R\cos(\varphi), y_0 + \frac{L_y}{2} + R\sin(\varphi)) \tag{2.14}$$

where L_x and L_y are the width and the high of simulation area, L'_x and L'_y are the width and the high of control area and α is the angle between the x-axis and target $T_{x,y}$ (see Figure 2.20).

In this chapter, our mobility model is based on the collective motion mobility model which illustrates how groups can make consensus decisions and effective leadership in biological systems [53].

To prevent agents from leaving the simulation area, we used reflective boundary-conditions, where an agent position is reflected with an angle equal to the incident angle.

After the above process has been performed for every member, all members can turn through an angle of, at most, $\theta\Delta t$ radians towards the desired direction $\hat{\mathbf{d}}_i(t+\Delta t)$ at time $(t+\Delta t)$ by the turning rate $\theta\Delta t$; if the angle between $v_i(t)$ and $\hat{\mathbf{d}}_i(t+\Delta t)$ is less than $\theta\Delta t$, they achieve alignment with their desired vector, $v_i(t+\Delta t) = \hat{\mathbf{d}}_i(t+\Delta t)$, otherwise they turn $\theta\Delta t$ towards it. If $n_{ic} \neq 0$, the agent will tend to become attracted towards the center of the simulation area. We apply this process at each ime step Δt, where each member is able to independently perform behavioural responses to maintain interactions with other members in its neighborhood.

2.4.1.3 Simulation Parameters

The simulation parameters which have been considered in this work are given in Table 3.2 :

2.4.1.4 Performance Metrics

Model performance metrics used in the simulation are given as follows :

1. **Polarization :** The polarization which describes the overall order of the agents' group is defined as the degree of alignment among agents. It increases with stronger interaction between the neighboring agents in the group [54]. The polarization of the group is then given as follows :

$$\boldsymbol{P}_{group}(t) = \frac{1}{N}\left|\sum_{i=1}^{N}\mathbf{v}_i(t)\right| \tag{2.15}$$

where N is the total number of agents.

2. **Accuracy :** The accuracy of the group is quantified as the angular deviation of group direction $g_d(t)$ around the preferred direction g. The accuracy of the group is then given as

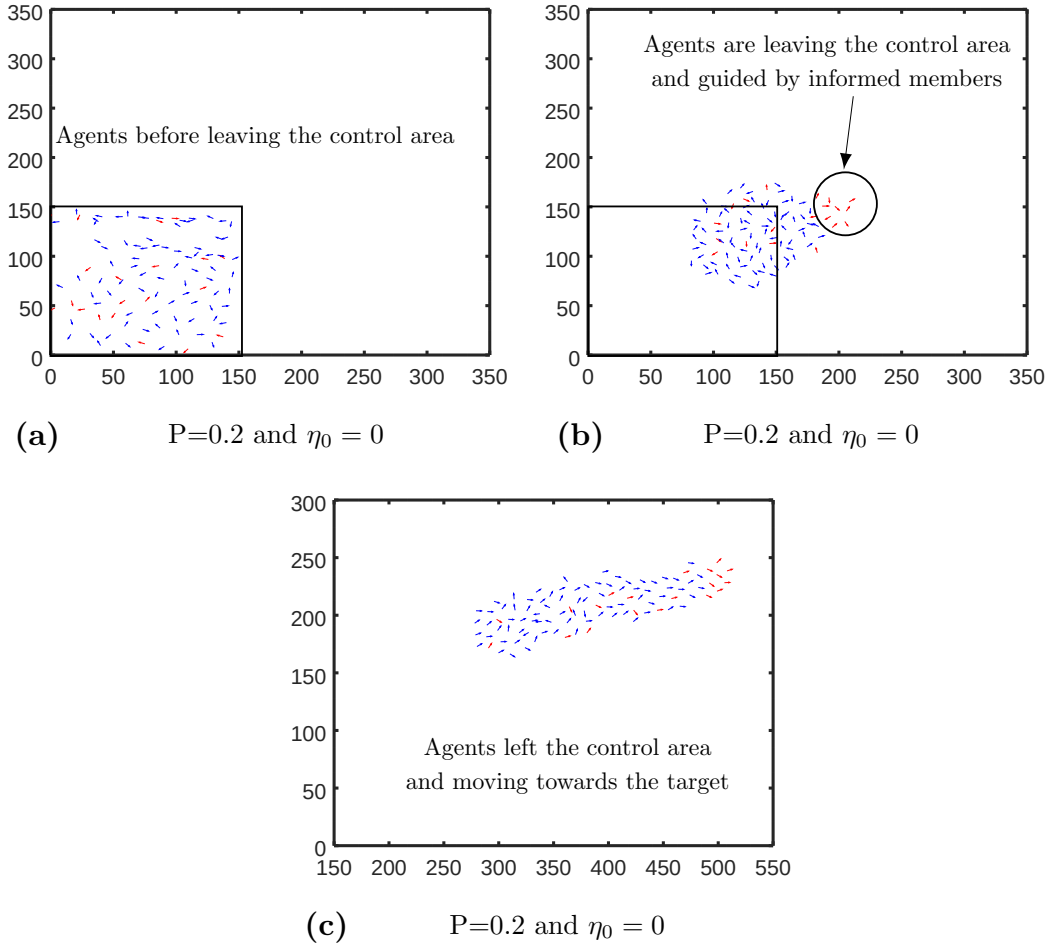

(a) P=0.2 and $\eta_0 = 0$ **(b)** P=0.2 and $\eta_0 = 0$

(c) P=0.2 and $\eta_0 = 0$

Figure 2.21 – Illustration of agents' group before and after exiting the control area with parameters P=0.2, $\phi = \pi/4$, R=1500m, $(L_x \times L_y) = 2500 \times 1500 m^2$. The red arrows represent informed agents, whereas blue arrows represent non-informed agents within the group.

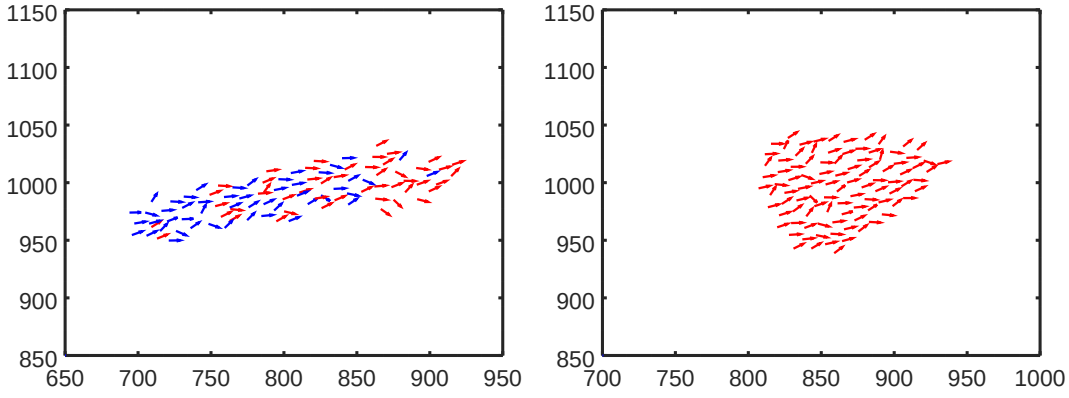

(a) P=0.5 **(b)** P=1

Figure 2.22 – Illustration of the agents' group with different percentages of informed agents P with parameters $\phi = \pi/4$, R=1500m, $(L_x \times L_y) = 2500 \times 1500 m^2$.

follows :

$$\boldsymbol{A}_{cc}(t) = \frac{\pi - |\psi(t)|}{\pi} \tag{2.16}$$

where $\psi(t)$ is the angular deviation between $g_d(t)$ and g at time t.

3. **Group elongation :** We define the group elongation by creating a bounding box around the group aligned with the direction of travel and calculating the ratio of the length of the axis aligned with the group direction, to that perpendicular to group direction. This value is 1 when both axes are identical, >1 as the group becomes more elongated in the direction of travel, and , <1 as it becomes elongated perpendicular to the direction of travel.

2.4.2 Results and discussion

We consider a group composed of N agents, where a proportion of informed individuals (P) are given information about the target T (see Figure 2.20). We recall that the parameter ω, allows informed individuals to balance the influence of their preferred direction and their social interactions. We perform extensive simulation experiments in order to analyze the impact of heterogeneity in terms of the level of knowledge (P) and the quality of information that each informed agent has about the target. To mimic real-world occurrences of various possible situations and their outcomes, we used three different distributions of ω including, two Gaussian distributions $\sim N = (0.3, 0.2), (0.4, 0.1)$ and an uniform distribution $\sim U = (0, 0.5)$. We compare all these distributions with that used by the Couzin in [53], where ω is considered fixed and equal to 0.5. This comparison is done in terms of a scenario, where information about the target T with a directional angle $\alpha = \frac{\pi}{4}$, is given to the informed agents.

In our simulations, we consider several performance metrics such as polarization, group elongation, accuracy and the crossed distance by the agents' group. These metrics are considered to figure out how informed members can impact the group dynamic, movement speed, and the group structure.

Figure 2.23 a shows that polarization increases sharply as soon as P takes a small value (Pc $\backsim$ 0.15). Beyond this value, the polarization takes approximately a constant value, reaching the maximal value of 1. The same observation can be seen from Figure 2.23 c-d where the accuracy and crossed distance are described in terms of P. This shows also that there is a strong correlation between the polarization and both the accuracy and the crossed distance. In Figure 2.23 b we show the group elongation descriptor, which is a measure that the group remains cohesive. The introduction of the group elongation is necessary to detect situations where the informed individuals leave the group. Interestingly, our results show that the group elongation descriptor is a good candidate for describing the agent's cohesion inside a mobile group. Indeed, the cohesion is as strong as P increases up to the critical value Pc$\backsim$0.15. Beyond this value, the cohesion strength decreases with increasing P. When P is great,all the agents are almost informed about the target and hence the repulsion interaction becomes the most dominant. In this situation, collective decision–making is not consensual, since the informed individuals fail to lead themselves along the informed orientation. Moreover, we figure out that, in contrast with the other descriptors, group elongation is more sensitive to random distributions of ω.

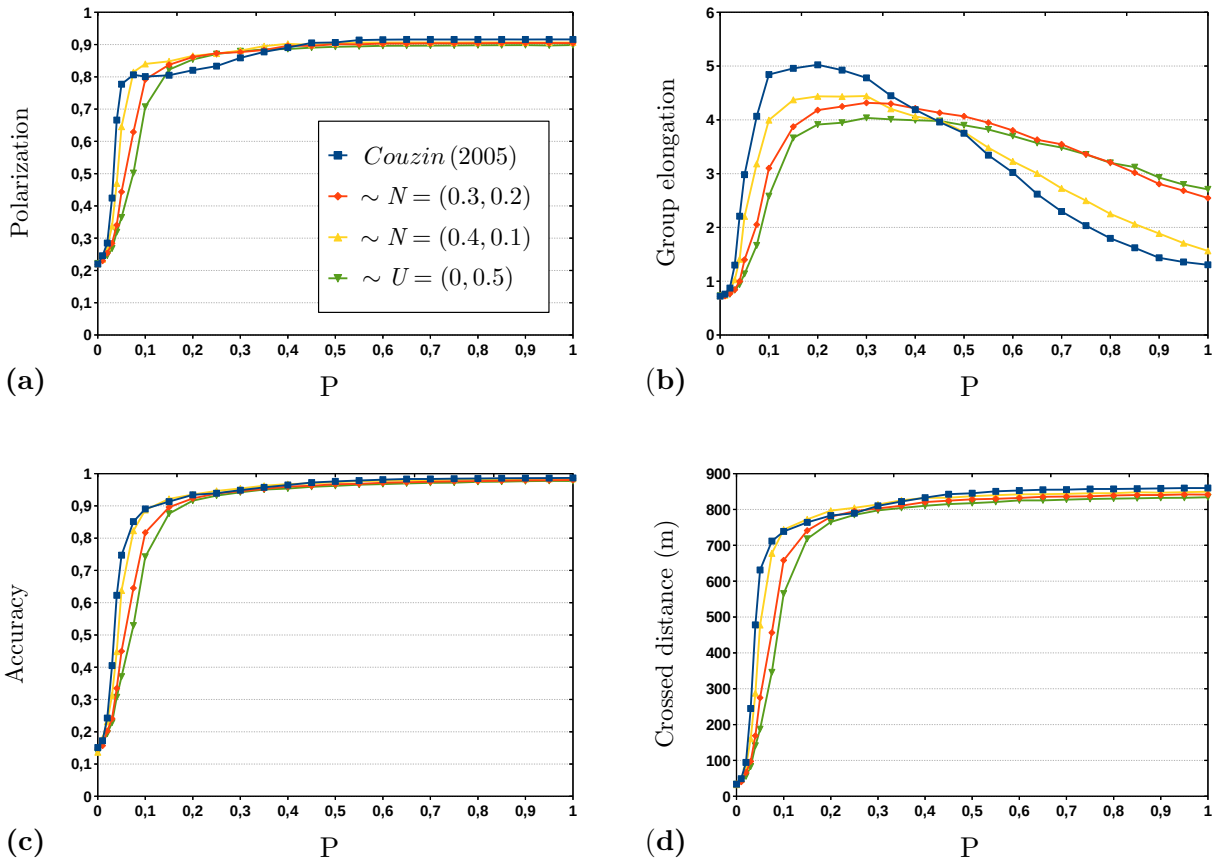

Figure 2.23 – Effect of increasing the proportion of informed agents under different distributions of ω in the case of scenario 1 with parameters $v_0 = 1$, $\phi = \frac{\pi}{4}$ and N= 100 : (a) Polarisation, (b) Group elongation, (c) Accuracy and (d) Crossed distance.

2.5 Conclusion

In this chapter, we have provided a fundamental review in the context of both microscopic traffic models and group mobility models. We have proposed two different mobility models in the context of vehicular traffic mobility and collective motion. For vehicular traffic system, we have considered a two-dimensional CA traffic model for studying the traffic flow and car accidents in a city with multiple roundabouts. Our results can be summarized as follows : 1. Urban traffic without turning behavior exhibits a transition from free flow to the congested state as the density exceeds a critical density of ρ_c. 2. The principal cause of the appearance of gridlock is the turning movement of vehicles. 3. Flow, accidents and waiting time are influenced by the turning rate as well as by the geometry of the urban city.

To give more insight and background in understanding the complex collective motion, we proposed a group mobility model based on a multi-agent system for studying the impact of heterogeneity within the agents' group cohesion. We concluded that a proportion of informed agents can bring cohesion inside the entire group to lead the non-informed agents along the target. However, a large proportion of informed agents may provide a non-consensual collective decision–making, due principally to repulsion interaction between informed agents.

The next chapter will deal with a general review of the most known tactical mobility models in the literature, including those related to operations in disaster areas, battlefield operations and area-based movement scenarios. Our attention will be oriented principally towards tactical mobility modeling and simulation of dismounted soldiers dynamic in the battlefield and

paying particular attention to some challenging problems encountered in tactical networks such as frequent topology change and wireless communication reliability. We will perform extensive simulation experiments of tactical networks in terms of several performance metrics. Also, we will highlight the impact of tactical mobility on energy consumption in WSNs.

Chapter 3

On the Simulation in Tactical Networks

« *The thing about quotes on the internet is that you can not confirm their validity* »

Abraham Lincoln

Contents

This chapter provides two main parts. Firstly, we review the most known tactical mobility models in the literature, including those related to operations in disaster areas, battlefield operations, and area-based movement scenarios. Secondly, we will provide a detailed presentation and validation of our proposed tactical mobility models related to different group movements and tactical scenarios based on ad hoc networks. Our proposed models include a tactical group mobility scenario, a battlefield scenario between two groups of soldiers and enemies, a tactical movement formation of the squad. Also, we introduce a detailed evaluation of a sensor network formed by autonomous agents to analyze the impact of Collective Motion on Sensor Network's Lifetime. The evaluation of our proposed scenarios is done in terms of several metrics according to the major constraints of tactical networks. The main objective in this chapter is trying to model different tactical scenarios as realistically as possible and to provide an efficient investigation of agents' dynamics of each scenario in terms of wireless communications reliability, topology change, and energy efficiency.

3.1 Introduction

Recently, countries have been interested in developing new skills and competencies based on new technologies of information and communication. The arrival of this revolution has facilitated cooperation and communications for tactical operations that represent cooperative tasks and a high level of movement coordination to complete the assigned mission as needed. The utilization of technologies is one of the major key elements of success of tactical operations to make easier the control of the area of interest. For example, the dismounted soldiers in a battlefield area would need to incorporate several new wireless technologies to exchange information in order to complete successfully the assigned missions, consisting of surveillance and/or tactical operations to prevent the intrusion of enemies [55]. This type of operation is usually done without preexisting communication infrastructure. The dismounted soldiers on the battlefield should cooperate with each other to complete their assigned mission. In other critical situations, dismounted soldiers need to perform sweep operations of houses or buildings, and may be divided into many battalions with each one having its proper mission e.g., searching and attacking the enemies during a sweep operation or escaping from an unexpected enemy attack.

3.2 Tactical mobility modeling

Tactical mobility modeling is considered to be the most important tool to perform various categories of tactical scenarios. The need for modeling of mobility is related to the fact that individuals can perform a wide variety of behaviors and movements depending on the situations encountered in the environment. In the context of wireless communications, the movements of agents have a direct impact on the tactical network. The evaluation test of the network performance during the execution of a tactical scenario in the real-world setting is often not feasible since the cost may be too high and sometimes it will be impossible to test it in the real world. For example, the deployment of soldiers on the battlefield in the presence of enemies cannot be tested for evaluation. Therefore, a simulation environment is very attractive for evaluating and studying the impact of soldiers' behaviors on the performance of the network and topology conditions during military operations.

3.3 Major encountered challenges in tactical networks

Here, we review the major encountered challenges in a tactical network where its network can passed through unstable states. These challenges are summarized in the following points :

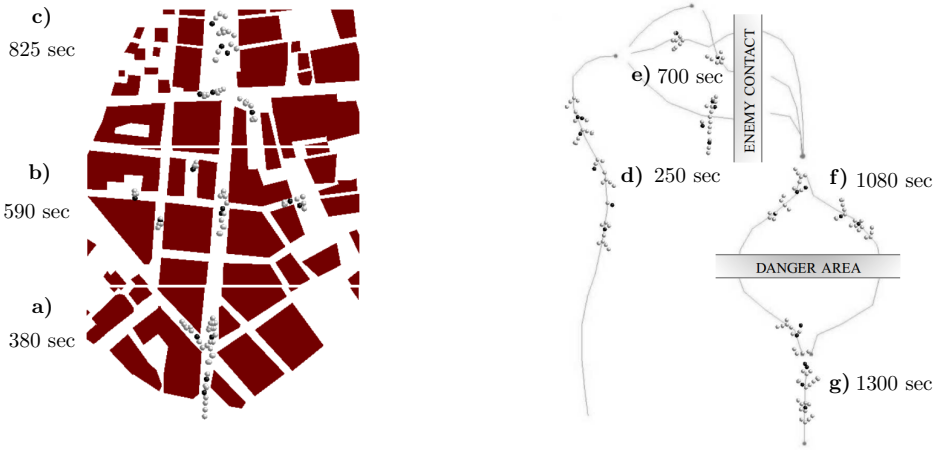

Platoon of soldiers tracing a city area

Platoon of soldiers traveling through hostile area

Figure 3.1 – Representation of Platoon model.

1. **Lack of centralized infrastructure :** The first encountered challenge for tactical networks is that this category of the network is not based on a centralized infrastructure. The network entities have to communicate in a distributed manner (end to-end or opportunistic communication) to ensure connectivity.
2. **Frequent topology change :** The network connectivity is worsened due to topology changes of wireless links driven by the unpredictable mobility of nodes within the network. Both the speed and the unpredictable behaviors of nodes can amplify the problem. Several methods have been proposed for link failure protection in ad hoc networks. We cite for example the method of [56] where a partition prediction and service replication on the server nodes are deployed. In [57], the authors introduce data replication at multiple nodes for dynamically deploying these nodes to disconnected partitions of the network. However, both data replication and topology information update undoubtedly increase memory and communication bandwidth overhead.
3. **Quality of Service and security :** Quality of service and security are also two important aspects to take into consideration when we need to carry critical information about missions or decisions, where the wireless communications may be vulnerable to cyber-attacks.
4. **Resource limitation :** Generally, the nodes that form the network have limited resources in terms of energy, processing capacity and memory, which may induce negative impacts on guaranteeing the delivery of messages. So, these nodes may behave selfishly (no-cooperatively) to preserve their resources for their benefit. Consequently, the communication protocols have to be efficient and well adapted to these limitations in order to maximize the lifetime of the network.

3.4 Tactical Mobility Models

3.4.1 Platoon of soldiers

We consider a model where a platoon of soldiers is moving for tracing a city area (scenario 1) or traveling through the hostile area in a battlefield (scenario 2). The movement of soldiers must take into account two main constraints, including spatial dependency and geographic constraints. During the movement in scenario 1, the platoon of soldiers may split up in multiple groups and regrouping afterwards. Moreover, when the platoon of soldiers is tracing a city area, the buildings are taken into account, either for soldier mobility, or either for the computation of radio signal propagation quality by considering the effects of obstacles (see Figure 3.1). For the scenario 2, the effects of obstacles are not taken into account in the simulation since the mobility of the soldiers in this scenario is performed in a hostile area and does not contain buildings.

3.4.2 Tactical scenario Model

This scenario describes a reconnaissance mission requiring special communication tools. The goal is to identify and secure a suspected biological weapons chemical factory for disarmament by United Nations weapons inspectors. The tactical scenario is operationalized in the narrative based on conventional warfare in future high-intensity and high-tech level conflicts. There is some realistic scenario which considered a less artificial approach instead of random movement for analysis of routing protocol performance. In this realistic scenario, catastrophe scenario is also there which focuses on the relatively slow and fast movement of the nodes. It could be considered for obstacles, group movements and tactical scenario (see Figure 3.2).

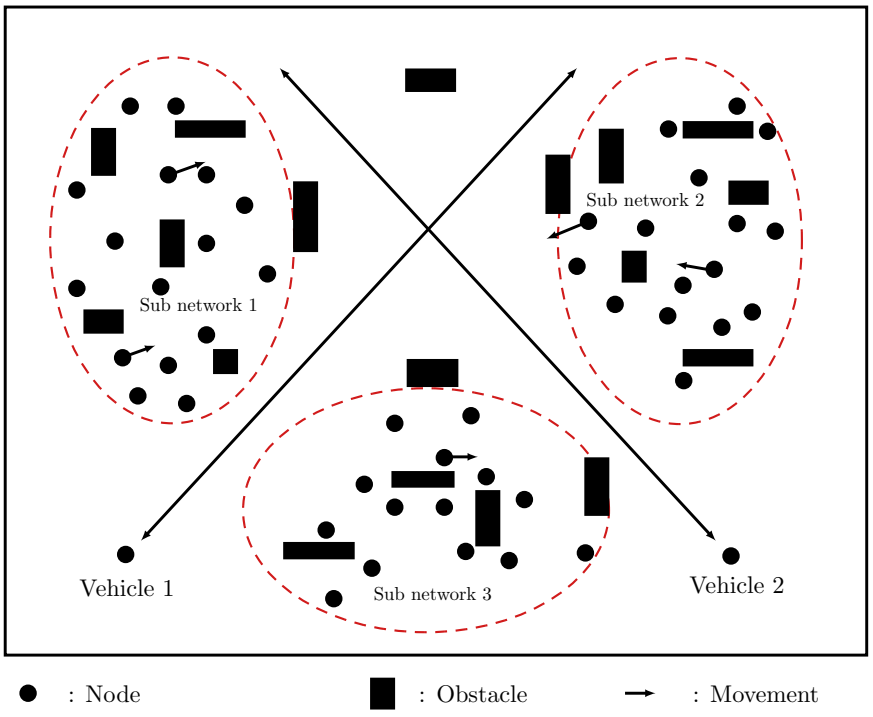

Figure 3.2 – Representation of Disaster area scenarios.

3.4.3 Disaster-area model

The purpose of this model is to realistically represent the movements in a disaster area scenario (see Figure 3.3). The disaster-area model is based on an analysis of tactical issues of civil protection. The model is a heterogeneous area-based, where areas are divided into polygonal tactical areas and each area uses its specific design of mobility. The movement in each area is realistically provided based on optimal paths selection witch support obstacles avoiding, dynamic joining and leaving of nodes. Within each area, a set of nodes moving according to a randomly based mobility model, as well as other nodes called transport nodes that carry the patients to a specific area with a cyclic movement behavior.

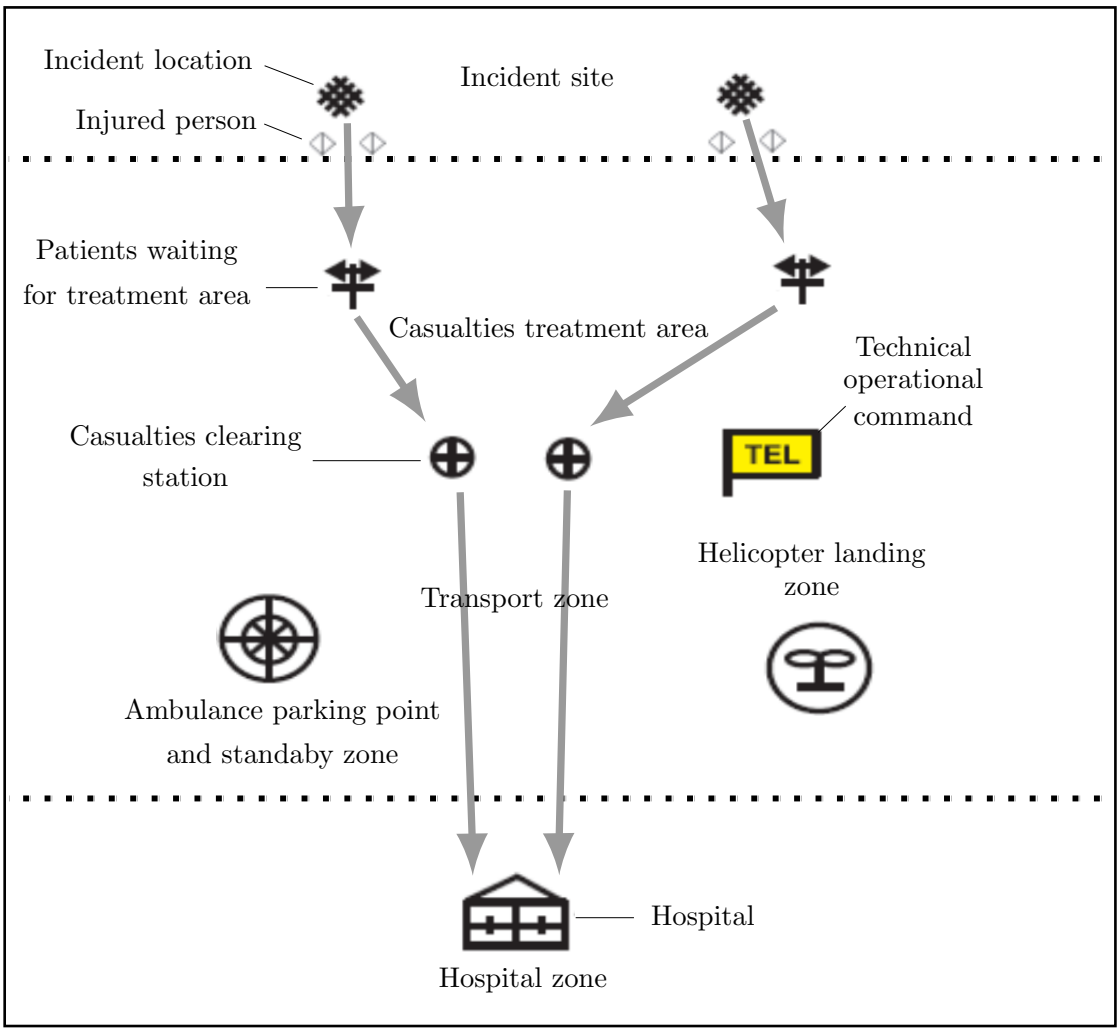

Figure 3.3 – Representation of Disaster-area model.

3.5 Contribution 1 : Simulation of dismounted soldiers' dynamics in Manets

3.5.1 Scenario 1 : Simulation of a dismounted soldiers' group

This section presents the basic concept of our proposed group mobility model, describing how the movement of dismounted soldiers and enemies is modeled on the battlefield based on a set of simple rules. It illustrates how the superposition of these simple rules is used to govern the dynamics of autonomous agents belonging to two distinct groups (soldiers and enemies).

The most important consideration of the group mobility model in trying to simulate the self-organizing behaviors of dismounted soldiers and enemies is because this model is the most appropriate one for modeling and simulation of mobility on the battlefield area [18, 19, 58]. In this context, we assume that dismounted soldiers are equipped with wireless communication devices based on IEEE 802.11 and can communicate directly with the soldier leader or indirectly via multi-hop routing (see Figure 3.5.1).

In this chapter, we introduce a group mobility model based on a collective motion approach for military wireless communications on the battlefield, where a group of dismounted soldiers moves in a limited battlefield area. A potential field algorithm is used to generate movement for each soldier. The perceptual field of each dismounted soldier is divided into the zone of repulsion (ZoR), the zone of orientation (ZoO) and the zone of attraction (ZoA), as shown in Figure 3.4 .

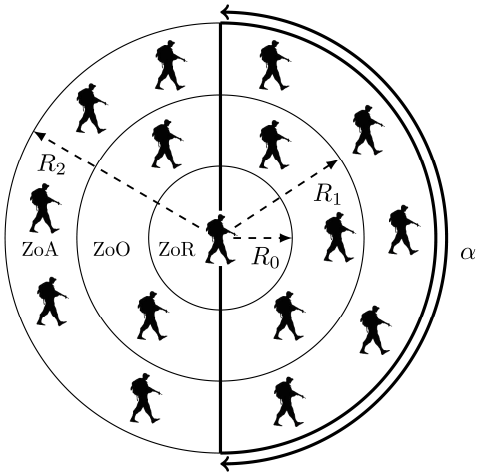

Figure 3.4 – Representation of a member in the model centered at the origin : zor=zone of repulsion, zoo=zone of orientation, zoa=zone of attraction, zore=zone of repulsion from enemies, α=field of perception ahead of the member.

Each dismounted soldier attempts to maintain a minimum distance from others within the ZoR. Within the ZoO, a dismounted soldier aligns itself with its neighbors and within the ZoA, a dismounted soldier moves towards the group so as not to be on the periphery or be left behind. Soldiers cannot see too far, thus, there is no interaction with others located outside the ZoA.

The proposed strategy of collective motion in this article is similar to the rule-based process in Couzin's model [54] and Reynolds's model [59]. However, to model the interaction of soldiers and enemies, we need to define some new behavioral rules assigned to soldiers when detecting enemy attacks and vice-versa (see subsection 3.1).

3.5.1.1 Definition of Scenario

Here, we considered N soldiers capable of moving at a constant speed of v_0 units per second. Each soldier is characterized by his location $\mathbf{p}_i(t)$ and velocity $\mathbf{v}_i(t) = v_0 \times \mathbf{d}_i(t)$ of direction $\mathbf{d}_i(t)$ at time t. In each time step t, a member i assesses the position and/or orientation of neighbors in its local neighborhood within three non-overlapping behavioral zones (Figure 3.4) to determine its desired direction of motion $\mathbf{d}_i(t+dt)$ at time $t+dt$. After that, the member i turns towards the direction vector $\mathbf{d}_i(t+dt)$ by the turning angle α_i, where

$$\alpha_i = \varphi + \xi_i \tag{3.1}$$

where $\varphi = \sigma \times dt$ is the turning angle and σ is the turning rate. $\xi_i = \theta \times dt \times rand(0,1)$, is a random uncertainty variable and θ is a noise parameter. The location of the member i at time

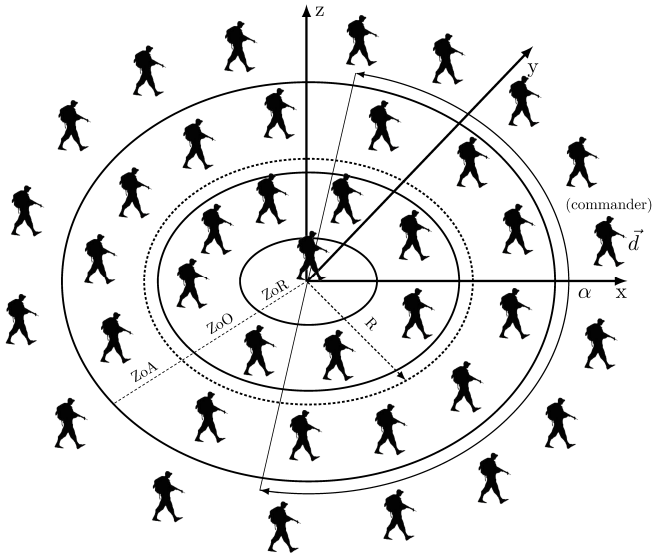

Figure 3.5 – Representation of the area around a dismounted soldier placed in the center : ZoR is the zone of repulsion, ZoO is the zone of orientation and ZoA is the zone of attraction. α degrees is the field of view, R is the communication range, $\vec{d}$ is the direction of movement for commander member (leader soldier).

$t + dt$ is given by :

$$\mathbf{p}_i(t+dt) = \mathbf{p}_i(t) + \mathbf{v}_i(t+dt)dt \tag{3.2}$$

Also, introducing the uncertainty in the movement of the military group may be useful to simulate encountered perturbation of soldier mobility such as difficult terrains and probable exiting obstacles (e.g. mountains, forests, and rivers) or some factors related to the assigned mission as surveying a military region or buildings from enemies.

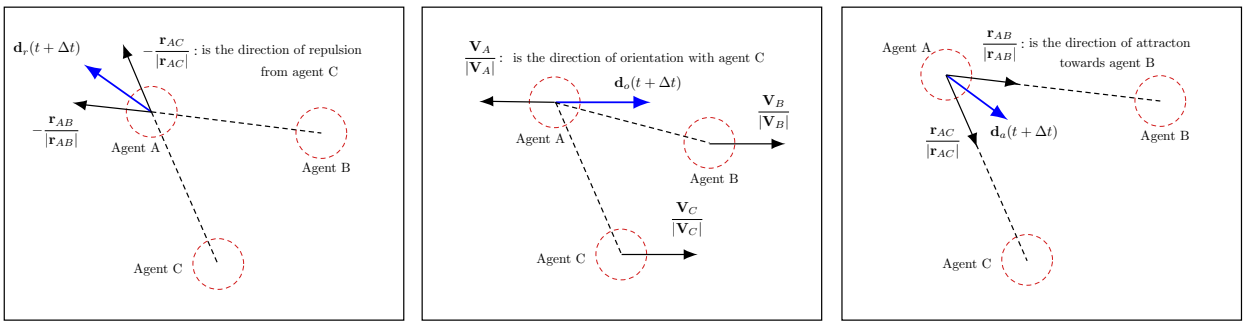

(a) Repulsion behavior (b) Orientation behavior (c) Attraction behavior

Figure 3.6 – Representation of a soldier's direction $d_i(t+dt)$ when performing a repulsion behavior, orientation behavior or an attraction behavior.

3.5.1.2 Behavioral rules assigned to dismounted soldiers

1. A Dismounted soldier attempts to maintain a minimum distance between himself and the other soldiers within the zone of repulsion. This rule has also the highest priority (less than rule 1 or rule 2).
2. If the dismounted soldier is not performing rule 3 he tends to align himself with the leader dismounted soldier within the zone of orientation(ZoO) and towards the position of the leader dismounted soldier within the zone of attraction (ZoA).

3. If the leader dismounted soldier is neither in ZoO nor in ZoA, the dismounted soldier tends to align himself with his neighbors within the zone of orientation(ZoO), and towards the group within the zone of attraction (ZoA) (see Algorithm 3.16).

3.5.1.3 Modeling of repulsion behavior from neighbors

A dismounted soldier i attempts to maintain a minimum distance from the other soldiers within a zone of repulsion (ZoR), modeled as a circle, centered on the dismounted soldier i, with radius R_0. If n_r neighbors are present in this zone at time t, the direction of repulsion from neighbors is given as follows :

$$\mathbf{d}_r(t+dt) = -\sum_{j\neq i}^{n_r} \frac{\mathbf{r}_{ij}}{|\mathbf{r}_{ij}|} \tag{3.3}$$

This behavioral rule has a priority compared to other behaviors, but, less than repulsion from enemies' behavior priority. This zone can be interpreted as soldiers maintaining personal space, or avoiding collisions. Moreover, this repulsion behavior corresponds to the frequently observed behavior of animals in nature (Krause and Ruxton, 2002)[54]. If no neighbors are within the zone of repulsion ($n_r = 0$), the dismounted soldier responds to other rules within the zone of orientation (ZoO) and the zone of attraction (ZoA).

3.5.1.4 Modeling of Cohesion behavior

Cohesion behavior is the opposite of repulsion behavior. This behavior encourages a dismounted soldier to move closer to other neighbors. The cohesion direction of a dismounted soldier i is given as follows :

$$\mathbf{d}_i(t+dt) = \begin{cases} \frac{1}{2}\left[\mathbf{d}_o(t+dt) + \mathbf{d}_a(t+dt)\right] & n_o >= 1,\ n_a >= 1, \\ \mathbf{d}_o(t+dt) & n_o >= 1,\ n_a = 0, \\ \mathbf{d}_a(t+dt) & n_a >= 1,\ n_o = 0. \end{cases}$$

where n_o and n_a are the number of neighbors in the zone of orientation (ZoO) and attraction (ZoA) respectively, $\mathbf{d}_o(t+dt)$ is the direction of alignment with neighbors within the zone of orientation (ZoO), and $\mathbf{d}_a(t+dt)$ is the direction of attraction towards the positions of soldiers within the zone of attraction (ZoA). The widths of zones (ZoO) and (ZoA) are defined as $\Delta r_o = r_o - r_r$ and $\Delta r_a = r_a - r_o$. Both r_o and r_a are used to determine the zones boundaries respectively. The cohesion direction is given as follows :

$$\mathbf{d}_o(t+dt) = \sum_{j=1}^{n_o} \frac{\mathbf{v}_j}{|\mathbf{v}_j|} \tag{3.4}$$

$$\mathbf{d}_a(t+dt) = \sum_{j\neq i}^{n_a} \frac{\mathbf{r}_{ij}}{|\mathbf{r}_{ij}|} \tag{3.5}$$

3.5.1.5 Network model and performance metrics

Our network contained N mobile nodes/soldiers deployed close to each other in a simulation area of $5000\times5000\ m^2$. The movement pattern is based on a collective motion approach. At each time step dt [1], the soldiers/nodes can send data packets towards the sink node/commander

1. The time step dt equals 1 second.

Table 3.1 – Simulation configuration.

Parameter	Symbol	Value	Parameter	Value
Number of soldiers	N	50	Simulation area	5000×5000 m^2
Enemy numbers	η	4-52	Transmission range	80 m
Zone of repulsion	r_r	10 m	Propagation model	TwoRayGround
Zone of orientation	$\Delta r_o(r_o - r_r)$	40 m	Interface queue model	PriQueue
Zone of attraction	$\Delta r_a(r_a - r_o)$	150 m	Queue size	64
Turning rate	σ	0.1	Routing protocol	AODV
Noise	θ	[0,1]	Transport protocol	UDP
Data generation rate	λ	[0,1]	Packet generator	CBR
Initial velocity of nodes	v_0	1 (m/s)	Packet size	1000 bytes

based on Ad Hoc On-Demand Distance Vector (AODV) routing protocol with a data generation rate (λ). Also, we define several metrics related to the performance of network measurement. We monitor the change in topology status caused by the motion of soldiers on the battlefield with and without the enemy's presence. Our main concern is the dynamic nature of the network topology and its effect on network performance. The measured performance metrics are described in detail as follows.

1. Metric 1 : The throughput, defined as the average rate of successful packets delivery over a communication channel to the sink node.
2. Metric 2 : The forwarded throughput, defined as the average rate of successfully forwarded packets through intermediate nodes over a communication channel.
3. Metric 3 : The packet loss, defined as the total dropped packets by source or intermediate nodes during transmission.
4. Metric 4 : The system speed, V_a, defined as the average velocity of soldiers during the simulation, can be calculated as :

$$V_a = \frac{1}{N v_0} \left| \sum_{i=1}^{N} \mathbf{v}_i(t) \right| \tag{3.6}$$

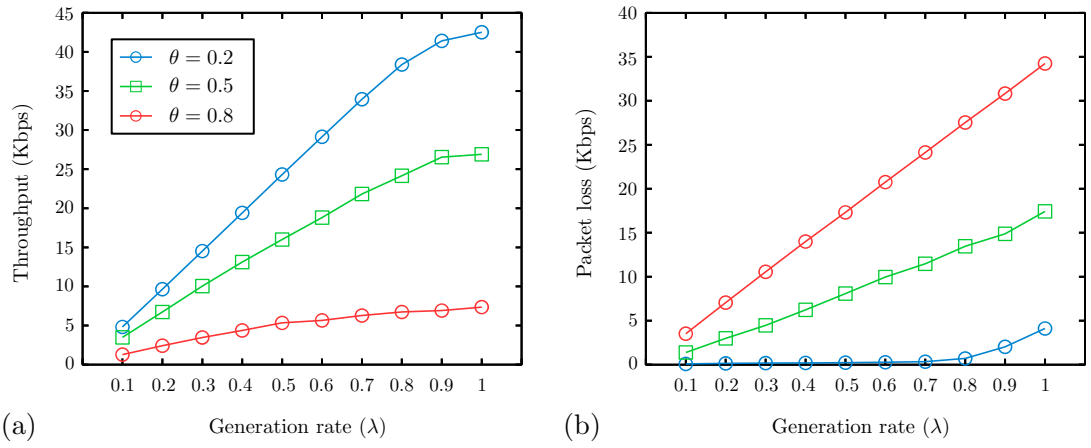

Figure 3.7 – Effect of increasing the generation rate (λ) with parameters $v_0 = 1\,(m/s)$: (θ) the noise probability parameter.

where N is the number of soldiers on the battlefield, and v_0 is the initial velocity assigned to soldiers at the beginning of the simulation execution.

5. Metric 5 : The path lifetime indicates how long the path is still valid before receiving a path update or path error message.
6. Metric 6 : The path length, defined as the total number of hops traveled by the packet to reach the destination.
7. Metric 7 : The packet delivery ratio, defined as the number of successfully received packets at the destination to the total number of packets that are expected to be received at the destination.
8. Metric 8 : The group size : defined as the number of soldiers who are geographically isolated from others by a distance d_{ig} [2] and share a membership in the group.

3.5.2 Results and discussion

3.5.2.1 Validation of scenario versus λ and v_0

Figure 3.7 a-b show the effect of data generation rate λ on both the average throughput and the average packet loss with varying values of noise θ. The figures show that the throughput gradually increases as λ increases. It is quite reasonable according to the network bandwidth availability. On the contrary, the noise has an obvious impact on the throughput, i.e., it decreases drastically in proportion to the noise. The reason for this is that noise exerts a perturbation on the mobility of soldiers. Therefore, the topology change has a great impact on routing performance. As opposed to the throughput, packet loss is taken into account. Figure 3.7 b shows that the average packet loss increases significantly with λ, because of buffer-overflow and collisions due to network congestion. Furthermore, noise strongly affects the packet loss rate.

The reason for this is that noise exerts an influence on the stability of links, by causing an unpredictable mobility behavior, which has the direct effect of increasing the packet loss, due to link failures and indirectly on the increasing buffer overflow because of unreachable nodes. In the next subsection, we will extend the analysis to noise effect on different network performance metrics to investigate how noise (θ) can affect on the collective motion of soldiers and network topology, and then its impact on inter-node communication within the network resultant topology.

We assume that our network will be strongly affected by the initial velocity of agents, whereby the communication efficiency of agents may be reduced ; and especially when associated with the increase of noise, in which case agents may unexpectedly lose connections with their neighborhood due to the relatively quick change in the direction of the velocity vector of the agents. It has been shown that if v_0 goes to infinity, the agents become completely mixed between two states, similar to the mean-field behavior of a ferromagnetic [50]. The first state corresponds to the perfect alignment of the group while the second corresponds to a pure random state. Therefore, we expect that the average velocity of the group will be exactly equal to 0.5. While extreme of v_0 equaling zero, the agents are stationary where the agents do not move.

To evaluate the effects of the mobility on the wireless network of soldiers, we analyzed, with simulations, the effect of initial velocity v_0 on different performance metrics with varying values of θ ={0.2,0.5}. The results of our simulation show that for θ = 0.2, increasing the initial velocity v_0 will affect slightly the mean velocity until it reaches $v_0 \approx 4$ (see Figure 3.8 c).

But beyond this value, it decreases strongly until reaches the value of 0.5 for $v_0 \geq 8$. However, for θ = 0.5, we found that the mean velocity decreases until it reaches a minimum and then

2. The distance between two isolated groups $d_{ig} = 80m$.

increases until reaches a value of 0.5. Moreover, just as it was predicted, we find that for higher values of v_0, the mean velocity remains constant at the value of 0.5 regardless of noise value.

Figure 3.8 a-b show that for lowest initial velocities, the network performs better, in terms of average throughput and packet loss, because low velocities provide favorable conditions that are sufficient for establishing very stable paths and also avoid network partition. On the contrary, it produces worse results under the highest initial velocities because high velocities cause sudden and severe disruptions to ongoing network routing ; resulting in lower throughput and high packet loss.

Figure 3.8 d shows that, for low values of noise, the forwarded throughput is decreased gradually when increasing initial velocity, while, in the case of high noise, it decreases exponentially. The impact of increasing both the initial velocity of soldiers and the noise provokes a drastic dispersion of the network topology, leading to a segmentation of the network topology into several small groups sizes or even into isolated nodes. Figure 3.9 plots the performance of the network, in the case of low noise value, in terms of the distributions of paths lifetimes, path length, hop length and group size. Figure 3.9 a-b show how the established paths can be affected by different values of v_0 (i.e., the initial velocity). We can see that when v_0 is low, communication channels of long lifetimes and short path lengths persist in the network. Also, the appearance of communication channels of long lifetimes is principally linked to the collective motion of nodes in the network. This can be seen clearly from Figure 3.9 d where only one large group exists in the system. However, increasing mobility causes the appearance of a high number of established paths and most of them have short lifetimes. Thus, nodes aren't able to keep connectivity for a long time. Indeed, higher mobility will disperse the nodes into small

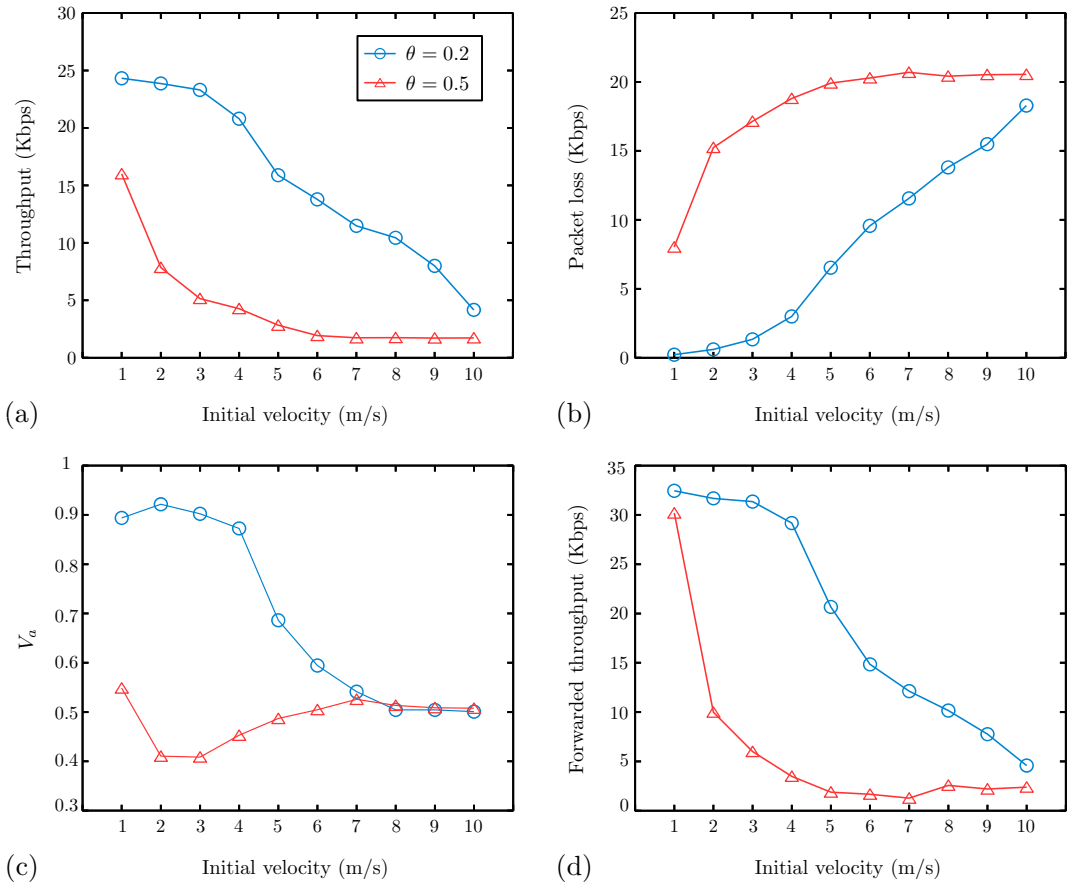

Figure 3.8 – Effect of increasing initial velocity v_0 with parameters $\lambda = 0.5$: (a) Average throughput, (b) Average packet loss, (c) Average velocity of soldiers, and (d) Group frequency.

groups, and data can be transferred to the sink only through communication channels having long paths. This confirms well the instability of the network due to a frequent topology change, where a lot of paths should be created to conduct packets towards the commander. Hence, much overheads are required to send traffic from the soldiers to the commander; affecting badly the network efficiency. To achieve better network efficiency, the soldiers must move slower to maintain the stability of their network. Indeed, we can see from Figure 3.9 c that when the initial velocity is low, the packet delivery rate is improved and a higher percentage of packets are received by the commander through short paths.

Moreover, to investigate the effect of initial velocity associated with a high level of noise, we repeated the same network scenario and calculations with different initial velocities and for $\theta = 0.5$.

This decision may highlight some features concerning the relationship between initial velocity and noise. We see from Figure 3.10 that, for $v_0 = 1$ and $\theta = 0.5$, the distribution of path lifetimes consistently shows a greater number of shortest lifetime paths compared with results in the case of $v_0 = 1$ and $\theta = 0.2$ (see Figure 3.10 a). This is obvious since, as we have depicted before, noise invokes randomness and perturbations to the structure of the communication network. More interestingly, we show that when both the initial velocity and noise are very high, the nodes are rarely able to establish paths to the destination, due mainly to the high uncertainty of nodes' mobility within the network area (see Figure 3.10 b). Also, we can expect that the association of higher levels of initial velocity and noise expands greatly the problem of the network partition and then causes severe topology destruction (see Figure 3.10 d). This can

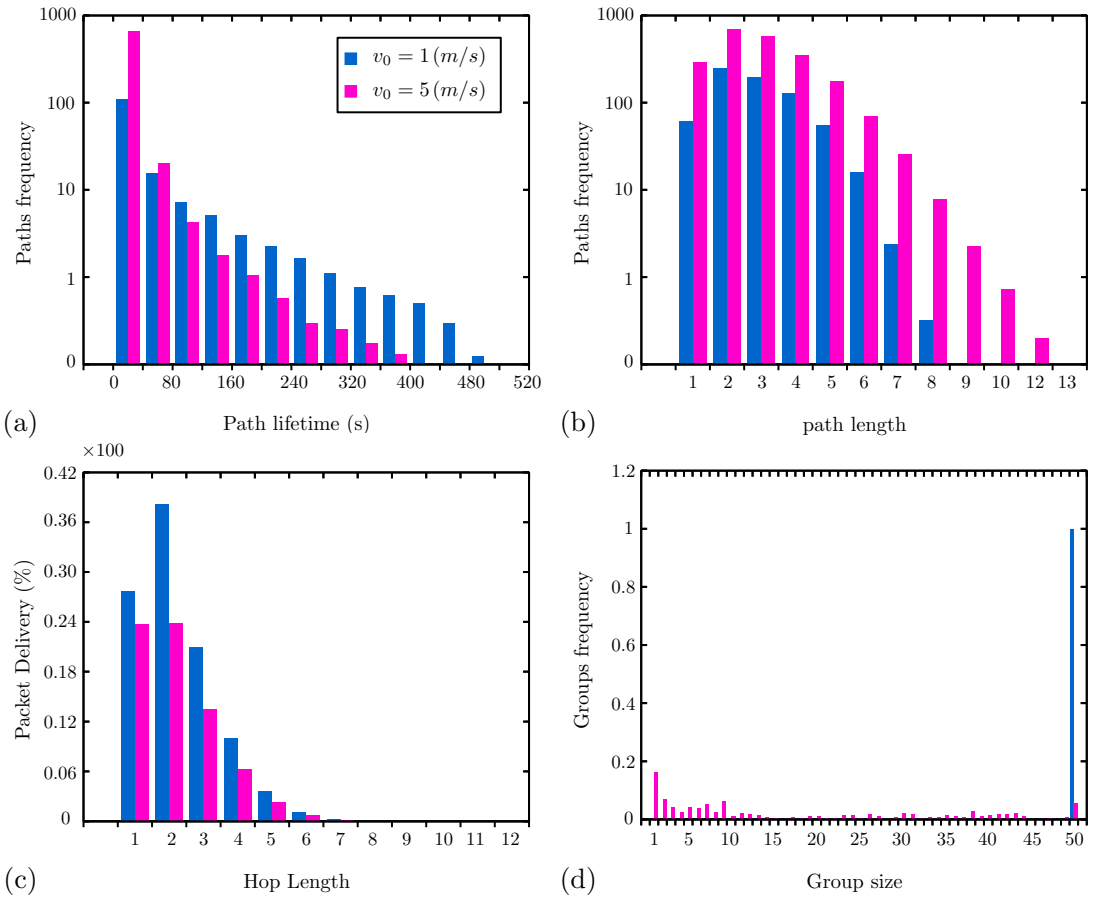

Figure 3.9 – Effect of increasing initial velocity v_0 with parameters $\theta = 0.2$, and $\lambda = 0.5$: (a) Average path lifetime, (b) Average path length, (c) packet delivery ratio, and (d) Group frequency.

be seen clearly from experiment results shown in Figure 3.10 c, where the network efficiency is almost absent.

3.5.2.2 Effects of noise θ

It has been demonstrated that collective motion models [50] exhibit a phase transition that occurs when the noise is increased. Indeed, for small values of noise, the average system speed is approximatively equal to one (see Figure 3.11 c). This phase which is called "finite net transport phase" corresponds to a coherently moving phase where almost all nodes move in the same direction. However, for high values of noise, this means that velocity is approximately zero ; reflecting the random aspect of the directions of the moving nodes. This phase is called, "no transport phase". Hence, a phase transition from "finite net transport phase" to "no transport phase" occurs at some critical value $\theta_c \approx 0.6$ (see Figure 3.11 c).

From Figure 3.11 a, we see that the average throughput decreases significantly versus noise. Hence, the throughput remains almost constant in the finite net transport phase ; while it decreases rapidly towards small values in a no transport phase. The main effect on decreasing throughput results especially from increasing noise, which hardly causes topology change due mainly to perturbation of the collective motion model. Thus, an arbitrary partition of the network occurs when noise increases.

Figure 3.11 b illustrates the effect of noise on average packet loss. It is found that the packets will begin to be removed from the network when the noise exceeds a certain level. Beyond

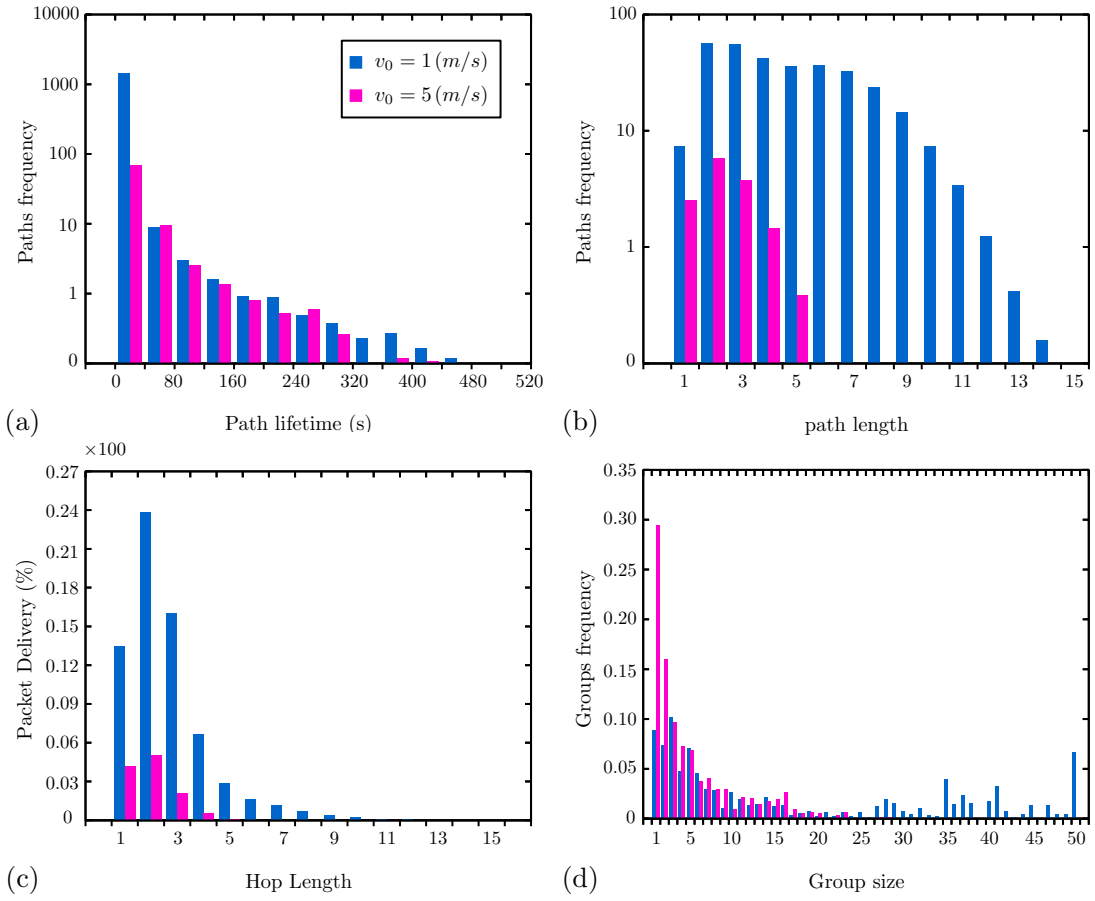

Figure 3.10 – Effect of increasing initial velocity v_0 with parameters θ = 0.5, and λ = 0.5 : (a) Average path lifetime, (b) Average path lifetime, (c) Average connection lifetime, and (d) Groups frequency.

this value, the network enters into the congested phase. The results show also that under the highest noise, packet loss is high, due mainly to the bad condition of the network topology where the link failures rate is very important.

In wireless mobile networks, nodes move frequently and to cover the disconnected segments of the network, nodes may act as a router to forward packets to other nodes. To study the influence of noise on the appearance of relay nodes in the network, we show in Figure 3.11 d the average forwarded throughput versus noise under different generation rates values λ. The average forwarded throughput significantly increases with increasing noise until reaching a maximized value and then decreases at higher values of noise. If the noise value is very small, then all the nodes move closer to each other and there is no need for relay nodes to transfer the data to the sink node. Moreover, increasing noise will provoke a considerable dispersion of nodes in the network area and then lead to the appearance of long paths and link failures, whereas direct transmission may be insufficient to reach the destination. Hence, this will increase the appearance of rely nodes in the system. However, if the noise value is very high, the nodes become almost disconnected and then no communications could be achieved via relay nodes. This explains the decreasing of the forward throughput (see Figure 3.11 d).

Figure 3.12 a-b illustrate the distributions of the path lifetime and the path length in the communication soldiers network. The results show that for higher values of noise, paths with the shortest lifetimes are the most prevalent in the network (see Figure 3.12 a).

The reason for this is that both the commander and the soldiers move separately in a disordered fashion. Thus, smaller path lifetimes are due principally to the incapability of nodes

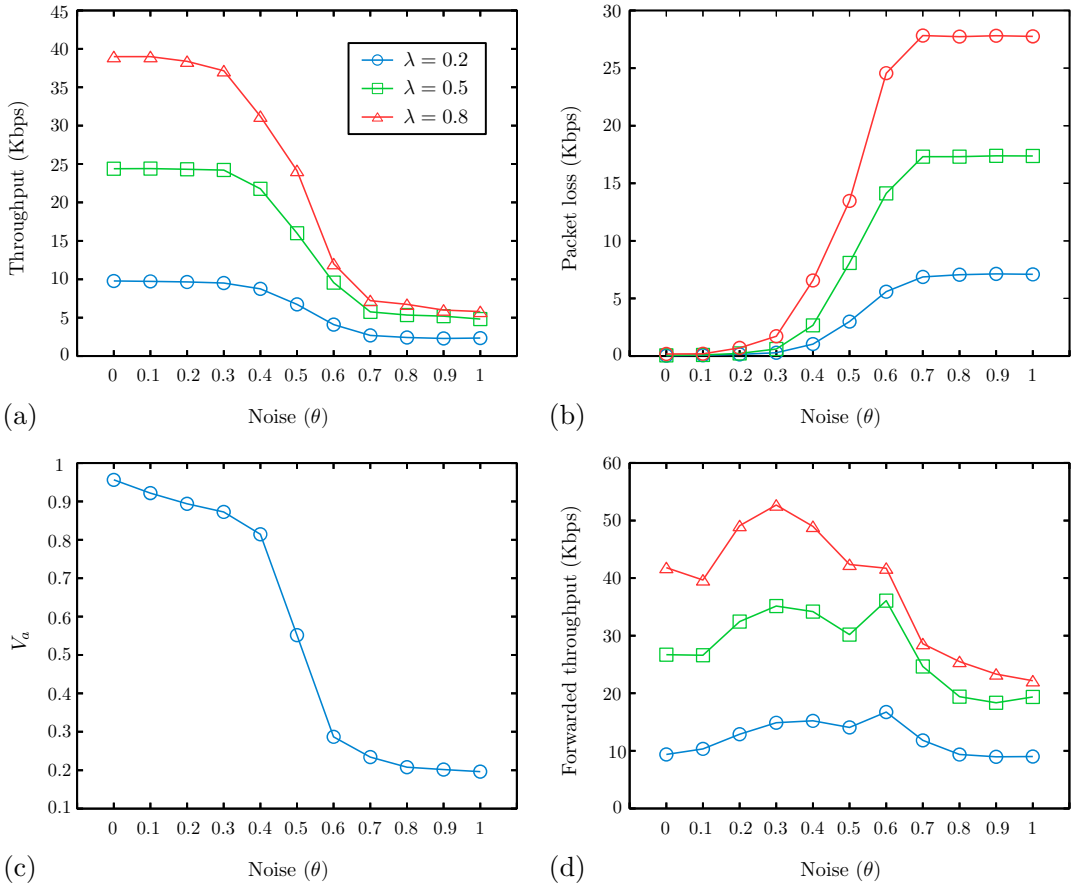

Figure 3.11 – Effect of increasing noise θ with parameters $v_0 = 1\,(m/s)$: (a) Average throughput, (b) Average packet loss, (c) Average velocity, and (d) Average forwarded throughput.

to keep connectivity for a long time because of the high dispersion of nodes. Furthermore, we see clearly from Figure 3.12 b that high values of noise lead to the establishment of long paths to reach the destination. However, these paths are frequently perturbed by unexpected movements of soldiers on the battlefield. As a consequence, this situation will lead to a significant reduction in the capacity of communication between the soldiers and leader soldiers on the battlefield (see Figure 3.11 a).

Figure 3.12 c reports the performance of the network obtained in terms of packet delivery ratio under different values of θ. Figure 3.12 c shows that the network achieves an overall higher rate of received packets under lower values of noise. The reason for this is that under the low value of noise, soldiers move coherently in a collective motion structure (finite net transport phase) and then the communication paths are more stable and reliable. Therefore, most existing communication paths are those emanating from soldiers that are a single hop from a commander. Furthermore, under low noise values, all nodes are located close to each other. So, there is no need for establishing longer paths. This optimizes the capacity of the overall communication network. But, under higher values of noise, the network is segmented into several groups sizes which are changing frequently over time (see Figure 3.12 d). Hence, we see that at low values of noise, only one large group exists in the network. However, increasing noise may create the dispersion of nodes and then several groups of different sizes may appear in the system. In particular, the high frequency of disconnected nodes is present in the network. Thus, this segmentation into different groups has a direct effect on the degradation of network performance as seen from (Figure 3.11 a and Figure 3.12 c).

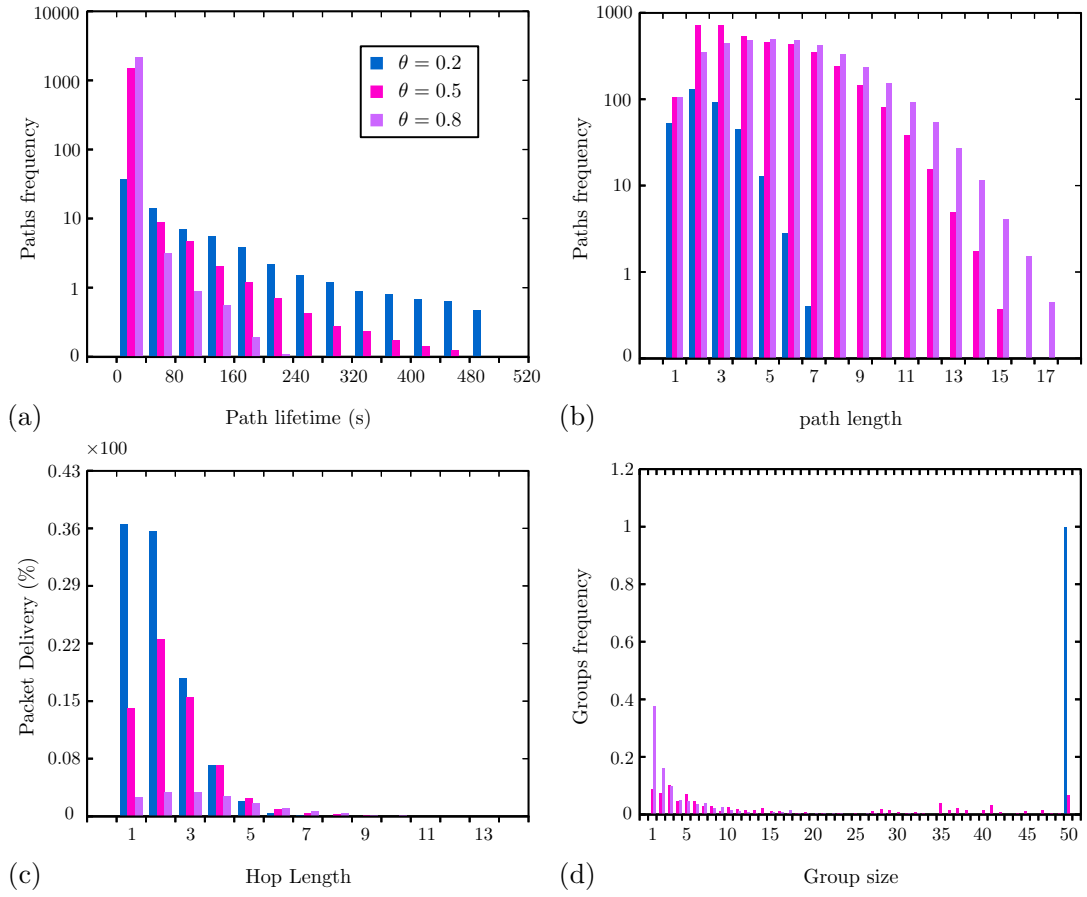

Figure 3.12 – Effect of increasing noise θ with parameters $v_0 = 1\,(m/s)$, and λ = 0.8 : (a) Average path lifetime, (b) Average path length, (c) packet delivery ratio, and (d) Group frequency.

3.5.3 Comparison with other existing mobility models

Our study used several monitoring metrics to reveal the performance of our group mobility model in a complex environment (the battlefield). This model is designed to simulate the movement of dismounted soldiers with a leader on the battlefield. To quantify the reliability aspects and features of our model, a comparison with other mobility models is expected. Since the simulation of enemy attacks is not treated in most of the existing group mobility models including recent works ; only a comparison without the presence of enemies can be performed in this section.

The unexpected mobility of soldiers on the battlefield leads to performance degradation of path length and path lifetime because speeding up or slowing down leads to changes in the network topology. Comparing our model and other models in terms of path length and path lifetime is expected to give extra merit to their strengths and other features.

Performance comparison of our proposed Group Mobility Model along with some existing mobility models is provided for the perturbation factors of network topology similar to the noise effect defined in our model. Indeed, our mobility model was compared with RPGM[19], Nomadic[60], GFMM[21], Spatio-Temporal Parametric Stepping (STEPS) [3][61] and Self-similar Least Action Walk (SLAW) [4][62].

3. At the beginning of each simulation, the set of nodes is deployed within an area of 500×500 m^2. As the value of α decreases, the nodes will be distributed over the whole area.

4. SLAW was evaluated over a coverage area of 1000×1000 m^2.

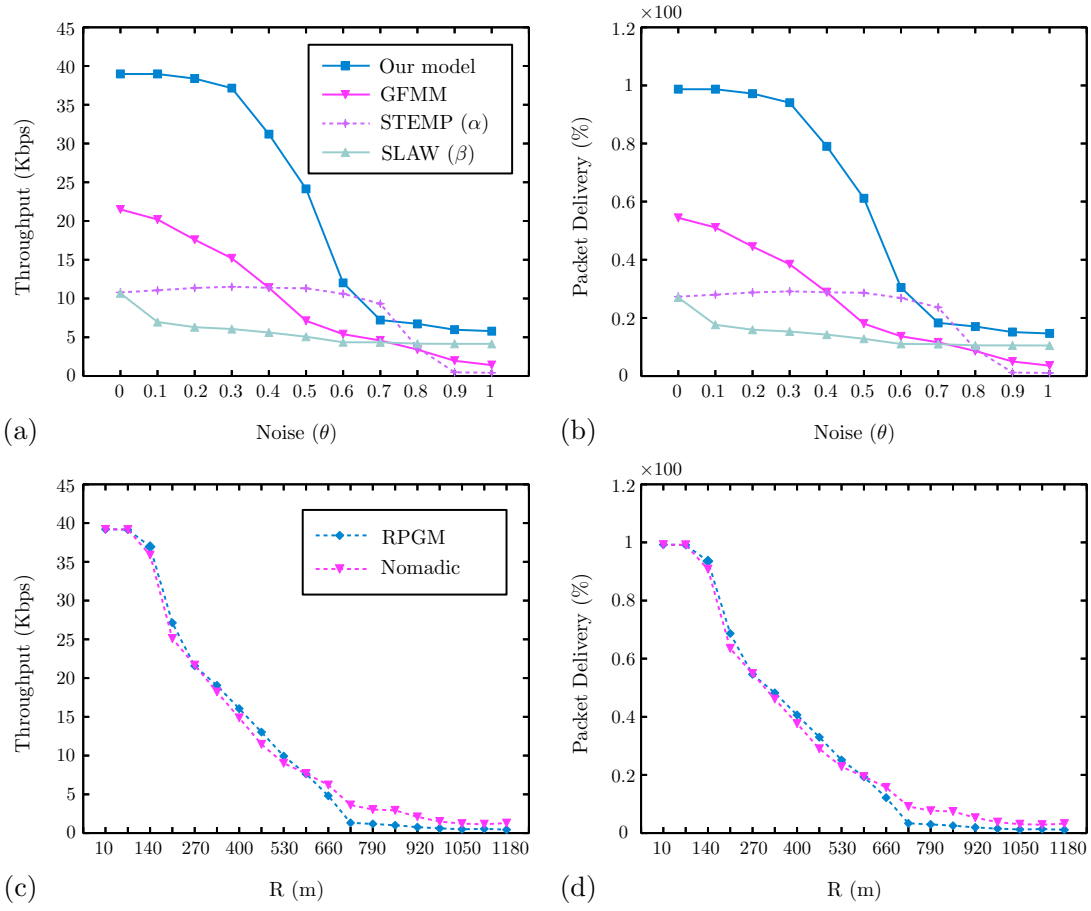

Figure 3.13 – Comparative evaluation between different mobility models in terms of the network performance, with parameters $v_0 = 1\,(m/s)$, $\lambda = 0.8$, $\alpha = 10 \times (1-\theta)$ and $\beta = (100 \times \theta) + 10$.

For this comparison, we have implemented the above mobility models with a scenario that considers a special node as the sink node (Commander) whereas the other members are considered as senders (Soldiers). To provide the randomness and perturbations to the structure of the network topology of existing mobility models as provided in our model via the noise parameter (θ), we identified through simulation the most appropriate parameters which could provoke a perturbation of nodes mobility for each mobility model as follows :

1. RPGM : In each group defined by this model, every member moves to a randomly chosen location within a circular neighborhood of radius R around its reference point location. The movement around the reference point is based on the RWM. The analysis and the simulation experiments demonstrated that the greater the radius the more the fluctuation and the uncertainty in the mobility are important.
2. Nomadic Community Mobility Model (NCMM) : It is similar to RPGM where every member moves also to a randomly chosen location within a circular neighborhood of radius R around its reference point location. NCMM is considered as a special case of the RPGM model.
3. GFMM : It supports a logical design of the noise defined as a speed deviation ratio based on a predefined parameter. This parameter is used to control the deviation range of nodes' speeds from the Group speed under GFMM.
4. STEPS : It is a simple parametric mobility model that is inspired by observable characteristics of human mobility behavior, specifically the Spatio-temporal correlation of human movements. It supports an attractor power parameter named (α). We are interested in the variation of α from low to high value, where under the highest value of α, the nodes have a higher probability to stay close to each other and so the preferential zone plays the attraction role instead of a repulsion one.
5. SLAW : This model expresses the human walking patterns based on synthetic mobility traces. Under SLAW, people would always randomly choose places to visit in random order. These places are defined as a set of waypoints and the choices of the next places or destinations to visit are completely random. Simulation experiments have demonstrated that the increase in the number of waypoints (β) is a determinant factor of the perturbation degree of network topology.

Figure 3.13 shows the average throughput as well as the packet delivery ratio in terms of different perturbation factors of network topology. As can be observed from Figure 3.13 , our model, RPGM and NCMM exhibit the highest throughput as well as having the highest packet delivery (≈100%) under the low value of noise and radius R, whereas the other mobility models exhibit the worst performance results. By looking at Figure 3.14 a and Figure 3.15 a, the benefit of long path lifetimes and the cohesion between soldiers could be seen clearly for our model, RPGM and NCMM. Furthermore, the existence of long path lifetimes, in these three mobility models, is an indication that there is an important mobility coherence between soldiers. This may lead to a significant increase in the number of relaying packets and therefore to optimizing the use of network resources. Figure 3.15 a also shows that GFMM exhibits similar results in terms of group size compared with the three previous models. However, in terms of network performance, it exhibits a medium level of throughput as well as the packet delivery ratio (≈50%).

This can be explained because nodes under GFMM can overlap or collide with each other ; and then can generate collisions because of the reception of a high number of packets within a limited coverage area.

As the level of perturbation factors increases, the network performance exhibits a degradation for all models except for the STEPS model, where it shows a very slight increase in the

network performance when α >= 5. However, when α is below the value of 5, indicating that the network in the STEPS model becomes scattered, the nodes move in a highly unpredictable manner causing segmentation of the network. By observing the results presented in Figure 3.13 , Figure 3.14 and Figure 3.15 , it is seen that the SLAW model depicts the worst network performance as β increases. This can be explained because the mobility of nodes under the SLAW model is based on a purely random strategy where each node randomly tries to visit a selected waypoint from the total number of waypoints (β). In this situation, the topology is quite unstable, and consequently, the communication links between nodes will be unstable or may even become disconnected. On the other hand, our model still exhibits the best performance compared to the other mobility models in terms of throughput, packet delivery ratio and path lifetime under the medium value of noise. Figure 3.15 b shows clearly that the highly stable communications in our model are achieved by wide group distributions of nodes within the network area. This keeps the stability of links between nodes such that the network topology is effectively static. Under high enough values of perturbation factors of network topology, the link quality is more unstable, and thus the probability of transmission failure increases, thereby increasing the packet loss probability. Therefore, the appearance of disconnected network segments Figure 3.15 c is particularly due to the degradation of the cohesion behavior between nodes. On the other hand, it could be also noticed that both RPGM and NCMM outperform our model in terms of packet delivery and path lifetimes (see Figure 3.14 c). This is because the topology connectivity in the case of our model depends on the dynamic of neighbors, whereas in the case of RPGM or NCMM the lead point has a significant impact on each group mem-

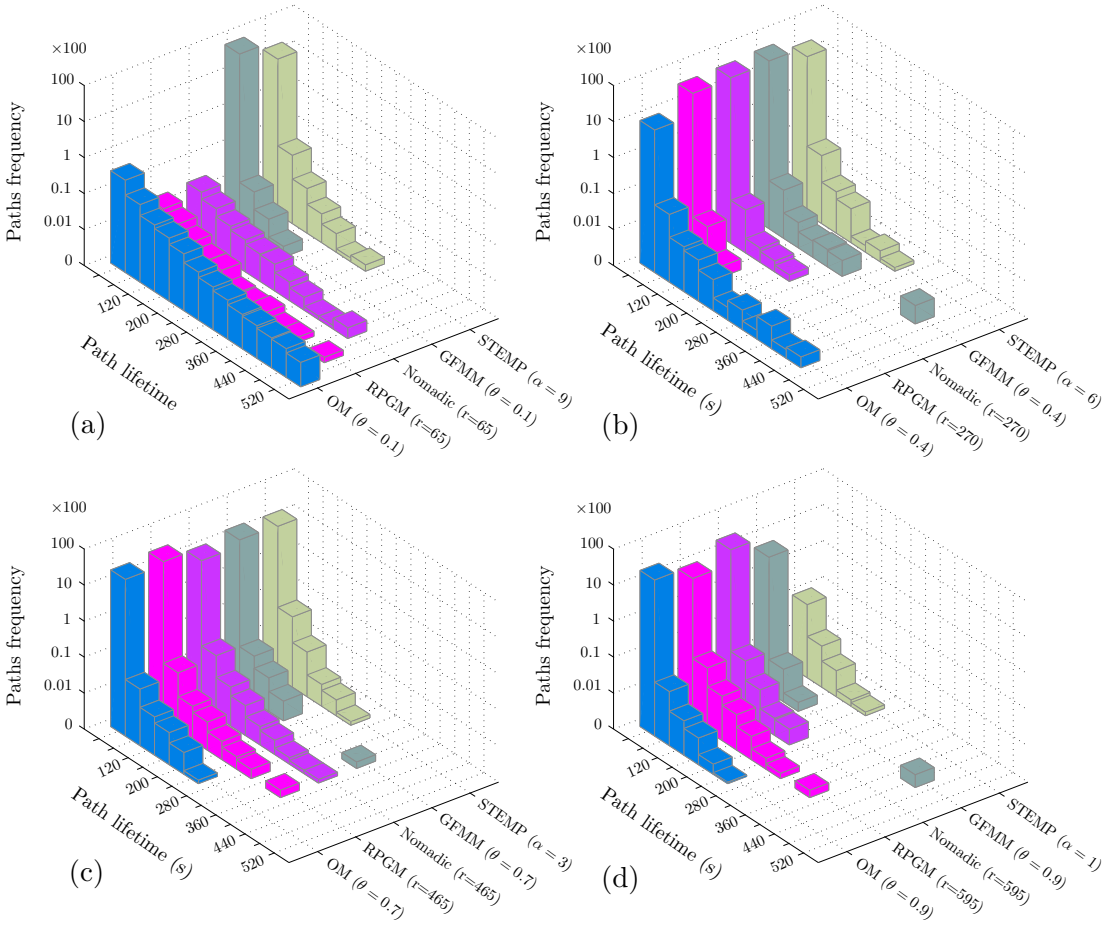

Figure 3.14 – Comparative evaluation between different mobility models in terms of the path lifetime distributions. OM denotes our model.

ber. This leads to keeping the stability and the availability of communication links for a long time as shown in (see Figure 3.14 c). However, both RPGM and NCMM depict a high frequency of isolated nodes, where the probability to get large group size is very small (see Figure 3.15 c). Finally, under very high values of perturbation factors, all the mobility models lead to the worst performance degradation. This is due principally to the fact that the nodes move in a highly unpredictable manner with randomly chosen speed and direction within the network area. Therefore, unexpected network segmentation may occur as the network topology and link capacities dynamically change over the time as shown in (Figure 3.15 d and Figure 3.14 d).

From the obtained results, we conclude that our model displays a realistic behavior compared with other mobility models. Only the nearby nodes to the leader are directly affected by its trajectory, whereas the other nodes are affected by their neighbors as in the real world. On the contrary, under RPGM and Nomadic, every node is affected by the lead point considered as a leader-member. GFMM does not support repulsion between the neighbors within the same group which is considered as a natural human behavior. Under both SLAW and **STAMP!** (**STAMP!**), the nodes can move freely according to a random mobility model without considering some aspects of cohesion or collective motion behavior.

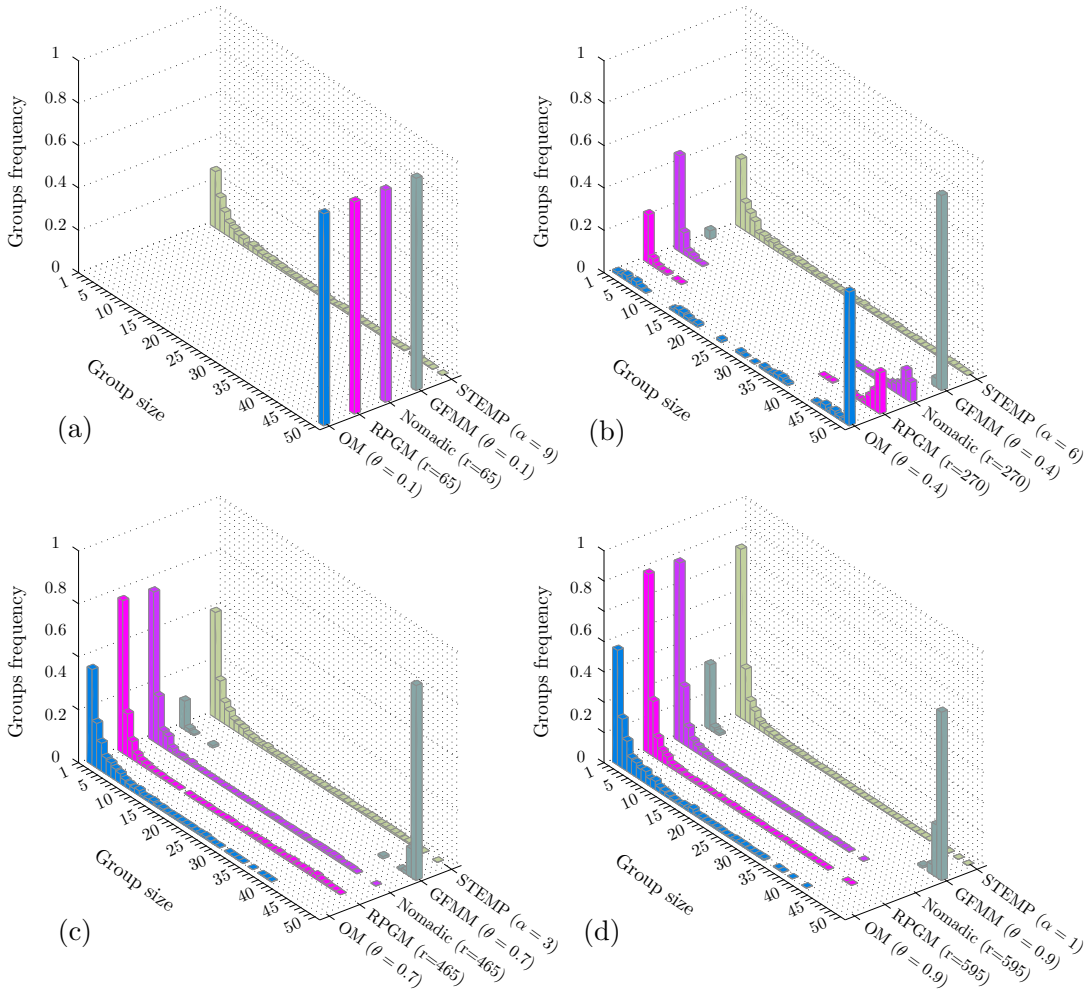

Figure 3.15 – Comparative evaluation between different mobility models in terms of the group size distributions.

3.5.4 Scenario 2 : Simulation of dismounted soldiers' with presence of enemy

3.5.4.1 Definition of Scenario

Here, we considers the same previous scenario described in Section 3.5.1.1 , but we deploy M enemies away of dismounted soldiers of 300 m (see Algorithm 3.16).

3.5.4.2 Behavioral rules assigned to dismounted soldiers

1. A Dismounted soldier attempts to maintain a maximum distance between himself and the enemies in his neighborhood, at all times regardless of his location zone. This rule has the highest priority.
2. The dismounted soldier leader attempts to move in any direction if there aren't enemies in his neighborhood.
3. If the enemy is located away from dismounted soldiers, they can follow the same rules as described in Section 3.5.1.2 .

3.5.4.3 Behavioral rules assigned to enemies

1. The enemy leader attempts to move towards the soldier leader, whenever he is within his neighborhood, to attack the soldier's group.
2. The enemy attempts to attack soldiers if there are one or more soldiers in his neighborhood, regardless of his location zone. For that, the enemy moves towards the group of soldiers within his neighborhood. This rule has the highest priority for enemies.
3. If the enemy is located away from dismounted soldiers, enemies can follow the same rules as dismounted soldiers except for the enemy leader (see Figure 3.5.1.2).

3.5.4.4 Modeling of repulsion behavior from enemy

Each dismounted soldier i (this may be the leader soldier) attempts to maintain maximum distance from n_{en} enemies in its neighborhood regardless of their location zone. In most cases, enemies are detected once they are within the zone of attraction (ZoA) of the dismounted soldier i. The direction of repulsion from enemies is given as follows :

$$\mathbf{d}_{re}(t+dt) = -\sum_{j=1}^{n_{en}} \frac{\mathbf{r}_{ij}}{|\mathbf{r}_{ij}|} \tag{3.7}$$

where $\mathbf{r}_{ij}$ is the unit vector from the location point of i in the direction of the enemy j. This behavioral rule has the highest priority in the model, so that if $n_{en} > 0$, the desired direction $\mathbf{d}_i(t+dt) = \mathbf{d}_{re}(t+dt)$. This repulsion behavior can be interpreted as soldiers avoiding danger space, or attacks from enemies. If no enemies are within any zone, the dismounted soldier responds to other behavioral rules.

3.5.4.5 Modeling of enemy attack behavior

In the strategy attack of the enemies, that is considered in this chapter, the leader enemy attempts to move towards the soldier leader, whenever he is within his neighborhood, to attack the soldiers' group. Moreover, an enemy i attempts to attack soldiers if there are one or more soldiers in his neighborhood, regardless of his location zone. For that, the enemy moves towards the group of soldiers within his neighborhood. In the simulations, we suppose that this

neighborhood is limited by the zone of attraction (ZoA). Hence, if n_{sol} soldiers are within ZoA (centered at the position of the enemy i), the direction of attack is given as follows :

$$\mathbf{d}_{at}(t+dt) = \sum_{j=1}^{n_{sol}} \frac{\mathbf{r}_{ij}}{|\mathbf{r}_{ij}|} \tag{3.8}$$

where $\mathbf{r}_{ij}$ is the unit vector from the location point of i in the direction of the dismounted soldier j. This behavioral rule has the highest priority in the model, so that if $n_{sol} > 0$, then the desired direction $\mathbf{d}_i(t+dt) = \mathbf{d}_{at}(t+dt)$. If no soldiers are within ZoA, the enemy responds to other behavioral rules.

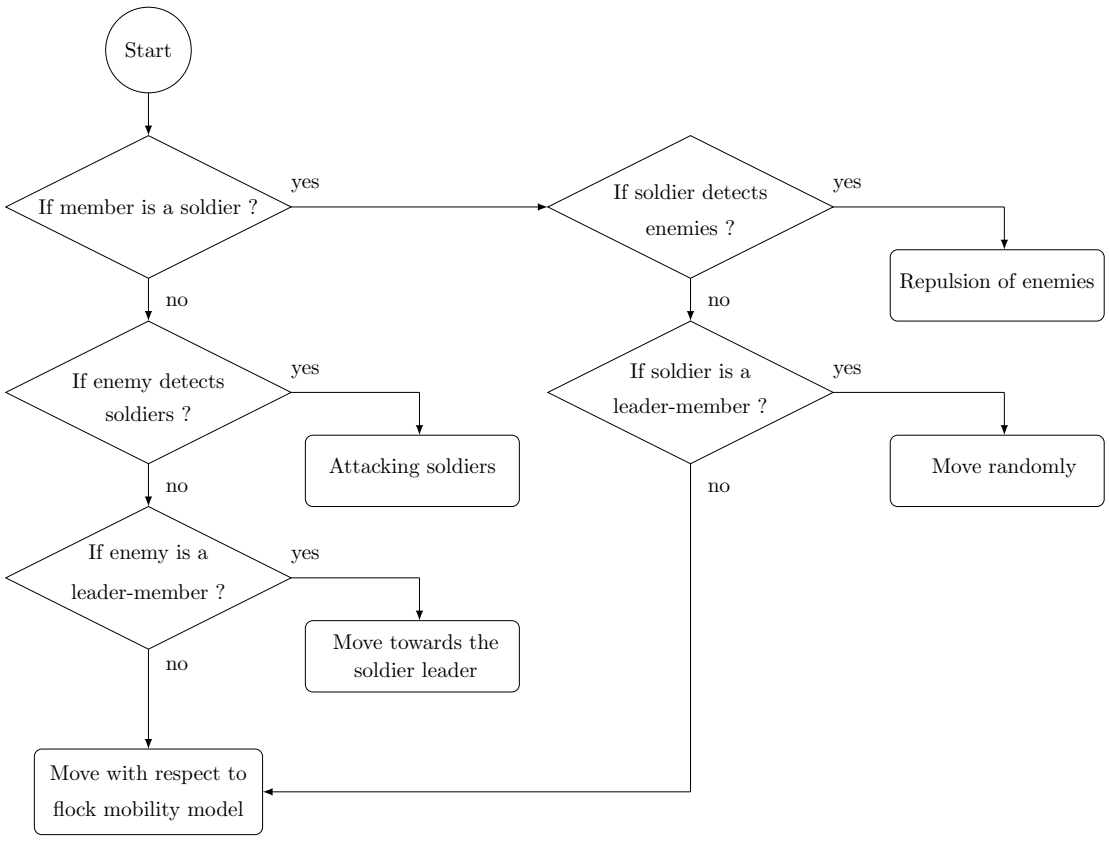

Figure 3.16 – The followed algorithm for defining different behaviors of dismounted soldiers with and without presence of enemy.

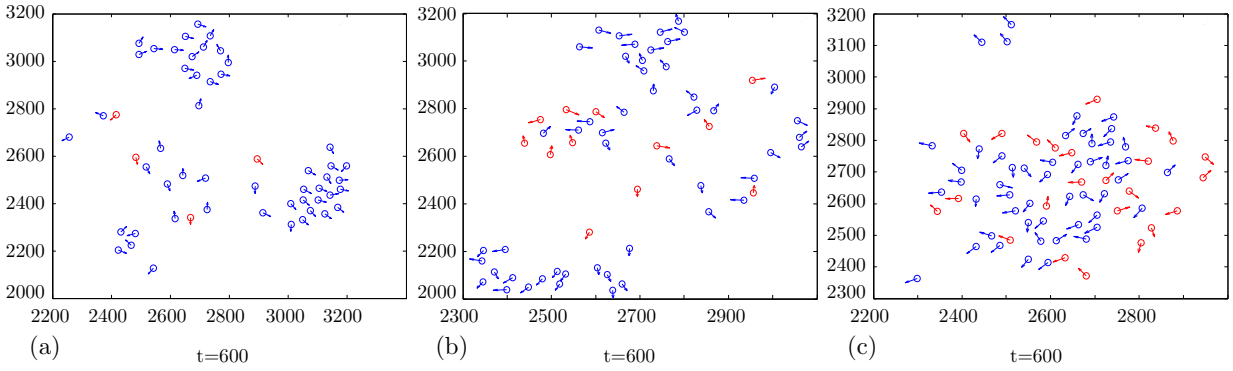

Figure 3.17 – Illustration of dismounted soldiers on the simulation area under different enemy numbers η : (a) $\eta = 4$, (b) $\eta = 12$, and (c) $\eta = 24$.

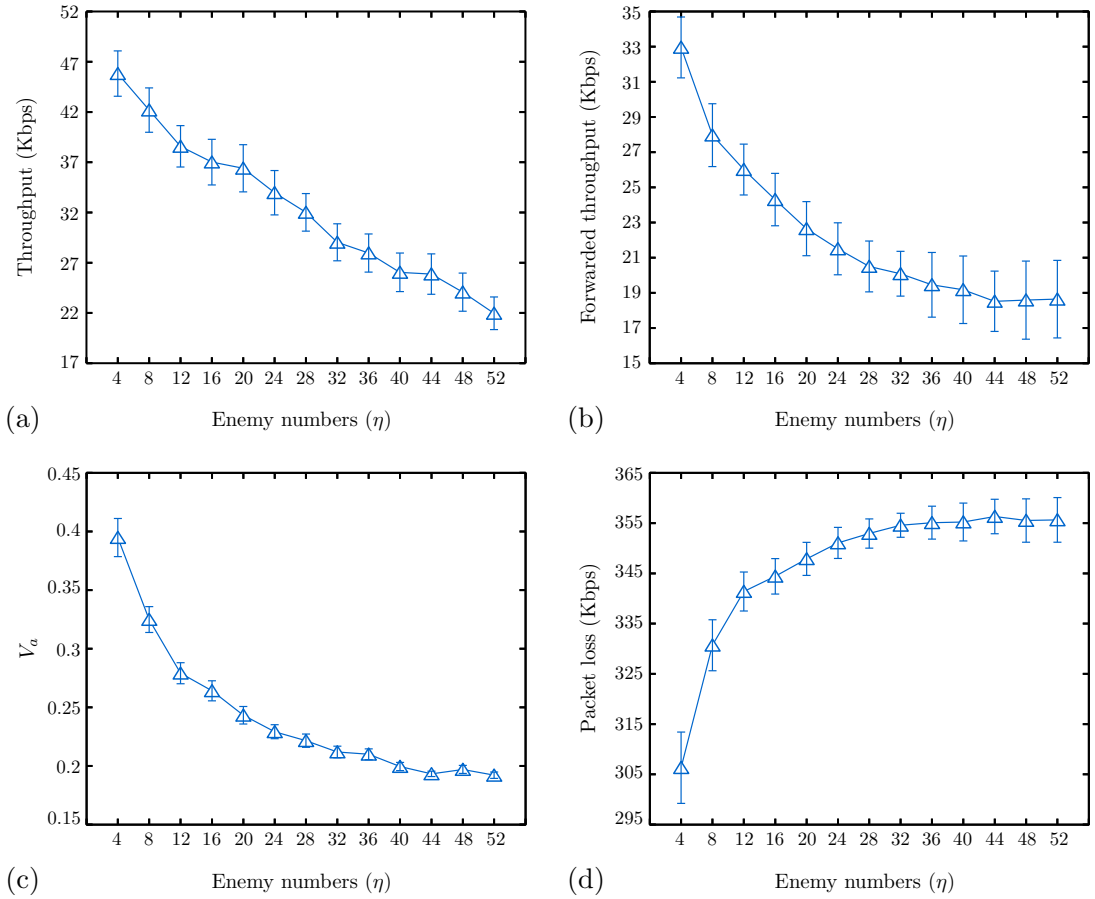

Figure 3.18 – Effect of increasing the enemy numbers η in the battlefield with parameters θ = 0, λ = 0.5, and $v_0 = 1\,(m/s)$: (a) Average throughput, (b) Average forwarded throughput, (c) Average velocity, and (d) Average packet loss.

3.5.4.6 Modeling of repulsion and cohesion behaviors for enemy

The repulsion behavior from neighbors (enemies) and the cohesion behavior are identical with those of the soldiers because these behavioral rules govern individual-level interactions within their group.

After the above process has been performed for every member (soldier and enemy), all members move towards the desired direction $d_i(t+dt)$ at time $(t+dt)$ by a vector velocity $\mathbf{v}_i(t+dt)$. We apply this process at each time step dt, where each member can independently perform a specific rule according to the significant interaction with other members in its neighborhood.

3.5.5 Results and discussion

3.5.5.1 Evaluation of dismounted soldiers' network versus enemy number

In this part, we use the same previous network configuration and the same group of soldiers, but, we add varied enemy numbers on the battlefield near the group of soldiers. We assume that the enemy's leadership can move towards the soldier's leadership based on Military-intelligence, whereas the soldier's leadership can move randomly in the battlefield area. Furthermore, soldiers and enemies must necessarily follow the collective motion pattern separately. But, the enemies can attack soldiers in the case when an enemy remarks one or more

soldier's existence in their field of view. Accordingly, enemies can't establish communication with soldiers or forward data flow to soldiers.

We analyzed the effect of increasing the enemy numbers (η) on the battlefield on different system metrics. In Figure 3.17 , we show snapshots of the model where we see clearly that increasing the enemy numbers disperse the collective motion of the soldiers.

Figure 3.18 shows that with increasing η, the average throughput at the sink node decreases almost linearly. It shows also that the average velocity exponentially decreased when increasing η (Figure 3.18 a and Figure 3.18 c). The presence of enemies on the battlefield provokes the dispersion of the group of soldiers to escape the enemy's attacks. This can be seen clearly from the distribution of the group size in the system Figure 3.19 d, where maximized percentage of isolated nodes are present.

Also, we see that both the decreasing of the forwarded throughput and the increasing of the packet loss, are correlated with the average velocity variation (see Figure 3.18 b-d). Indeed, with increasing η, we observe an exponential decrease of the average velocity while, on the other hand, exponential increases and exponential decreases are found, for the forwarded throughput and the packet loss respectively. Moreover, even when the average velocity is stabilized for η >= 44 they are also stabilized at the same value of η. Finally, we believe that the presence of enemies not only disperses the group of soldiers but also destroys the communication network of the soldiers, so that the quantity of data flow transmitted to the commander decreases while increasing the enemy numbers.

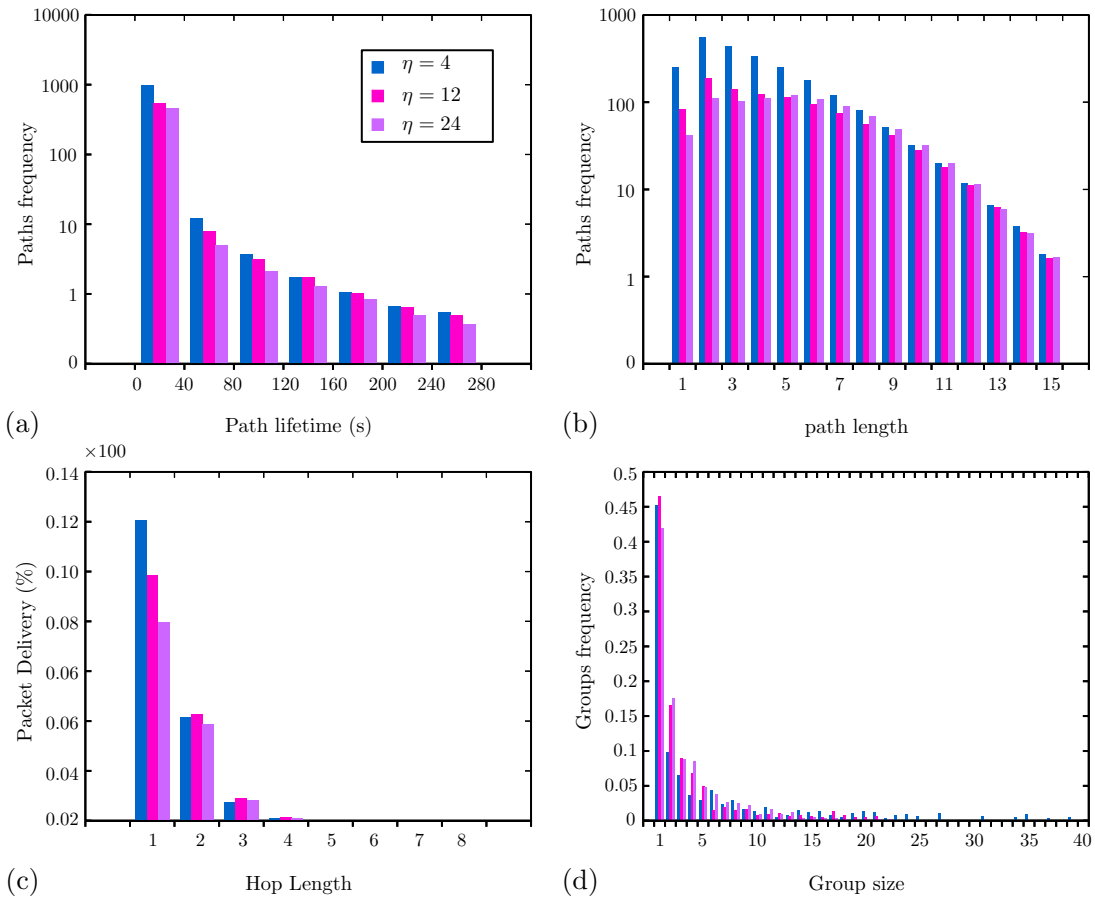

Figure 3.19 – Effect of increasing the enemy numbers (η) in the battlefield with parameters θ = 0, λ = 0.5, and $v_0 = 1\,(m/s)$: (a) Average path lifetime, (b) Average path length, (c) Packet delivery count, and (d) Average groups size.

Figure 3.19 depicts the results of the distributions of path lifetimes, path lengths, hop lengths and group sizes under a different enemy number. Figure 3.19 a-b clearly show the appearance of a high number of long paths with short lifetimes in the wireless communication network of the soldiers.

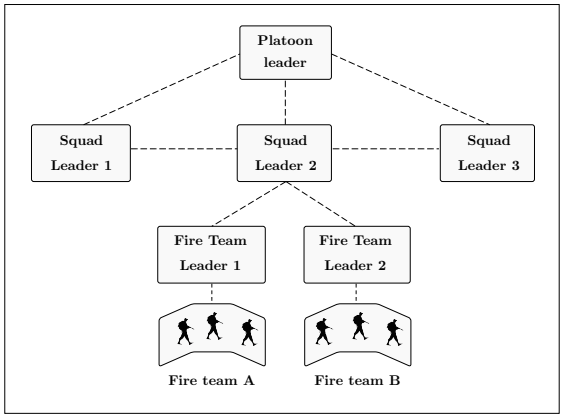

Figure 3.20 – Organizational structure of a platoon.

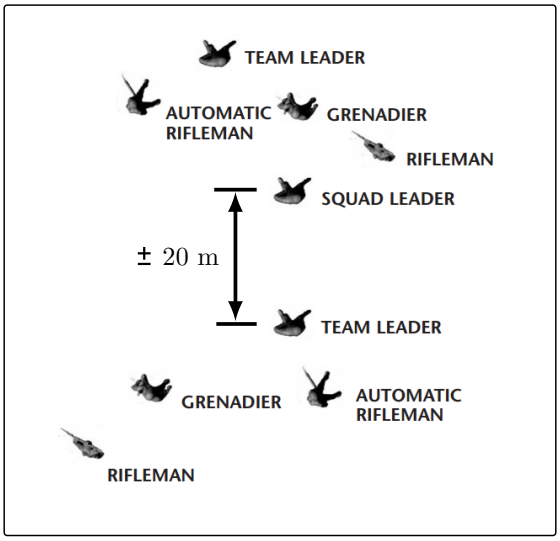

Figure 3.21 – Squad Traveling.

Thus, the presence of enemies on the battlefield causes a segmentation and disruption of the network topology and therefore causes a degradation of the network performance (see Figure 3.19 c). The enemy attacks are somewhat similar to the effect of the noise parameter. However, the main difference lies in the fact that the enemy attacks are more realistic than the noise effect. While increasing the noise level decreases exponentially the throughput at the sink node, the increase of enemy numbers decreases proportionally the throughput. This implies that although the network may suffer from higher link failures and topology changes because soldiers are escaping from the enemy. As a consequence, only the short paths may be established between the soldiers. Finally, the results show that the performance of the network was affected negatively by the presence of enemies on the battlefield. From these results, a high rate of dropped packets and a low rate of packets delivery have been observed. Indeed, in the presence of enemies, the highly dynamic and the sparse distribution of soldiers in the battlefield, lead to a decrease in path lifetimes and an increase in path lengths, which sharply degrades the network performance. Thus, there is a need to develop new decentralized infrastructures based on mobile ad hoc networks capable of routing the urgent data of soldiers on the battlefield in a short time.

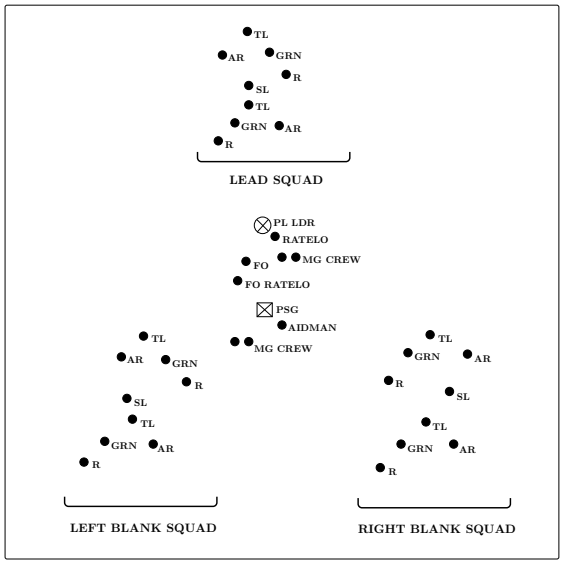

Figure 3.22 – Illustration of wedge formation which has two squads in the rear that can overwatch or trail the lead squad.

3.5.6 Scenario 3 : Simulation of a dismounted soldiers' squad

Here, we extend our model described in Section 3.5.1 to support the ability of dismounted soldiers to follow a preferred direction towards a predefined target. This can be done via choosing a proportion p of the individuals who are already given information about a preferred direction (simulated as a unit vector $\mathbf{g}$) representing the destination to a known resource or enemy location [63]. All other individuals are naïve and are not aware that there is a preferred direction, nor do they know which members of the group have this information. Then, the informed individuals balance the influence of their preferred direction towards a target $\mathbf{T}$ and their social interactions with weighting term ω, as described in [53].

We assume that N dismounted soldiers move at a constant speed of v_0 units per second. Each soldier is characterized by his location $\mathbf{p}_i(t)$ and velocity $\mathbf{s}_i$ of direction $\mathbf{d}_i(t)$ at time t. In each time step t, a member i assesses the position and/or orientation of neighbors in its local neighborhood within only two non-overlapping behavioral zones (Figure 3.23) to determine its desired direction of motion $\mathbf{d}_i(t+\Delta t)$ at time $t+dt$. After that, the member i turns towards the direction vector $\mathbf{d}_i(t+\Delta t)$ by the turning angle $\alpha_i \Delta t$, where

$$\alpha_i = \sigma + \chi \tag{3.9}$$

where σ is the turning rate, χ is a random angle taken from a circular-wrapped Gaussian distribution, centered on 0, with standard deviation χ radians gaussian-distributed angle. The location of the member i at time $t+\Delta t$ is given by :

$$\mathbf{p}_i(t+\Delta t) = \mathbf{p}_i(t) + \mathbf{v}_i(t+\Delta t)\Delta t \mathbf{s}_i \tag{3.10}$$

3.5.6.1 Behavioral rules description

In this section, we take into account the ability of grouping individuals within two independent groups (e.g., the lead team and trail team) and the degree of interaction between them needed to develop dominance relationships. These relationships allow individuals to move together as one group forming a rifle squad. Based on the interactions between soldiers and teams, our potential purpose is further to model a squad column known as a movement

Table 3.2 – Mobility model parameters used in the simulation.

Parameter	Symbol	Value
Number of soldiers	N	9
Zone of repulsion	Z*o*R	10 m
Zone of attraction	Z*o*A	50 m
Zone of orientation	Z*o*O	50 m
Number of groups	-	1
Number of teams	-	2
Turning rate	σ	2 rad
Initial velocity of nodes	v_0	1 (m/s)
Packet sending rate	λ	2 and 5 (packets/s)
Time step	dt	0.2 (s)
Standard deviation	χ	[0,2] rad

formation and a movement technique used in the battlefield area. In the battlefield area, the squad traveling movement technique is used when enemy contact is not likely. This movement technique offers the best speed and control during the maneuver, the trail team follows closely behind the lead fire team. In this chapter, we are interested in incorporating both the movement formation and movement technique of a squad by considering mathematical modeling and a set of simple rules responsible for soldiers' behaviors.

3.5.6.2 Repulsion behavior

We use the definition of repulsion behavior described in Section 3.5.1.3 .

3.5.6.3 Attraction and orientation behaviors

Each dismounted soldier i attempts to become attracted towards n_a, and aligned with n_o neighbors within both the zone of attraction and orientation (ZoA and ZoO), centered on the

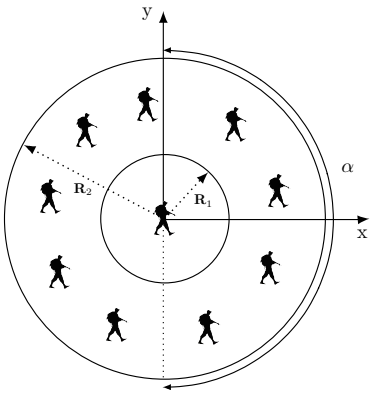

Figure 3.23 – Representation of a member in the model centered at the origin : R_1=zone of repulsion, R_2=zone of orientation and attraction, and α is the field of perception ahead of the member.

dismounted soldier i with radius R_2.

$$\mathbf{d}_i(t+\Delta t) = \sum_{j}^{n_o} h_j \frac{\mathbf{v}_j}{|\mathbf{v}_j|} + \sum_{j\neq i}^{n_a} h_j \frac{\mathbf{r}_{ij}}{|\mathbf{r}_{ij}|} \tag{3.11}$$

where $\mathbf{v}_j$ is a unit direction vector of soldier j. In our scenario, h_j is always equals to 1 except of squad leader, where $h_j = 2$ so as to give him a higher priority [64].

Here $\mathbf{d}_i(t+\Delta t)$ is converted to the corresponding unit vector $\hat{\mathbf{d}}(t+\Delta t) = \mathbf{d}_i(t+\Delta t)/|\mathbf{d}_i(t+$

Table 3.3 – Network model parameters used in the simulation.

Parameter	Value
Propagation model	Propagation/TwoRayGround
Network area	$5000m \times 5000m$
Packet generator	CBR
Transmission range	60 m
Simulation time	1000 s
Queue size	64 packets
Transport protocol	UDP
Routing Protocol	AODV
CBR packet size	1000 bytes

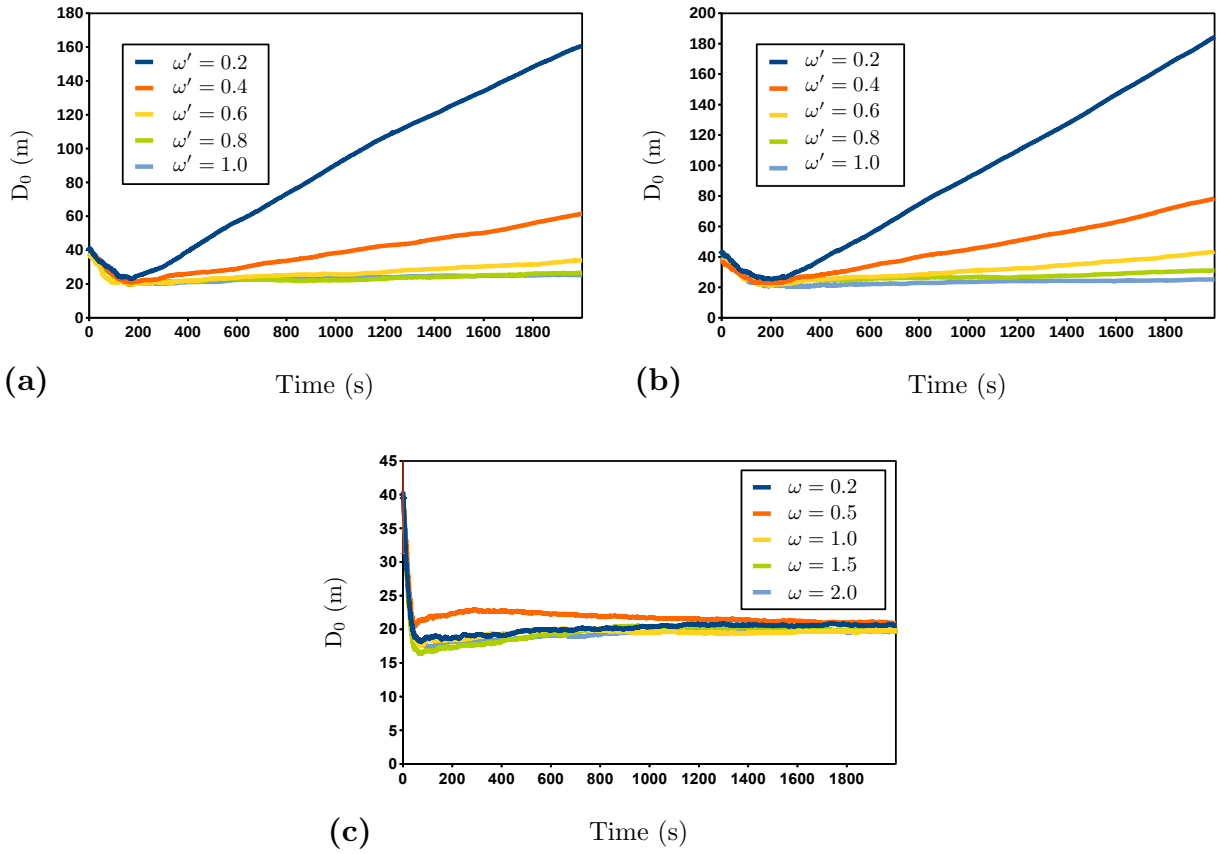

Figure 3.24 – Effect of increasing the weighting term ω′ on the distance between trail team and lead team in the case of ω=0.5 (a) and ω=1 (b). (c) shows the variation of the distance between the trail team and the lead team when using our mathematical model as a function of ω value.

$\Delta t)|$.

To incorporate the influence of informed group members, a proportion of the individuals p are given information about a preferred direction (simulated as a unit vector g) representing the destination to a known resource or enemy location [53]. However, in our considered scenario with ($p = 1$). The informed individuals balance the influence of their preferred direction and their social interactions with weighting term ω, as follows :

$$\mathbf{d}_i'(t+\Delta t) = \frac{\hat{\mathbf{d}}_i(t+\Delta t) + \omega g}{|\hat{\mathbf{d}}_i(t+\Delta t) + \omega g|} \tag{3.12}$$

where ω is weighting term used by the members of lead team, whereas the members of trail team use ω′ as weighting term towards the lead team (e.g. the destination of trail team is the lead team). The destination position is chosen randomly within the simulation area.

After a detailed analysis of the variation of ω′ as a function of ω (see Figure 3.24), we found that ω′ is given as follows :

$$\omega' = \begin{cases} \dfrac{d}{d_0}\left[\exp(d-d_0) + \ln(\dfrac{\omega}{4})\right] & \omega < 1, \\ \dfrac{d}{d_0}\left[\exp(d-d_0) + \omega\right] & Otherwise. \end{cases} \tag{3.13}$$

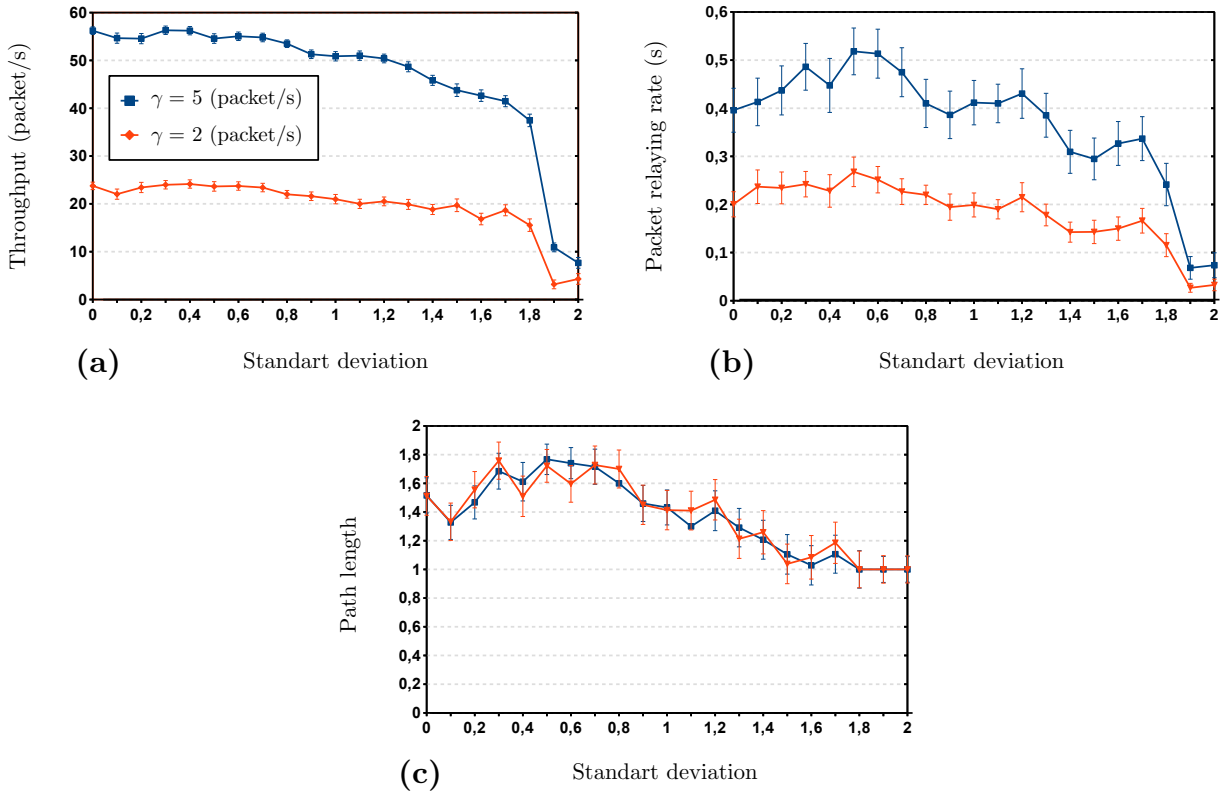

Figure 3.25 – Effect of increasing the standard deviation : (a) Throughput, (b) Packet relaying rate and (c) Path length.

3.5.7 Results and discussion

3.5.7.1 Network Model and simulation parameters

Our group mobility model has been implemented using Java and can generate mobility traces. To evaluate our model in terms of network performance, we perform Network Simulator (NS)-2 simulations to observe and analyze the impact of soldiers' dynamics on the reliability of communications using the mobility traces of soldiers in the battlefield area generated from our Java simulator.

Our network contained N mobile nodes/soldiers deployed close to each other in a simulation area of 5000×5000 m^2. At each time step dt. The soldiers/nodes can exchange data packets based on AODV routing protocol with a data generation rate (λ). The squad leader can exchange communications with their neighbors in the squad.

3.5.7.2 Evaluation of dismounted soldiers network versus standard deviation

Here, we consider the squad mobility scenario to study the impact of soldiers' dynamic in the battlefield area on the performance of the network. We evaluated the network performance under different packet sending rate λ and perturbation levels χ (standard deviation). The perturbation of the soldiers' mobility is expected to simulate several effective factors in the mobility environment such as obstacles, crossing forests, and rivers.

From Figure 3.25 a, it is shown that the average throughput decreases significantly as a function of the standard deviation. Moreover, when the standard deviation becomes higher, the throughput decreases significantly, especially in the range [1.8, 2]. We can explain that by the fact that the increase in the standard deviation can hardly cause a topology change due mainly to perturbation of the collective motion of dismounted soldiers allowing soldiers to move with low accuracy. As a consequence, an arbitrary partition of the network topology occurs when the standard deviation reaches a higher level.

Figure 3.25 b shows the effect of increasing the standard deviation on the relaying rate of packets by intermediate nodes. It is observed that the relaying rate of packets is also affected by the increase in the standard deviation. This illustrates that the nodes encounter a difficulty to find stable paths for relaying unrelated packets as the standard deviation increases. This is due mainly to the bad condition of the network topology which results from an increase in the link failures when the distance between two soldiers becomes higher than the transmission range.

Figure 3.25 c shows that the path length increases as the standard deviation increases until reaching a maximum length of 0.5. But, it starts decreasing as the standard deviation continues increasing. We can explain that by the fact that the network topology is elongated when the standard deviation is (<= 0.5). However, when the standard deviation is increased enough (> 0.5), the network is partitioned info small clusters and isolated nodes. This is sufficient to explain why the path length is decreased : the source node cannot establish a path with the destination node if there are not sufficient nodes that can participate as relay nodes in this path.

3.6 Contribution 2 : On the relationship between tactical mobility and energy-efficiency in WSN

Recently, WSNs have been emerged among the most attractive research field for enabling different categories of applications [65]. A wireless sensor network is a group of multiple detection stations called sensor nodes. Every sensor node is equipped with a transducer, micro-

computer, transceiver and power source. The transducer generates an electrically measurable signal based on the environmental and physical variations. The microcomputer processes and stores the sensor data. The power for each sensor node is derived from a battery. Many applications for wireless sensor networks are proposed in different application fields, including animal behavior classifying and Health Monitoring [66, 67], Energy generation [68, 69], and localization techniques [70].

The efficiency of these applications, however, is hampered by requirements such as reliability, battery-life, transmission range, frequencies, size of the network, etc. Wireless sensor networks are formed by small sensor nodes communicating over wireless links without using fixed network infrastructure. Sensor nodes have a limited transmission range, and their processing and storage capabilities, as well as their energy resources, are also limited. There have been many attempts to improve the efficiency of wireless sensor networks in terms of energy consumption by introducing varying protocols. These protocols can be classified into three classes. Protocols in the first-class make routing decisions based on residual energy. These protocols are known as clustering-based protocols, where sensors are distributed into many clusters capable of communicating the detected events to a central location. A clustering-based protocol can utilize the randomized rotation of local cluster base stations (cluster-heads) to evenly distribute the energy load among the sensors in the network. This method can provide scalability and robustness by incorporating the collected data within each cluster into the routing protocol to reduce the amount of information that must be transmitted to the base station. Moreover, the collected data can be transmitted by the cluster heads via single-hop [71] or multi-hops communications [72]. Protocols in the second class make routing decisions based on the control of the transmission power level at each node to increase network scalability [73]. This implies that the node chooses the transmission power level for every packet in a wireless ad hoc network. In this context, different properties are taken into consideration to control the transmission power. For example, the solution proposed in [74], where a network layer protocol called COMPOW, ensures that the transmit power used by all the nodes would converge to a common power level : the lowest power level at which the network is connected. However, these types of protocols take into consideration the additional relaying burden as they use in most cases a low transmitting power level to send packets which causes an increase in the number of hops and the end-to-end delay [75]. Protocols in the third class take into consideration the control of the network topology by determining which nodes should be awake to participate in the multi-hop network topology and which should remain asleep [76–78]. This method allows nodes to reduce energy consumption by using multi-hop communications to avoid sending large amounts of data over long distances. However, the selection of sensors which should be awake or not remain a challenging problem due to unpredictable propagation effects in the environment. This means that sensors are not able to have uniform connectivity.

Another class of approaches is based on using different flooding algorithms to reduce the consumption of the energy and collision occurrence in sensor networks related mainly to an increase in density of sensor nodes. Several solutions were proposed in the literature, for example : reducing the number of rebroadcasts [79], considering a selection of eligible neighbors to rebroadcast [80], or introducing a new routing algorithm based data-centric routing and address-based routing schemes [81].

Recently, many studies have proposed applications based on the behavior of the flock in sensor networks for different purposes. For example, in [66, 69], authors introduced novel sources of energy generation rather than operating sensors only on limited power. The proposed conversion of energy from mechanical to electrical based on the head movements of individual sheep in a flock during grazing were monitored to investigate the amount of energy that can be generated by these movements. In [82], the authors proposed a simple motion control algorithm

in the field of autonomous robotic sensor networks that operates in a pure autonomous manner. Based on the proposed algorithm, a sensor can move, sense and communicate with each other in a cooperative way. Also, these algorithm models the coverage demand into the virtual force field, and hence each sensor can simply obey the effect of force field onto it to move. In the same context, authors in [83] address the problem of coverage in sensor networks using a Voronoi-based algorithm that leverages the converged movement towards Voronoi cells centers with the intelligent nodes provisioning an algorithm to deliver a fully automated and autonomous sensor network. On the other hand, authors in [84] introduced an attempt to mimic the scale-free behavior in swarms of autonomous agents, specifically in Unmanned Aerial Vehicles using an agent-based model. In [85], the authors proposed a new flocking control algorithm and distributed filter to solve the two-targets tracking problem. All mobile sensors can split into two groups to track their target and form a cohesive flock with their neighbors based on the interaction between followers in different groups. In [66], the authors introduced an application scenario of a group of animals' group equipped with sensors that monitor their health state.

In this chapter, we considered a scenario that is frequently observed in the real-world and it may be one of the scenarios that will get increasing attention in the next generation of sensor networks applications. Our attention is oriented to simulate sensor networks in the context of some scenarios such as a military group of soldiers equipped with sensors, a squad of multiple teams with a soldier leader who must be informed about the health of their neighbors, or a sensor network formed by a group of mobile robots capable of tracking a target and monitoring specific events around it. Accordingly, we consider a similar case of sensor networks applications, where a scenario includes a group of autonomous agents capable of moving collectively to reach a specific distant target is introduced. We aim especially to investigate the impact of some effective mobility parameters that can lead to an emergence of such a design of agents' dynamics within the group and therefore to identify a clear relationship between the emerged mobility design and its impact on the network lifetime in terms of energy consumption. We monitor the behavior of agents' dynamics and the sensor network based on two main performance metrics, including the residual energy and the number of sensors nodes still alive.

3.7 Conclusion

To simulate and analyze dismounted soldiers' dynamic aspects, the first important step in this chapter was modeling dismounted soldiers' mobility as realistically as possible. Our strategy is then based on the collective motion behavior, where dismounted soldiers' dynamics are governed by using three basic rules to allow individuals to interact collectively between each other [54, 59]. In this chapter, we studied three tactical mobility scenarios frequently encountered in realistic tactical networks. The first scenario represents a simulation of a dismounted soldiers' group dynamic in the battlefield based on collective motion behavior. The wireless network is evaluated in terms of several effective factors that are expected to perturb communications on the battlefield such as noise, speed and other parameters of the network model. Simulation results demonstrate the effectiveness of collective motion for more reliable paths and for improving the stability of the network. However, noise strongly affects the network topology state, causing partitioning and nodes dispersion.

The second scenario extends the first one by taking into account dismounted soldiers' dynamics with the presence of enemies. As the soldier's dynamics are constrained by the presence of enemy attack, the obtained results depicted that the throughput of packets received by the commander decreases as the number of enemies increases. This is due to limitations in terms of relay nodes and insufficient link quality, which are mainly due to the great dynamics of soldiers trying to escape enemy attacks.

In the third scenario, a dismounted soldier's squad consisting of two teams, including a lead team and a trail team is introduced. We perform simulations for the dismounted soldiers' movement in the case of the traveling squad. We provided detailed modeling and analysis of the dynamic of both teams in the battlefield area. The simulation results show that the network performance is more sensitive to the dynamic of soldiers in the simulation area. Moreover, the standard deviation of the soldiers' movement direction has a much higher impact on the throughput, related/unrelated packets and path lengths.

In the last considered scenario, we used another tactical mobility scenario designed to analyze the relationship between tactical mobility and energy efficiency. Our results show that the sensor network is very sensitive to agents' dynamics in the simulation area. It is found that noise has negative effects on both the cohesion of the group and on the sensor network's lifetime while the weighting term has positive effects on both the level of group's attraction towards the target and sensor network.

The next chapter will deal with a general review of the most known services provided by smart cities, including a detailed description of smart mobility and new wireless technologies. Next, we will introduce two intelligent mobility strategies. The first strategy concerns Real-Time Path Planning in road networks to reduce vehicle traveling times. The second strategy concerns a collision probability estimation method in an urban environment that uses DSRC-based V2V Communications, to avoid collisions at intersections between approaching vehicles.

Chapter 4

On the Simulation in Smart Cities

« *A person who never made a mistake never tried anything new.* »

Albert Einstein

Contents

This Chapter provides two main parts. In the first part, we present an overview of intelligent mobility as a fundamental feature of smart city technologies and wireless communication standards. In the second part, we propose two different smart city strategies. The first strategy, which is called Real-Time Path Planning strategy, is developed to reduce vehicle traveling time and to avoid congestion problems due either to an increase of the car density or to some unexpected events such as car accidents. This strategy allows vehicles to select reliable paths from a central server based on V2V and V2I communications. The second strategy we propose a novel collision prediction method in an urban environment by using DSRC-based V2V Communications. This method is designed to predict collisions at intersections between approaching vehicles based on the calculation of probability of collision. The main purpose of our strategy is providing an estimation of risk for each pair of approaching vehicles based on a probability of collision by using a cooperative awareness message (CAM) that vehicles can exchange periodically. Each massage can includes vehicles information such as current position, speed and acceleration.

4.1 Smart Cities

The appearance of the smart city's concept is related to many factors. These factors include cities which have been increasingly afflicted by spatial issues due to high urban growth, technological developments and people trying to get a high quality of life. All these causes have participated in the appearance of smart cities revolution in the whole world. Smart cities focus on the exchange of information between different technological components and infrastructures. Additionally, the term governance plays an important role in the concept of smart cities as well as networking and partnerships between different sectors like businesses, non-profit organizations, governments, and citizens. Also, smart cities focus on energy transition in different smart cities' projects as a principal parameter that can have a high influence on the success of such project. Several services are identified as the main areas of services needed as requirements to take into consideration to create a smart city.

1. **Urban planning :** Urban planning is a very important and basic element in smart cities due to its ability to define the fundamental needs in terms of urban environments design. It then helps to determine the needs linked to a specific design of infrastructure that the other services should be created for. It is considered as the main part of the smart city which aims to connect all the other parts of the city by providing flexible interactions in terms of needs and efficient control of all parts in the smart city.
2. **Smart energy :** Is one of the fundamental components of Smart Cities that defines the criteria of efficient energy dissemination and optimization within the entire community to achieve a high quality of living. This can include efficiency in public lighting, renewable energy installations and smart energy. This is expected to reduce carbon in the society and also to make harder control of energy sources in the smart city.
3. **Smart security :** The goal of security in smart cities is to ensure a high level of safety for citizens based on smart emergency services. These services can include identifying the emergency type and notification method and finally selecting the related emergency service. The main parts of emergency services include Ambulance, rescue service and Police, but with smart management based on new technologies of communication and localization.
4. **E-Health :** As heath is the most important issue for humans ; in smart cities, the E-Health will play an important role in the treatment and monitoring of health problems based

on a broad range of information and communication technology systems. These technologies are capable of giving an efficient control of health data for the patient to provide health services in real-time. Also, there will be smart systems and software supporting

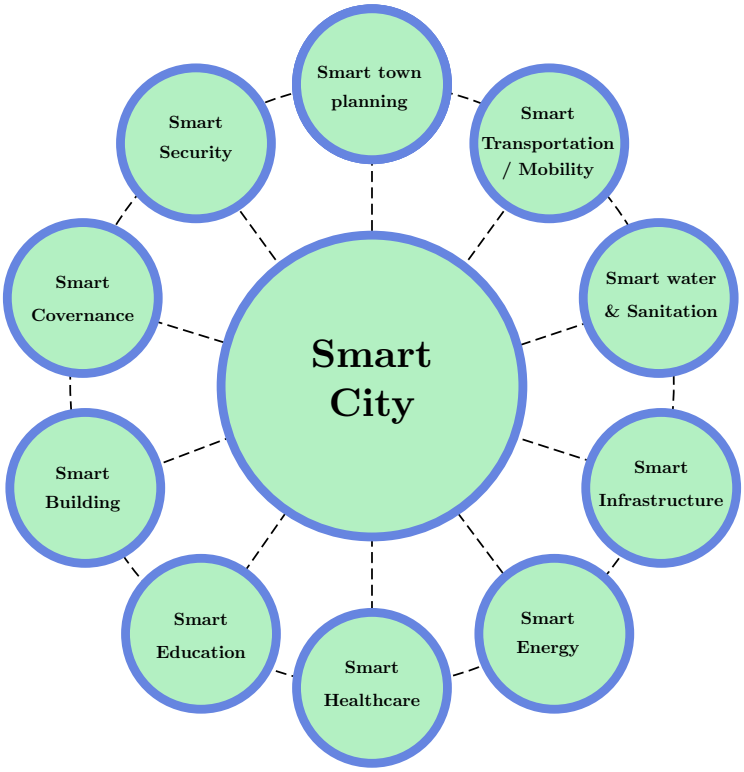

Figure 4.1 – Smart city structure : the main areas of services within smart cities.

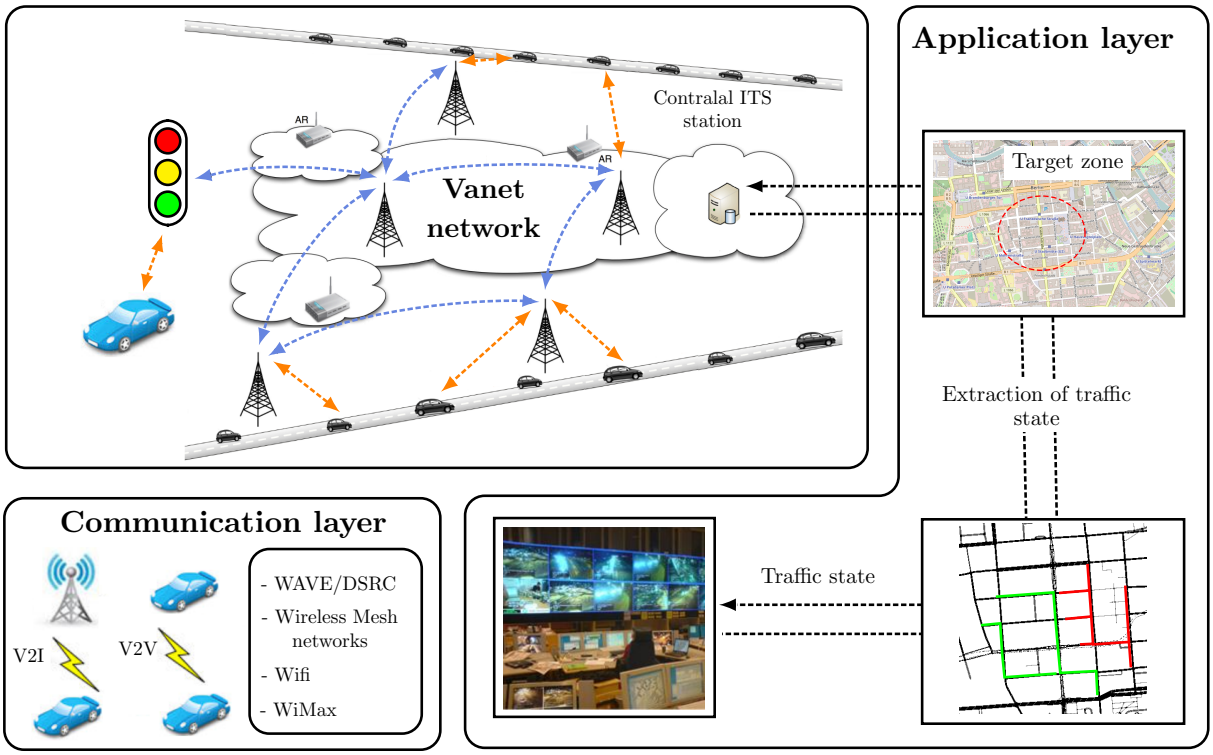

Figure 4.2 – Intelligent Transportation Systems and Vehicular Wireless Communication Networks.

health care messaging and medical devices.

5. **E-Government :** The E-government refers to the government which uses the ICT to provide easy access to different types of information for citizens. The goal of E government is to make the relationship between the government and the citizens more transparent, democratic and efficient. This can allow the establishing of a confidential relationship between the government and citizens and can participate in increasing the development of businesses due to a high level of engagement by all actors.

4.2 Smart Mobility

Smart mobility is one of the core services of smart cities as it is linked directly to human quotidian activities and dependent on a set of sectors that are characterized by high dynamics, including transportation systems and mobility of the citizens. The objective of smart cities is to improve the modes of transport and traffic management within transport networks to efficiently and safely use the transport infrastructure. Also, smart cities focus on reducing energy and resource consumption and greenhouse gas and other polluting emissions while considering traffic management within transport networks. Moreover, Smart mobility may provide more efficient services due to its intelligent infrastructure based on new communication technologies such as **VANET!** (**VANET!**).

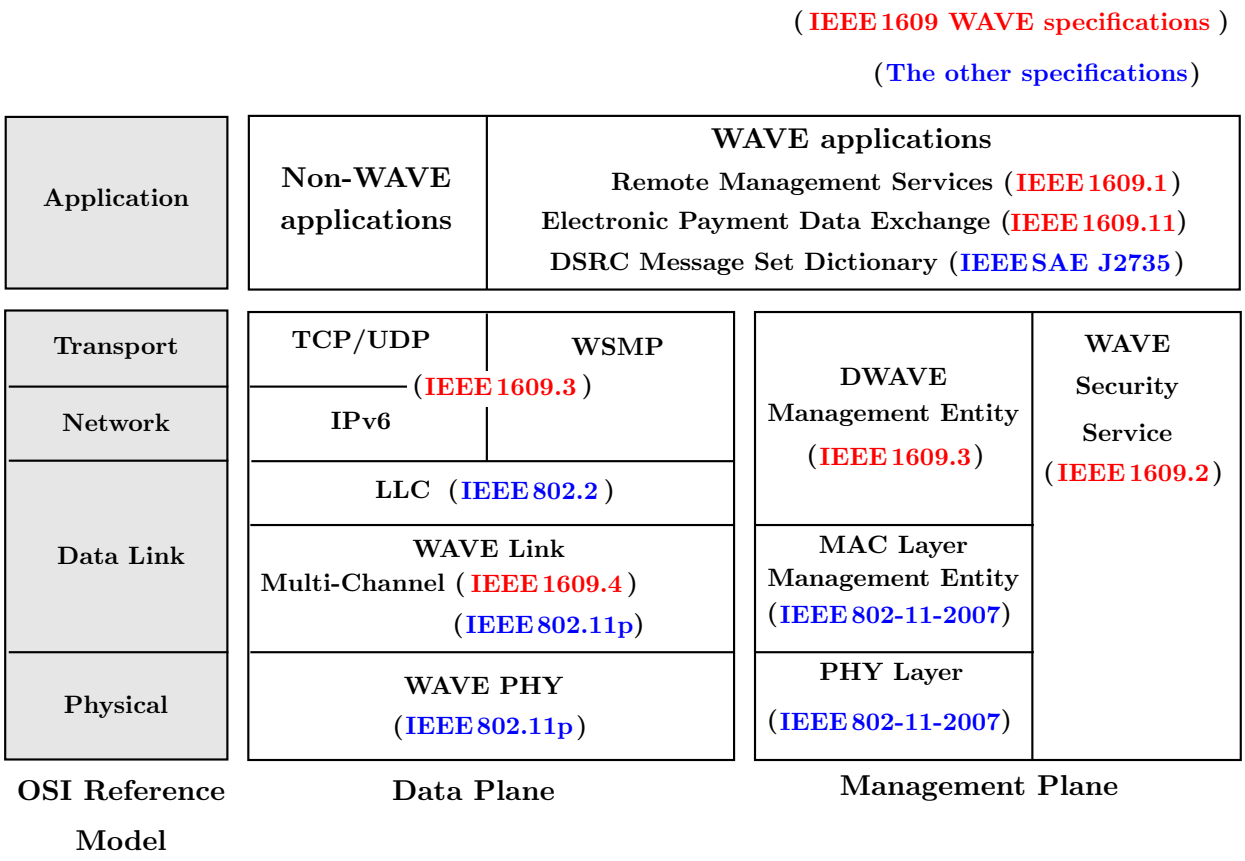

Figure 4.3 – Communication Standards.

4.2.1 Adhoc Network Technologies

Wireless Ad-hoc Networks (WANETs) is designed to enable wireless communications based on a decentralized approach. Nodes in WANET can communicate between themselves when they are in the communication range of each other or participate in routing by forwarding data for other nodes as routers. The ability of nodes to forward data for other nodes is considered a basic functionality that makes WANET work more dynamically, especially when a routing algorithm is used to allow connectivity with distant nodes from the source nodes. We can classify WANET into two main types of wireless networks : MANETs and VANETs.

MANET is designed to enable wireless communication between nodes in dynamic topologies without any infrastructure. The goal of considering MANETs is to adapt wireless communication to topology changes. For this purpose, MANET nodes must exchange control messages to establish the routes used to forward data packets based on a forwarding strategy or a routing protocol. The need for such routing protocol is because the network connectivity is worsened due to topology changes driven by wireless links and unpredictable mobility of nodes. This problem can be observed especially in some tactical scenarios in which dismounted soldiers move on the battlefield during the execution of their missions.

In the last decade, VANET have known a rapidly increasing development because it is considered as a promising concept to enable numerous categories of applications for improving traffic safety, avoiding traffic road congestion, and for other real-time applications [86]. Moreover, VANET is expected to allow drivers to receive information from nearby vehicles on events that are detected on the road as well as to receive data from the RSUs deployed on the road infrastructure. This received information enables drivers to take the right and the timely decisions as a better reaction to some sudden events on the road. Moreover, VANET can also provide V2V and V2I communications to allow vehicles to communicate with each other anywhere in the urban environment. For example, the RSUs can allow vehicles to exchange information between each other under long distances. This makes VANETs capable of providing the reliability of communications under even low density of vehicles. Unlike MANET, VANET suffer from some problems such as high speed of vehicles, unexpected turning of vehicles participating in already established routes, and sudden stopping of vehicles when they reach their destinations.

4.2.1.1 Wireless Communication Standards

In the past, the development of wireless technology concerned two main types of networks : voice and data networks. The voice-oriented networks come in the first order, followed by data-oriented networks. Recently, the progress of communication technology allowed the market for data oriented products and services to increase mush faster than voice-oriented products and services. Moreover, the current wireless technology can efficiently transport voice, audio, and video in addition to data.

Before reviewing the existing communication standards, we first need to give a short representation of the standard Institute of Electrical and Electronics Engineers (IEEE). The IEEE is a professional association for advanced technologies. This professional association is the leader for advanced technologies and is also responsible for the definition of most existing communication standards, including IEEE802.15.1 for Bluetooth, IEEE802.11a/b/g for Wireless LAN whereas IEEE802.11p is defined to support vehicular communications. The publication of IEEE 802.11p standard was in 2010 due to the need of a mobile vehicular environment which is characterized by a high dynamic and high speed of vehicles. This standard is an approved amendment to the IEEE 802.11 standard to add Wireless Access in Vehicular Environments (WAVE). This standard comes to support ITS applications. This includes data exchange between high-speed vehicles and between the vehicles and infrastructure, so-called V2V and

V2I communications.

However, several limitations hindering the development of WAVE networking service protocols such as those related to communication between the vehicle and service provider, those related to high-speed of vehicles, and those related to a lack of homogeneous communication between different automotive industries. All these limitations were sufficient to express the need for a strong WAVE architecture capable of responding to all WAVE application requirements. The arrival of the IEEE 1609 family of standards has the purpose of overcoming these limitations. The IEEE 1609 describes the WAVE architecture and all services necessary for multi-channel DSRC/WAVE devices to exchange data in a mobile vehicular environment. The standard IEEE 1609.1, for example, explains the level of the application layer to allow WAVE applications at remote sites to communicate with On-Board Units (OBUs) through Roadside Units (RSUs). In Data Plane, based on the OSI model, Figure 4.4 shows that IEEE 1609.3 incorporates other specifications related to Data plane for both existing applications and WAVE applications. These specifications include data in the Transport layer and Network layer, by either using TCP/UDP/IPv6 to support existing Non-WAVE applications or either Short Message Protocol (WSMP) to support WAVE applications. In the data link layer, Logical Link Control (LLC) uses specifications defined by the standard IEEE 802.2, whereas WAVE MAC follows the specification of both IEEE 802.11p and IEEE 1609.4 to support multi-channel operations including Control Channel (CCH) and Service Channel (SCH), respectively. In Management Plane, IEEE 1609.3 comes to explain how to adopt suitable secure message formats and how to process them within WAVE systems. For this purpose, this standard also describes administrative functions needed to respond to the constraints of security, including both MAC Layer Management Entity (MLME) and PHY Layer Management Entity (PLME).

4.2.1.2 Channel propagation models

Among the main characterization of wireless channels, is the propagation of electromagnetic wave propagation between the transmitter and the receiver which can be modeled as falling off as a power-law function of the distance due to the attenuation phenomenon. Thus, only a portion of the transmitted wave's energy will reach the receiver antenna. If there is not a direct line-of-sight path between the transmitter and the receiver, the transmitted electromagnetic

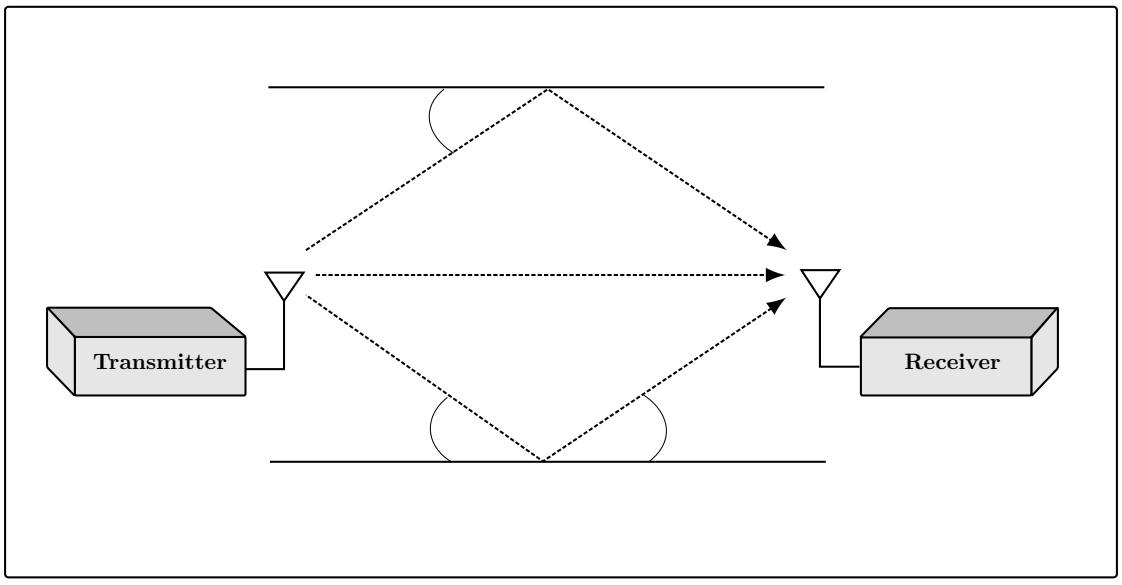

Figure 4.4 – Propagation of electromagnetic wave propagation between the transmitter and the receiver.

wave will encounter different types of objects in the environment. This will allow it to arrive at the receiver from different paths at different times.

1. **Free-space Model :** It is the most basic model of Radio Frequency (RF) propagation. The free space propagation model is used when there is a direct LOS wave propagation between the transmitter and receiver. It predicts the received signal strength versus the crossed distance by the transmitted electromagnetic wave. As the transmitted wave energy decays with the increase of distance between the transmitter and the receiver, the free-space model models the degradation of signal strength with an inverse square rule, or 20 decibels (dB) per decade. So, the received power will be given by the free space equation as follows :

$$\mathbf{P}_r(d) = \frac{\mathrm{P}_t \mathrm{G}_t \mathrm{G}_r \lambda^2}{(4\pi d)^2 \mathrm{L}} \tag{4.1}$$

   where $\mathbf{P}_r(d)$ is the received power given a transmitter-receiver separation of d, P_t is the transmit power, G_t is the gain of the transmitting antenna, G_r is the gain of the receiving antenna, d is the distance between the transmitter and the receiver, and $\mathrm{L} > 1$ is the system loss factor not related to propagation.

2. **Two-ray Interference Model :** The two-ray ground propagation model models electromagnetic wave propagation in the case where there is no direct line-of-sight path between the transmitter and the receiver. In this case, the transmitted wave will encounter different types of obstacles such as buildings or the ground which will cause reflection, diffraction or diffusion of the wave depending on the distance between the sender and receiver and the type of obstacles encountered. This phenomenon is called multipath fading, which can also be modeled as a power-law function of the distance between the transmitter and receiver as follows :

$$\mathbf{P}_r(d) = \frac{\mathrm{P}_t \mathrm{G}_t \mathrm{G}_r h_t^2 h_r^2}{d^4} \tag{4.2}$$

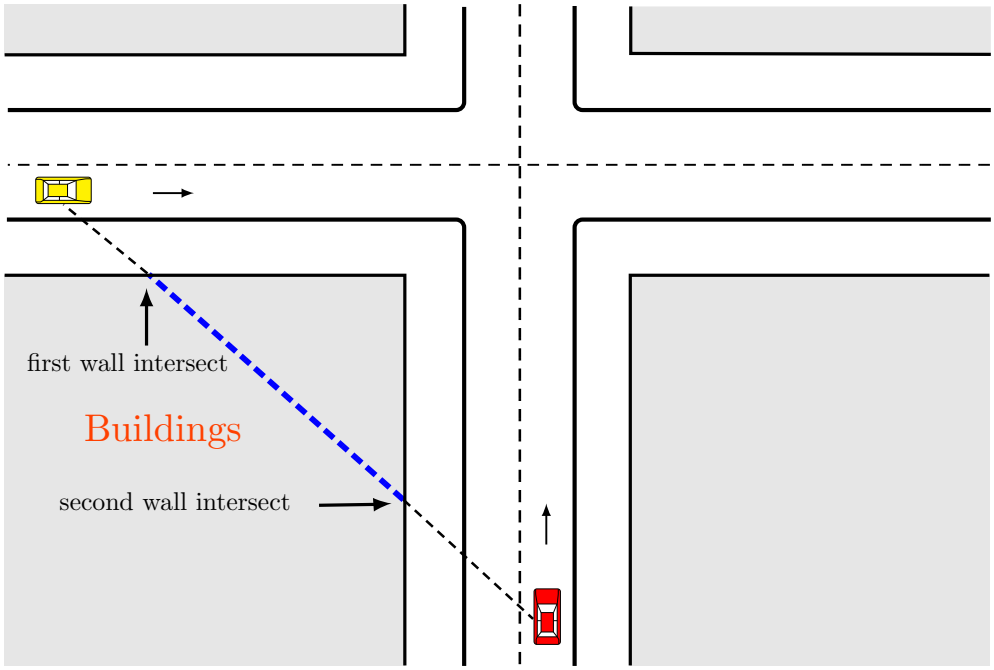

Figure 4.5 – Illustration of the Obstacle Shadowing Model

where h_r is the height of the receiving antenna above ground, h_t is the height of the transmitting antenna above ground.

3. **Obstacle Shadowing Model :** This model is interested in the effects of obstacles between the transmitter and the receiver. These obstacles can therefore inaccurately overstate network performance by causing a considerable path loss when the signal is received. The Obstacle Shadowing Model combines different approaches for calculation of the signal propagation path loss by accounting for the attenuation caused by walls and the distance within obstacles (see Figure 4.5). It considers path loss exponents when the wireless signal is traveling through matter and free-space. The model allows calculating the attenuation based on the number of walls that need to be penetrated.

4.3 Contribution 1 : The Impact of Real-Time Path Planning on Reducing Vehicles Traveling Time

ITS have received wide interest in academia and industry research due to the development of VANET and its ability to enable different categories of applications. These applications can include strategies to improve traffic safety, avoiding traffic moving congestion, and Global Position System (GPS)-based navigation systems [86].

Congestion problems are known as a transition phase between free-flow state and complete gridlock. Imperfect driving plays an important role in the formation of traffic jams within the transportation system, especially when it is combined with the increase of the density of vehicles [26]. Indeed, when the density of cars increases, drivers' attention reduces and the imperfections in their driving styles increase. Most often traffic jams are observed at roundabouts, crossings of roads, and intersections of highways [87]. For example, a jam may appear just due to some traffic interweaves at roundabouts caused by imperfect driving styles.

In the last decade, there have many attempts to solve traffic congestion problems caused by high increase of car density, imperfect driver behavior or accident events. However, most of the proposed approaches, such as modifying traffic road network or modernizing road infrastructure, do not satisfy the requirements due to the limitation of resources (e.g., cost and spaces) and the rapid increase in the number of vehicles. Recently, the appearance of ITS and the development of VANET have initiated the tentative of resolving traffic problems with a different way : they adopt recent technological solutions and intelligent applications based on wireless communications between vehicles or between vehicles and the infrastructure. Most of the proposed ideas have considered strategies such as path planning or vehicle-to-vehicle communications for cooperative congestion avoidance.

All these strategies are based on a real-time exchange of information about traffic conditions between vehicles and RSUs. For example, the authors in [88] proposed a new method to dynamically calculate the current traveling time in a street by using RSUs at the start and the end of each street. The efficiency of the proposed method is investigated in a real city using as a VANET scenario based on a simulation framework including SUMO, OMNET++, and Veins. However, the authors did not report how vehicles trigger broadcasts of the calculated travel time when they reach the end of the street. In [88], the authors proposed a real-time path planning algorithm, which not only improves the overall spatial utilization of a road network but also reduces average vehicle travel cost and prevents vehicles from getting stuck in congestion as well. The proposed algorithm is based on a stochastic Lyapunov optimization technique that is exploited to address the globally optimal path planning problem. The results show that the proposed path planning algorithm outperforms the traditional distributed path planning in terms of balancing the spatial utilization and drivers' travel cost. In [89] the authors intro-

duced a novel dynamic vehicular path planning solution. The proposed solution does not rely on infrastructures to collect traffic information. Instead, it utilizes a density-speed traffic flow model to predict the traffic condition. Also, a dynamic candidate path selection algorithm is developed to reduce the redundant data collection overhead. This approach has been extensively evaluated using large scale traffic trace-based simulations. The obtained results show that the proposed approach outperforms some existing solutions in terms of communication efficiency and path planning effectiveness. In [90] the authors proposed a route planning algorithm to calculate the route with the shortest traveling time based on real-time traffic information by using VANET. At each road segment, a traveling vehicle can exchange information about traffic information with other neighboring vehicles by using the IEEE 802.11p standard and GPS navigation application implemented on the Android platform. This approach uses the average recorded driving speed as an indicator of traffic state at road segments. Another class of approaches is based on using path planning to reduce road traffic congestion and avoiding traffic jams in large cities. For example, in [91], to avoid traffic jams in large cities, the authors proposed an intelligent traffic system called CIDMERA, which improves the overall spatial utilization of the road network. CIDMERA also can reduce the average vehicle travel costs by preventing vehicles from getting stuck in traffic. In [92] the authors proposed a distributed and collaborative traffic congestion detection and dissemination system that uses VANET. This system is based on the use of the smart phone by each driver to detect a location through GPS. This information is sent to a remote server that detects traffic congestion. Once congestion is confirmed the congestion information is disseminated to the end-user phone through RSUs.

4.4 Contribution 2 : Estimating Vehicle Collision Probability at Intersections

The lack of safety at intersections is related to several factors, including bad weather conditions, imperfect driving styles, aggressiveness of some drivers, drivers who disregard traffic rules or traffic lights at intersections. However, with the development of ITS[93] and standardization of dedicated short-range communication DSRC using IEEE 802.11p [94], it will be possible to estimate a driver's safety level when approaching the intersection and then to adopt an effective strategy to alert the driver so he can react as quickly as possible. For example, in [95, 96], the authors introduced category applications defined as Intersection Collision Warning Systems (ICWSs), which can detect and warn the driver up to fully automated reactions. In [97], the authors investigated the issue of the timing for successfully detected collisions at intersections in the case of avoidance systems assuming DSRC transmission delays of 25 and 300 ms in normal and poorer channel conditions, respectively. For this purpose, the authors investigated mainly the time-to-avoid collision metric when the driver has received an alert about a probable collision and how it can avoid that within a limited time interval. They highlighted some events (the alert moment of the driver, the reaction of the driver, and the deceleration capability) and identified in which situation the driver can avoid the collision. To avoid arbitrary collisions with bicycles, authors in [98], proposed an algorithm that can estimate drivers' behaviors such as when the driver can steer, brake, or accelerate. It is based on lateral and longitudinal movements and vehicle dynamics and provides various approaches to model intersection approaching vehicles. In [99], authors focused on accidents at an intersection caused by driver error. Accordingly, they proposed a novel approach to risk assessment to identify dangerous situations by detecting conflicts between intention and expectation, i.e. between what drivers intend to do and what is expected of them. In [100], authors have highlighted the possibilities of future trajectory prediction based on an estimation and communication of vehicle positions and prediction using simple GPS receivers and motion sensors. In the same context, authors in [101], presented an evaluation scheme based on safety metrics to estimate future crash at intersections by quantifying the collision probability between vehicles approaching an intersection. For this purpose, each approaching vehicle can receive a beacon message that includes vehicle information such as position, velocity, and current acceleration. The authors investigated the impact of safety messaging between vehicles approaching an intersection with different beacon time intervals.

4.4.1 The critically of collisions at intersections

The safety at intersections is a critical issue that needs to be handled carefully due to difficulty related mainly to the prediction of drivers' behaviors at roads. Recently, several studies based on vehicular ad hoc networks were proposed to solve the problem of collision at intersections. However, most of them investigate the performance of the safety applications by highlighting only some problems related to wireless networks, while the challenges related to safety metrics still need more attention from the research community. So, here we take into account the importance of this issue and try to define efficient safety metrics in the first order to be able to provide confident safety applications for the driver. In the final part of our goal, we will validate and show the performance of our strategy when using it with simple beaconing based communications similarly as [101].

Chapter 5

General Conclusions and Future Work

« *The thing about quotes on the internet is that you can not confirm their validity* »

Abraham Lincoln

Contents

5.1 General Discussion

Motivated by the importance of mobility issues and the effective role it plays in ad hoc networks illustrated through different perspectives of applications, this thesis focuses on studying and analyzing mobility models designed for tactical networks and smart cities.

The first contributions of this thesis are devoted to developing models such as traffic flow model and flock-based mobility model, as a preliminary step towards investigating the more complex and interesting problems related to smart cities and tactical networks respectively. The goal of this first contribution is the development of intelligent mobility strategies to improve both traffic flow and safety in a city with multiple roundabouts. Hence, a two-dimensional cellular automata model is presented to model a city with multiple roads and roundabouts. Based on this model, traffic states were extensively analyzed in terms of traffic flow, average velocity, car accidents and waiting times in the entrance legs. We observed that bottleneck and gridlock states could occur when some critical car densities are reached. Also, we identified that both the increase in the car density and disequilibrium in the balance of turning rates are responsible for the appearance of bottleneck and gridlock states. The second contribution is devoted to studying a flock-based mobility model capable of simulating the collective motion of agents in the direction of a target. The results showed that agents' dynamics are governed by the decisions of their neighbors, in particular, when the majority of neighbors can make consensus decisions about a specific moving direction. Also, the emergence of leadership within the group depends on the quality of information received by informed agents which allows other agents to determine accurately their preferences.

The second step undertaken in this thesis was the investigation of the problem of mobility in tactical networks under three different scenarios. The first scenario is designed to simulate dismounted soldiers' dynamics on a battlefield without the presence of enemies. The second one incorporates the presence of enemies and their effect to wreck the collective motion of soldiers. The third scenario simulates tactical mobility of dismounted soldiers' squad. Our results showed that when enemies are not present in the battlefield, dismounted soldiers move in a collective manner whenever the noise is low enough. Both the soldiers' wireless communications and its related paths' lifetime are enhanced, due to the stability of network topology. In contrast, noise strongly affects the network topology state, causing partitioning and soldier's dispersion. In addition, our investigation also showed that soldier's dynamics are constrained by the presence of enemy attacks. The obtained results depicted that the throughput of packets received by the commander decreases as the enemy numbers increase, due to limitations in terms of relay nodes and insufficient link quality, which are mainly caused by the high dynamic of soldiers as they try to escape from enemy attacks. In the context of tactical mobility of dismounted soldier's squad, we found interesting results that links the impact between tactical mobility and energy-efficient in WSNs. Our findings show that noise has a negative impact on both the cohesion of the group and the sensor network's lifetime : the higher the value of η_0, the higher the group elongation and group split and therefore the higher the energy consumption by the sensor nodes. Secondly, the increase in the percentage of informed agents P causes a slight improvement in energy consumption as it has effects on both the cohesion of the group and on the sensor network's lifetime.

Motivated by the ability of VANETs to provide real-time communications based on V2V and V2I, we first decided to develop a real-time path planning for reducing vehicles' travel time in smart cities. Based on real scenarios, our strategy was sufficiently evaluated under varying beacon time intervals and the density of vehicles. Our results showed that our strategy significantly outperforms the obtained results when traditional strategy is used. Moreover, it is also shown that traffic lights have a significant impact on both travel time, the number of journeys and

average speed. Also, beacon time intervals have less impact on the traffic state when a high number of intersections use traffic lights. Secondly, we Secondly, we adopted a cooperative communication strategy between vehicles based on the Dedicated Short-Range Communication (DSRC) to study the ability of predicting collisions between vehicles approaching an intersection. The purpose of our strategy is two folds : first, providing a mathematical estimation of smallest distance between approaching vehicles an intersection with smallest estimation error. Second, we integrated the proposed estimation method of smallest distance with our V2V cooperative strategy to calculate the maximum probability of collision between approaching vehicles an intersection as a function of both exact data and beacons' time intervals. Our results showed that the accuracy of collisions prediction depends on the beacons' time intervals, where it increases significantly under small beacons' time intervals, while it decreases under higher beacons' time intervals.

5.2 Future work

Mobility modeling remains an interesting research area in the field of wireless communications, especially for transportation systems and tactical networks. Accordingly, we observe that many challenges still need to be overcome. So, in the future, we plan to work on the following ideas :

1. To incorporate soldiers' cognitive abilities based on memory and real-time interactions so that the soldier can make a tactical decision on the battlefield.
2. To use genetic algorithms to "evolve" operational tactics and targeting strategies.
3. To use SWARM for developing full-system models for training purposes and/or developing new tactical solutions to enhance real-world operations.
4. To develop 3D models for defining soldiers and the battlefield in a three-dimensional area. The 3D models will be combined with a network simulator like NS-2 to make simulations more realistic.
5. To extend the collision detection strategy to include the trust level of each driver's behaviors in the road network. The collected driver's trust level will be referred to as an indicator of aggressiveness' level for this driver at intersections.

Bibliography

[1] C. Bettstetter, Mobility modeling in wireless networks : categorization, smooth movement, and border effects, ACM SIGMOBILE Mobile Computing and Communications Review 5 (3) (2001) 55–66. 2

[2] M. M. Zonoozi, P. Dassanayake, User mobility modeling and characterization of mobility patterns, IEEE Journal on selected areas in communications 15 (7) (1997) 1239–1252. 2

[3] C. Song, T. Koren, P. Wang, A.-L. Barabási, Modelling the scaling properties of human mobility, Nature Physics 6 (10) (2010) 818. 2

[4] A. K. Saha, D. B. Johnson, Modeling mobility for vehicular ad-hoc networks, in : Proceedings of the 1st ACM international workshop on Vehicular ad hoc networks, ACM, 91–92, 2004. 2

[5] P. Holliday, SWARMM-a mobility modelling tool for tactical military networks, in : MILCOM 2008-2008 IEEE Military Communications Conference, IEEE, 1–7, 2008. 2

[6] L. Li, T. Kunz, Efficient mobile networking for tactical radios, in : MILCOM 2009-2009 IEEE Military Communications Conference, IEEE, 1–7, 2009. 2

[7] N. Aschenbruck, R. Ernst, E. Gerhards-Padilla, M. Schwamborn, BonnMotion : a mobility scenario generation and analysis tool, in : Proceedings of the 3rd international ICST conference on simulation tools and techniques, ICST (Institute for Computer Sciences, Social-Informatics and . . . , 51, 2010. 2

[8] B. C. da Silva, A. L. Bazzan, G. K. Andriotti, F. Lopes, D. de Oliveira, ITSUMO : an intelligent transportation system for urban mobility, in : International Workshop on Innovative Internet Community Systems, Springer, 224–235, 2004. 2

[9] M. Rondinone, J. Maneros, D. Krajzewicz, R. Bauza, P. Cataldi, F. Hrizi, J. Gozalvez, V. Kumar, M. Röckl, L. Lin, et al., iTETRIS : a modular simulation platform for the large scale evaluation of cooperative ITS applications, Simulation Modelling Practice and Theory 34 (2013) 99–125. 2

[10] S. Huang, A. W. Sadek, Y. Zhao, Assessing the mobility and environmental benefits of reservation-based intelligent intersections using an integrated simulator, IEEE Transactions on Intelligent Transportation Systems 13 (3) (2012) 1201–1214. 2

[11] A. Adelakun, C. R. Cherry, Exploring truck driver perceptions and preferences : Congestion and conflict, managed lanes, and tolls, Tech. Rep., 2009. 8

[12] C. H. Yang, A. Regan, Prioritization of potential alternative truck management strategies using the analytical hierarchy process, Tech. Rep., 2009. 8

[13] U. Sparmann, Spurwechselvorgänge auf zweispurigen BAB-Richtungsfahrbahnen, FORSCH STRASSENBAU U STRASSENVERKEHRSTECH 263 (263). 8

[14] Y. Regragui, N. Moussa, Modeling and simulation of VANET in traffic city, in : 2014 5th Workshop on Codes, Cryptography and Communication Systems (WCCCS), IEEE, 73–76, 2014. 8

[15] Y. Regragui, N. Moussa, A cellular automata model for urban traffic with multiple roundabouts, Chinese journal of physics 56 (3) (2018) 1273–1285. 8, 13, 14

[16] J. M. Ng, Y. Zhang, A mobility model with group partitioning for wireless ad hoc networks, in : Information Technology and Applications, 2005. ICITA 2005. Third International Conference on, vol. 2, IEEE, 289–294, 2005. 9, 11

[17] M. Musolesi, C. Mascolo, A community based mobility model for ad hoc network research, in : Proceedings of the 2nd international workshop on Multi-hop ad hoc networks : from theory to reality, ACM, 31–38, 2006.

[18] B. Zhou, K. Xu, M. Gerla, Group and swarm mobility models for ad hoc network scenarios using virtual tracks, in : Military Communications Conference, 2004. MILCOM 2004. 2004 IEEE, vol. 1, IEEE, 289–294, 2004. 9, 40

[19] X. Hong, M. Gerla, G. Pei, C.-C. Chiang, A group mobility model for ad hoc wireless networks, in : Proceedings of the 2nd ACM international workshop on Modeling, analysis and simulation of wireless and mobile systems, ACM, 53–60, 1999. 9, 40, 50

[20] K. H. Wang, B. Li, Group mobility and partition prediction in wireless ad-hoc networks, in : Communications, 2002. ICC 2002. IEEE International Conference on, vol. 2, IEEE, 1017–1021, 2002. 10

[21] S. A. Williams, D. Huang, Group force mobility model and its obstacle avoidance capability, Acta Astronautica 65 (7) (2009) 949–957. 11, 50

[22] K. Wu, Q. Yu, A multi-group coordination mobility model for ad hoc networks, in : MILCOM 2006-2006 IEEE Military Communications conference, IEEE, 1–5, 2006. 11

[23] K. Nagel, M. Schreckenberg, A cellular automaton model for freeway traffic, Journal de physique I 2 (12) (1992) 2221–2229. 13

[24] D. Chowdhury, L. Santen, A. Schadschneider, Statistical physics of vehicular traffic and some related systems, Physics Reports 329 (4) (2000) 199–329. 14

[25] P.-g. Hou, H.-w. Yu, C. Yan, J.-y. Hong, An extended car-following model based on visual angle and backward looking effect, Chinese Journal of Physics 55 (5) (2017) 2092–2099. 14

[26] F. Járai-Szabó, Z. Néda, Earthquake model describes traffic jams caused by imperfect driving styles, Physica A : Statistical Mechanics and its Applications 391 (22) (2012) 5727–5738. 14, 75

[27] M. Zamith, R. C. P. Leal-Toledo, E. Clua, E. M. Toledo, G. V. P. Magalhães, A new stochastic cellular automata model for traffic flow simulation with drivers' behavior prediction, Journal of Computational Science 9 (2015) 51–56. 14

[28] B. Persaud, R. Retting, P. Garder, D. Lord, Safety effect of roundabout conversions in the united states : Empirical bayes observational before-after study, Transportation Research Record : Journal of the Transportation Research Board (1751) (2001) 1–8. 14

[29] S. Eisenman, J. Josselyn, G. List, B. Persaud, C. Lyon, B. Robinson, M. Blogg, E. Waltman, R. Troutbeck, Operational and safety performance of modern roundabouts and other intersection types, Project NYSDOT C-01 47.

[30] L. Rodegerdts, Roundabouts in the United States, vol. 572, Transportation Research Board, 2007. 14

[31] S. Mandavilli, A. McCartt, R. Retting, Crash patterns and potential engineering countermeasures at Maryland roundabouts, Traffic Injury Prevention 10 (1) (2009) 44–50. 14

[32] M. E. Fouladvand, Z. Sadjadi, M. R. Shaebani, Characteristics of vehicular traffic flow at a roundabout, Physical Review E 70 (4) (2004) 046132. 14

[33] R. Wang, H. J. Ruskin, Modelling traffic flow at multi-lane urban roundabout, International Journal of Modern Physics C 17 (05) (2006) 693–710. 14

[34] D.-w. Huang, Modeling gridlock at roundabout, Computer Physics Communications 189 (2015) 72–76. 14

[35] N. Boccara, H. Fuks, Q. Zeng, Car accidents and number of stopped cars due to road blockage on a one-lane highway, Journal of Physics A : Mathematical and General 30 (10) (1997) 3329. 14

[36] N. Moussa, Car accidents in cellular automata models for one-lane traffic flow, Physical Review E 68 (3) (2003) 036127. 14, 24

[37] H. Echab, N. Lakouari, H. Ez-Zahraouy, A. Benyoussef, Simulation study of traffic car accidents at a single lane roundabout, International Journal of Modern Physics C 27 (01) (2016) 1650009. 14

[38] A. Pratelli, Design of modern roundabouts in urban traffic systems, in : Urban Transport XII, eds. Brebbia and Dolezel, WIT Press, 83–93, 2006. 18

[39] J. A. Cuesta, F. C. Martínez, J. M. Molera, A. Sánchez, Phase transitions in two-dimensional traffic-flow models, Physical Review E 48 (6) (1993) R4175. 23

[40] C. von Rueden, S. Gavrilets, L. Glowacki, Solving the puzzle of collective action through inter-individual differences, 2015. 26

[41] O. Petit, R. Bon, Decision-making processes : the case of collective movements, Behavioural Processes 84 (3) (2010) 635–647. 26

[42] G. Ariel, O. Rimer, E. Ben-Jacob, Order–disorder phase transition in heterogeneous populations of self-propelled particles, Journal of Statistical Physics 158 (3) (2015) 579–588. 26

[43] A. M. Menzel, Collective motion of binary self-propelled particle mixtures, Physical Review E 85 (2) (2012) 021912. 26

[44] B. Ferdinandy, K. Ozogány, T. Vicsek, Collective motion of groups of self-propelled particles following interacting leaders, Physica A : Statistical Mechanics and its Applications 479 (2017) 467–477. 26

[45] S. Mishra, K. Tunstrøm, I. D. Couzin, C. Huepe, Collective dynamics of self-propelled particles with variable speed, Physical Review E 86 (1) (2012) 011901. 26

[46] M. Zamani, T. Vicsek, Glassy nature of hierarchical organizations, Scientific reports 7 (1) (2017) 1382. 26

[47] L. F. Lafuerza, R. Toral, On the effect of heterogeneity in stochastic interacting-particle systems, Scientific reports 3 (2013) 1189. 26

[48] Y. Imry, M. Wortis, Influence of quenched impurities on first-order phase transitions, Physical Review B 19 (7) (1979) 3580. 26

[49] M. Aizenman, J. Wehr, Rounding effects of quenched randomness on first-order phase transitions, Communications in mathematical physics 130 (3) (1990) 489–528. 26

[50] T. Vicsek, A. Czirók, E. Ben-Jacob, I. Cohen, O. Shochet, Novel type of phase transition in a system of self-driven particles, Physical review letters 75 (6) (1995) 1226. 27, 44, 47

[51] T. Vicsek, A. Zafeiris, Collective motion, Physics Reports 517 (3) (2012) 71–140.

[52] Y. Regragui, N. Moussa, Agent-based system simulation of wireless battlefield networks, Computers & Electrical Engineering 56 (2016) 313–333. 27

[53] I. D. Couzin, J. Krause, N. R. Franks, S. A. Levin, Effective leadership and decision-making in animal groups on the move, Nature 433 (7025) (2005) 513. 28, 29, 31, 59, 62

[54] I. D. Couzin, J. Krause, R. James, G. D. Ruxton, N. R. Franks, Collective memory and spatial sorting in animal groups, Journal of theoretical biology 218 (1) (2002) 1–11. 29, 40, 42, 67

[55] N. R. Council, Energy-Efficient Technologies for the Dismounted Soldier, The National Academies Press, ISBN 978-0-309-05934-3, URL http://www.nap.edu/catalog/5905/energy-efficient-technologies-for-the-dismounted-soldier, 1997. 36

[56] K. H. Wang, B. Li, Efficient and guaranteed service coverage in partitionable mobile ad-hoc networks, in : INFOCOM 2002. Twenty-First Annual Joint Conference of the IEEE Computer and Communications Societies. Proceedings. IEEE, vol. 2, IEEE, 1089–1098, 2002. 37

[57] G. Karumanchi, S. Muralidharan, R. Prakash, Information dissemination in partitionable mobile ad hoc networks, in : Reliable Distributed Systems, 1999. Proceedings of the 18th IEEE Symposium on, IEEE, 4–13, 1999. 37

[58] A. Fongen, M. Gjellerud, E. Winjum, A military mobility model for manet research, Parallel and Distributed Computing and Networks (PDCN 2009), February 16 (2009) 18. 40

[59] C. W. Reynolds, Flocks, herds and schools : A distributed behavioral model, ACM Siggraph Computer Graphics 21 (4) (1987) 25–34. 40, 67

[60] M. Sánchez, P. Manzoni, ANEJOS : a java based simulator for ad hoc networks, Future generation computer systems 17 (5) (2001) 573–583. 50

[61] A.-D. Nguyen, P. Senac, M. Diaz, Modelling mobile opportunistic networks–From mobility to structural and behavioural analysis, Ad Hoc Networks 24 (2015) 161–174. 50

[62] K. Lee, S. Hong, S. J. Kim, I. Rhee, S. Chong, Slaw : A new mobility model for human walks, in : INFOCOM 2009, IEEE, IEEE, 855–863, 2009. 50

[63] Y. Regragui, N. Moussa, Dynamics of network connectivity in tactical manets, in : 2018 International Conference on Advanced Communication Technologies and Networking (CommNet), IEEE, 1–6, 2018. 59

[64] R. Freeman, D. Biro, Modelling group navigation : dominance and democracy in homing pigeons, The journal of navigation 62 (1) (2009) 33–40. 61

[65] I. F. Akyildiz, W. Su, Y. Sankarasubramaniam, E. Cayirci, A survey on sensor networks, IEEE Communications magazine 40 (8) (2002) 102–114. 63

[66] E. S. Nadimi, R. N. Jørgensen, V. Blanes-Vidal, S. Christensen, Monitoring and classifying animal behavior using ZigBee-based mobile ad hoc wireless sensor networks and artificial neural networks, Computers and Electronics in Agriculture 82 (2012) 44–54. 64, 65

[67] A. Kumar, G. P. Hancke, A zigbee-based animal health monitoring system, IEEE Sens. J 15 (1) (2015) 610–617. 64

[68] S. Sudevalayam, P. Kulkarni, Energy harvesting sensor nodes : Survey and implications, IEEE Communications Surveys & Tutorials 13 (3) (2011) 443–461. 64

[69] E. S. Nadimi, V. Blanes-Vidal, R. N. Jørgensen, S. Christensen, Energy generation for an ad hoc wireless sensor network-based monitoring system using animal head movement, Computers and Electronics in Agriculture 75 (2) (2011) 238–242. 64

[70] G. Mao, B. Fidan, B. D. Anderson, Wireless sensor network localization techniques, Computer networks 51 (10) (2007) 2529–2553. 64

[71] W. B. Heinzelman, A. P. Chandrakasan, H. Balakrishnan, An application-specific protocol architecture for wireless microsensor networks, IEEE Transactions on wireless communications 1 (4) (2002) 660–670. 64

[72] O. Younis, S. Fahmy, HEED : a hybrid, energy-efficient, distributed clustering approach for ad hoc sensor networks, IEEE Transactions on mobile computing 3 (4) (2004) 366–379. 64

[73] V. Kawadia, P. Kumar, Power control and clustering in ad hoc networks, in : INFOCOM 2003. Twenty-Second Annual Joint Conference of the IEEE Computer and Communications. IEEE Societies, vol. 1, IEEE, 459–469, 2003. 64

[74] S. Narayanaswamy, V. Kawadia, R. S. Sreenivas, P. Kumar, Power control in ad-hoc networks : Theory, architecture, algorithm and implementation of the COMPOW protocol, in : European wireless conference, vol. 2002, Florence, Italy, 156–162, 2002. 64

[75] P. Gupta, P. R. Kumar, The capacity of wireless networks, IEEE Transactions on information theory 46 (2) (2000) 388–404. 64

[76] A. Cerpa, D. Estrin, ASCENT : Adaptive self-configuring sensor networks topologies, IEEE transactions on mobile computing 3 (3) (2004) 272–285. 64

[77] Y. Xu, J. Heidemann, D. Estrin, Geography-informed energy conservation for ad hoc routing, in : Proceedings of the 7th annual international conference on Mobile computing and networking, ACM, 70–84, 2001.

[78] B. Chen, K. Jamieson, H. Balakrishnan, R. Morris, Span : An energy-efficient coordination algorithm for topology maintenance in ad hoc wireless networks, Wireless networks 8 (5) (2002) 481–494. 64

[79] C. Tang, L. Zhang, An Improved Flooding Routing Protocol for Wireless Sensor Networks Based on Network-Coding, in : ITM Web of Conferences, vol. 17, EDP Sciences, 02001, 2018. 64

[80] D. Chang, K. Cho, N. Choi, Y. Choi, et al., A probabilistic and opportunistic flooding algorithm in wireless sensor networks, Computer Communications 35 (4) (2012) 500–506. 64

[81] J. Son, T.-Y. Byun, A routing scheme with limited flooding for wireless sensor networks, International Journal of Future Generation Communication and Networking 3 (3) (2010) 33–40. 64

[82] H. Zhao, L. Mao, J. Wei, Coverage on demand : A simple motion control algorithm for autonomous robotic sensor networks, Computer Networks 135 (2018) 190–200. 64

[83] K. Eledlebi, D. Ruta, F. Saffre, Y. Al-Hammadi, A. Isakovic, A Model for Self-deployment of Autonomous Mobile Sensor Network in an Unknown Indoor Environment, in : Ad Hoc Networks, Springer, 208–215, 2018. 65

[84] S. Singh, M. M. Kokar, Simulation of Scale-Free Correlation in Swarms of UAVs, in : International Conference on Complex Systems, Springer, 91–97, 2018. 65

[85] H. Su, Z. Li, M. Z. Chen, Distributed estimation and control for two-target tracking mobile sensor networks, Journal of the Franklin Institute 354 (7) (2017) 2994–3007. 65

[86] T. Kosch, C. J. Adler, S. Eichler, C. Schroth, M. Strassberger, The scalability problem of vehicular ad hoc networks and how to solve it, Wireless Communications, IEEE 13 (5) (2006) 22–28. 72, 75

[87] A. Schadschneider, Traffic flow : a statistical physics point of view, Physica A : Statistical Mechanics and its Applications 313 (1-2) (2002) 153–187. 75

[88] H. Noori, M. Valkama, Impact of VANET-based V2X communication using IEEE 802.11 p on reducing vehicles traveling time in realistic large scale urban area, in : Connected Vehicles and Expo (ICCVE), 2013 International Conference on, IEEE, 654–661, 2013. 75

[89] Z. He, J. Cao, T. Li, Mice : A real-time traffic estimation based vehicular path planning solution using vanets, in : Connected Vehicles and Expo (ICCVE), 2012 International Conference on, IEEE, 172–178, 2012. 75

[90] H. Yu, J. Yoo, S. Ahn, A VANET routing based on the real-time road vehicle density in the city environment, in : Ubiquitous and Future Networks (ICUFN), 2013 Fifth International Conference on, IEEE, 333–337, 2013. 76

[91] A. M. de Souza, R. S. Yokoyama, G. Maia, A. Loureiro, L. Villas, Real-time path planning to prevent traffic jam through an intelligent transportation system, in : Computers and Communication (ISCC), 2016 IEEE Symposium on, IEEE, 726–731, 2016. 76

[92] C. Jayapal, S. S. Roy, Road traffic congestion management using VANET, in : Advances in Human Machine Interaction (HMI), 2016 International Conference on, IEEE, 1–7, 2016. 76

[93] G. Karagiannis, O. Altintas, E. Ekici, G. Heijenk, B. Jarupan, K. Lin, T. Weil, Vehicular networking : A survey and tutorial on requirements, architectures, challenges, standards and solutions, IEEE communications surveys & tutorials 13 (4) (2011) 584–616. 78

[94] Wireless Access in Vehicular Environments, IEEE (July 2010) Std 802.11p–2010. 78

[95] S.-H. Chang, C.-Y. Lin, C.-C. Hsu, C.-P. Fung, J.-R. Hwang, The effect of a collision warning system on the driving performance of young drivers at intersections, Transportation research part F : traffic psychology and behaviour 12 (5) (2009) 371–380. 78

[96] T. Mangel, F. Schweizer, T. Kosch, H. Hartenstein, Vehicular safety communication at intersections : Buildings, Non-Line-Of-Sight and representative scenarios, in : 2011 Eighth International Conference on Wireless On-Demand Network Systems and Services, IEEE, 35–41, 2011. 78

[97] A. Tang, A. Yip, Collision avoidance timing analysis of DSRC-based vehicles, Accident Analysis & Prevention 42 (1) (2010) 182–195. 78

[98] M. Brannstrom, E. Coelingh, J. Sjoberg, Model-based threat assessment for avoiding arbitrary vehicle collisions, IEEE Transactions on Intelligent Transportation Systems 11 (3) (2010) 658–669. 78

[99] S. Lefèvre, C. Laugier, J. Ibañez-Guzmán, Risk assessment at road intersections : Comparing intention and expectation, in : 2012 IEEE Intelligent Vehicles Symposium, IEEE, 165–171, 2012. 78

[100] H.-S. Tan, J. Huang, DGPS-based vehicle-to-vehicle cooperative collision warning : Engineering feasibility viewpoints, IEEE Transactions on Intelligent Transportation Systems 7 (4) (2006) 415–428. 78

[101] S. Joerer, M. Segata, B. Bloessl, R. L. Cigno, C. Sommer, F. Dressler, A vehicular networking perspective on estimating vehicle collision probability at intersections, IEEE Transactions on Vehicular Technology 63 (4) (2013) 1802–1812. 78

Appendix A

Using SUMO to simulate traffic in road networks

This Appendix contains a description of how to use SUMO to perform road traffic simulation.

The Simulator of Urban Mobility (SUMO) is open-source software (licensed under the GPL), highly portable, microscopic and continuous road traffic simulation package designed to handle large road networks. Sumo is developed and implemented in C++ by the DLR - Institute of Transportation Systems of DLR, the National Aeronautics and Space Research Center of the Federal Republic of Germany in Berlin. It uses only portable libraries that make it independent of any architecture. Based on SUMO's simulation platform, many features are provided, including microscopic simulation, online interaction and the simulation of multimodal traffic. Also, SUMO allows time schedules of traffic lights either by the user or via automatic generation. Moreover, in SUMO, there are no artificial limitations in the network size and the number of simulated vehicles. The simulation of traffic networks can be provided by importing maps encoded in many file formats such as OpenStreetMap, VISUM, VISSIM, and NavTeq. Also, SUMO allows users to define their preferred traffic networks based on netedit tool. Each module defined in SUMO is accompanied by extensive documentation and examples. The documentation is available on : http://sumo.dlr.de/wiki/Main_Page.

1 Importing maps in SUMO

There are many ways in which a map can be extracted from OpenStreetMaps. The simplest way of doing it is using a Web browser and access the web page at http://www.openstreetmap.org. However, another possibility is using some sort of stand-alone applications that support and are compatible with the OpenStreetMaps database. For example, one of best known pieces of software is JOSM, the Java OpenStreetMap Editor, which is available for download for free the Internet. In Figure 5.2 , an illustration example of the JOSM graphical user interface. This interface allows SUMO users to specify more details needed to define such a configuration of the map to be download. The map will be extracted in the OSM file format contains the necessary information needed to extract the road network by SUMO. Also, JOSM allows reducing the size of OSM files.

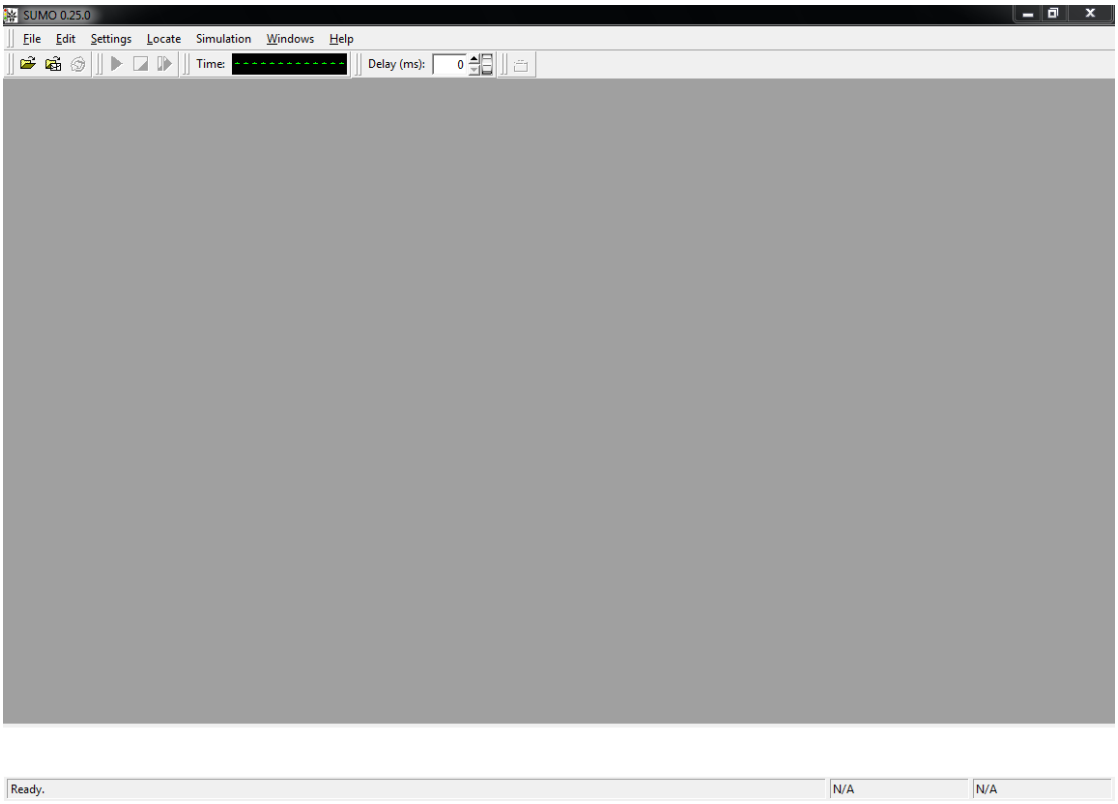

Figure 5.1 – Overview of SUMO's graphical simulation interface.

However, there are other possible ways to extract maps from OpenStreetMaps like a Python script which is called osmWebWizard.py.

On the other hand, when using the web Browser, we already have the coordinates of the bounding box surrounding the desired area illustrated with red color in 5.3 (which can be obtained e.g. from the www.openstreetmaps.org website. That is provided by a web service with the following URL : `http://api.openstreetmap.org/api/0.6/map?bbox=<coordinates>`, where <coordinates> = <SW-longitude,SW-latitude,NE-longitude,NE-latitude> as e.g. in `http://api.openstreetmap.org/api/0.6/map?bbox=15.218,50.473,15.471,50.552`.

2 Converting from an OSM file to a SUMO .net.xml file

Passing through all previous steps and different options, the final result will be an XML file, usually named <something>.osm or <something>.osm.xml, but in our case, we can rename it Berlin.osm. Now, we can use another tool called NETCONVERT to convert the OSM file to the Berlin.net.xml file format, to use it for the SUMO simulation. We used a line command prompt interface in windows 7 as follows.

$$netconvert\ --osm-files\ berlin.osm\ -o Berlin.net.xml\ --remove-isolated\ --remove-geometry\ --type-files\ C:\Users\MSDSGROUP\Desktop\sumo-0.25.0\data\typemap\osmNetconvert.typ.xm$$

Besides that OSM files include several generated information, like POI (Points of Interest), buildings drawings, regions, etc. However, SUMO usually simply discarded graphic information not important for simulation.

Now, using the generated Berlin.net.xml file by SUMO, we can generate a polygon file using the following command :

$$polyconvert\ --net-file berlin.net.xml\ --osm-files\ berlin.osm\ --type-file typemap.xml\ -o berlin.poly.xml$$

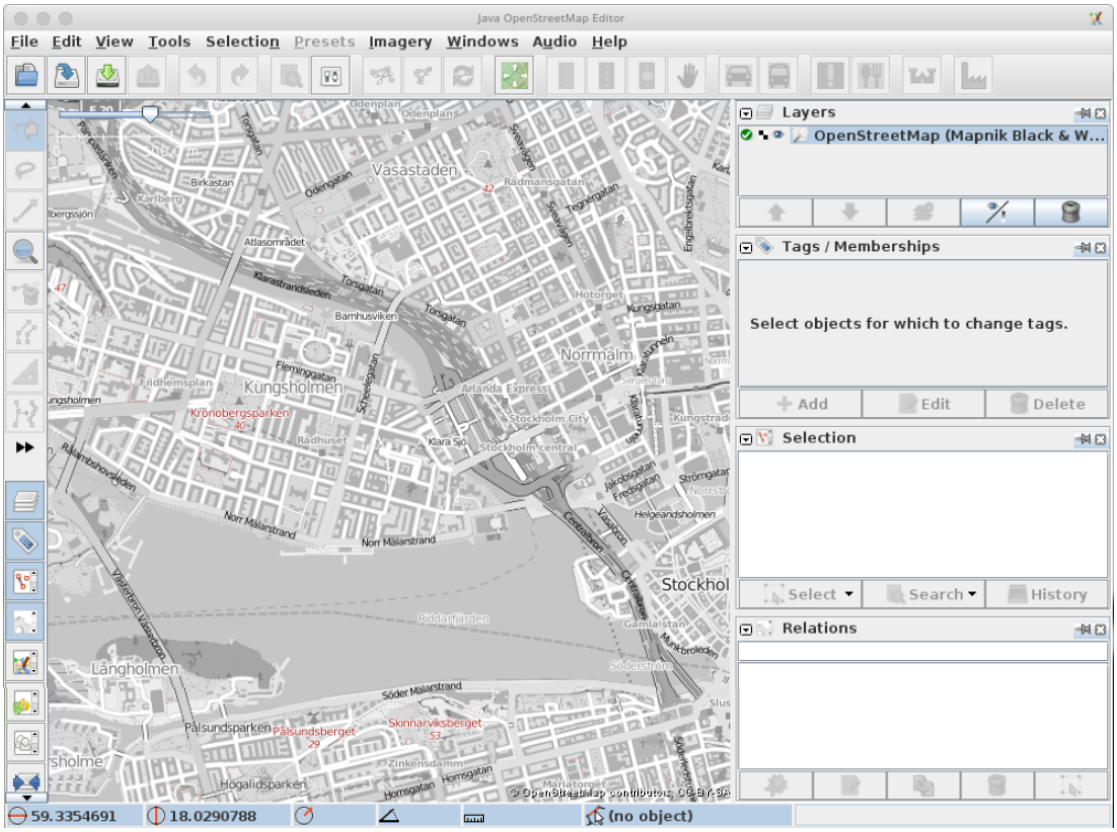

Figure 5.2 – Graphical User Interface of the software JOSM.

In this part, we will generate a set of random trips for a given network (option -n). It does so by choosing source and destination uniformly at random distribution. The tool used for this step is "randomTrips.py" with some options. The trips are distributed evenly in a time interval defined by begin time using (option -b, default 0) and end time using (option -e, default 3600) in seconds. The number of trips is defined by the repetition rate (option -p, default 1) in seconds. Every trip has an id consisting of a prefix (option –prefix, default "") and a running number. The probabilities for selecting an edge may also be weighted by edge length (option -l) or by the number of lanes (option -L). To generate trips in our case we use the following command line :

$$randomTrips.py\ -n\ Berlin.net.xml\ -r\ Berlin.rou.xml\ -e\ 4000 -l$$

Now, we can run the simulation scenario of the Berlin road network by using a configuration file Berlin.sumo.cfg Figure 5.4 that use the already extracted files, including Berlin.net.xml, Berlin.rou.xml, and Berlin.poly.xml as follows :

$$sumo-gui\ Berlin.sumo.cfg$$

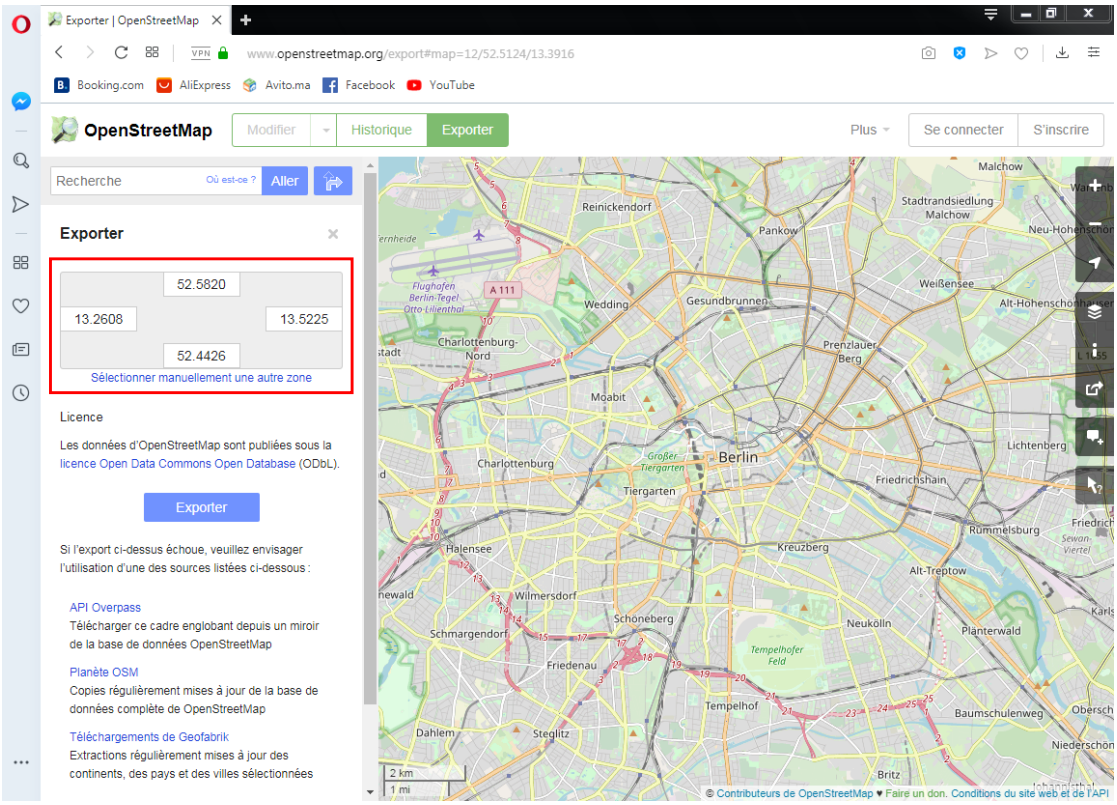

Figure 5.3 – Importing of a map from OpenStreetMaps.

2 Interaction between SUMO and TraCI

TraCI uses a TCP based client/server architecture to provide access to SUMO. To establish a connection between a TraCI client and SUMO, we need to define a remote port waiting for the command sent by the TraCI client. SUMO can start only with a few additional command-line options. When started, SUMO only prepares the simulation and waits for an external application to take the control traffic based on specific predefined TraCI command. The best known framework for developing the external application as TraCI clients is known as Veins framework. The Veins framework includes a set of models to make vehicular network simulations. The framework composed of OMNeT++, Veins and SUMO can be used for quickly setting up and interactively running simulations. Accordingly, to run a connection between a Veins application and SUMO, we use the following command which in turn calls a Python script to do the work :

```
cd /Python27
python C:\omnetpp-4.6\samples\veins\sumo-launchd.py -vv -c
C:\Users\MSDSGROUP\Desktop\sumo-0.25.0\bin\sumo.exe
```

```
<?xml version="1.0" encoding="iso-8859-1"?>

<configuration>

    <input>
        <net-file value="Berlin.net.xml"/>
        <route-files value="Berlin.rou.xml"/>
        <additional-files value="Berlin.poly.xml"/>
    </input>

    <time>
        <begin value="0"/>
        <end value="4000"/>
        <step-length value="0.01"/>
    </time>

</configuration>
```

Figure 5.4 – Generation of road network scenario based berlin map.

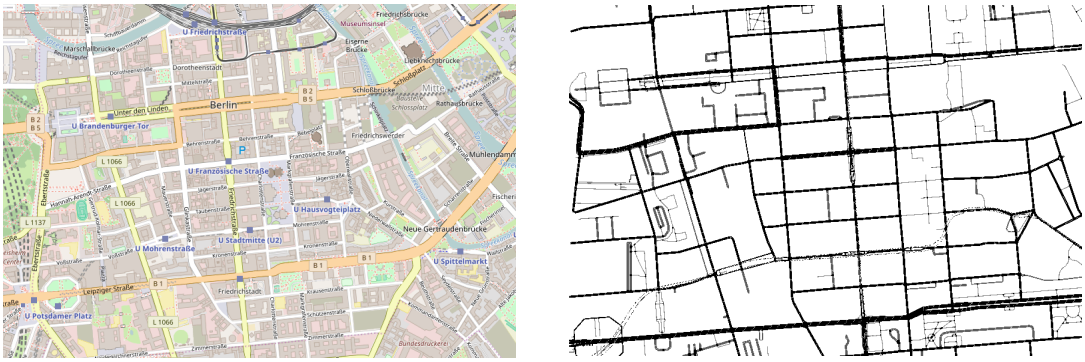

(a) Berlin map

(b) Berlin road network

Figure 5.5 – Generation of road network scenario based Berlin map.

Appendix B

Published papers

• Journal papers

1. Y. Regragui, N. Moussa, Agent-based system simulation of wireless battlefield networks, Computers & Electrical Engineering 56 (2016) 313–333.

2. Y. Regragui, N. Moussa, A cellular automata model for urban traffic with multiple roundabouts, Chinese journal of physics 56 (3) (2018) 1273–1285.

• Conference Papers

1. Y. Regragui, N. Moussa, Dynamics of network connectivity in tactical manets, in : 2018 International Conference on Advanced Communication Technologies and Networking (CommNet), IEEE, 1–6, 2018.

2. Y. Regragui, N. Moussa, Investigating the impact of real-time path planning on reducing vehicles traveling time, in : 2018 International Conference on Advanced Communication Technologies and Networking (CommNet), IEEE, 1–6, 2018.

3. Y. Regragui, N. Moussa, Simulation of wireless sensors in collective motion, in : 2018 6th International Conference on Wireless Networks and Mobile Communications (WINCOM), IEEE, 1–6, 2018.

4. Y. Regragui, N. Moussa, On the Self-Organization of Mobile Agents to Ensure Dynamic Multi-level Coverage in Sensor Networks, in : Proceedings of the 2nd International Conference on Networking, Information Systems & Security, ACM, 15, 2019.

5. Y. Regragui, N. Moussa, Modeling and simulation of VANET in traffic city, in : 2014 5th Work-shop on Codes, Cryptography and Communication Systems (WCCCS), IEEE, 73–76, 2014.